AMRL-TR-79-7

AN EVALUATION AND COMPARISON OF SEVERAL MEASURES OF IMAGE QUALITY FOR TELEVISION DISPLAYS

HARRY LEE TASK, Ph. D.

JANUARY 1979

AEROSPACE MEDICAL RESEARCH LABORATORY
AEROSPACE MEDICAL DIVISION
AIR FORCE SYSTEMS COMMAND
WRIGHT-PATTERSON AIR FORCE BASE, OHIO 45433

79 06

NOTICES

TECHNICAL REVIEW AND APPROVAL

AMRL-TR-79-7

This report has been reviewed by the Information Office (OI) and is releasable to the National Technical Information Service (NTIS). At NTIS, it will be available to the general public, including foreign nations.

This technical report has been reviewed and is approved for publication.

FOR THE COMMANDER

CHARLES BATES, JR.
Chief
Human Engineering Division
Aerospace Medical Research Laboratory

SECURITY CLASSIFICATION OF THIS PAGE (When Data Entered)

REPORT DOCUMENTATION PAGE

READ INSTRUCTIONS BEFORE COMPLETING FORM

1. REPORT NUMBER: 14 AMRL-TR-79-7	2. GOVT ACCESSION NO.
	3. RECIPIENT'S CATALOG NUMBER
4. TITLE (and Subtitle): 6 AN EVALUATION AND COMPARISON OF SEVERAL MEASURES OF IMAGE QUALITY FOR TELEVISION DISPLAYS.	5. TYPE OF REPORT & PERIOD COVERED: Doctoral Dissertation
	6. PERFORMING ORG. REPORT NUMBER
7. AUTHOR(s): 10 Harry L. Task Lee	8. CONTRACT OR GRANT NUMBER(s)
9. PERFORMING ORGANIZATION NAME AND ADDRESS: Aerospace Medical Research Laboratory, Aerospace Medical Division, Air Force Systems Command, Wright-Patterson Air Force Base, Ohio 45433	10. PROGRAM ELEMENT, PROJECT, TASK AREA & WORK UNIT NUMBERS: 62202F, 7184-11-21 16 17 11
11. CONTROLLING OFFICE NAME AND ADDRESS: 009 850	12. REPORT DATE: 11 January 1979
	13. NUMBER OF PAGES: 152
14. MONITORING AGENCY NAME & ADDRESS (if different from Controlling Office): 9 Doctoral thesis,	15. SECURITY CLASS. (of this report): UNCLASSIFIED
	15a. DECLASSIFICATION/DOWNGRADING SCHEDULE: N/A

16. DISTRIBUTION STATEMENT (of this Report)

Approved for public release; distribution unlimited

17. DISTRIBUTION STATEMENT (of the abstract entered in Block 20, if different from Report)

12 152 p.

DDC REPORT JUN 11 1979 C

18. SUPPLEMENTARY NOTES

19. KEY WORDS (Continue on reverse side if necessary and identify by block number)

DISPLAYS	DISPLAY EVALUATION	VIDEO DISPLAYS
IMAGE QUALITY	DISPLAY QUALITY	DISPLAY MEASUREMENT
TELEVISION	IMAGE EVALUATION	FIGURE OF MERIT
CATHODE-RAY-TUBE	TARGET DETECTION	
	TARGET RECOGNITION	

20. ABSTRACT (Continue on reverse side if necessary and identify by block number)

Television display systems are currently widely used for many image transmission applications other than home entertainment. For many military and commercial uses the quality of the displayed imagery is critical with respect to its effect on observer performance. This dissertation investigates 19 figures of merit (FOM's) that have been proposed as measures of television image quality. (Continued on reverse)

DD FORM 1 JAN 73 1473 EDITION OF 1 NOV 65 IS OBSOLETE

009 850

SECURITY CLASSIFICATION OF THIS PAGE (When Data Entered)

BLOCK 20. ABSTRACT CONTINUED

A target detection and target recognition study was implemented to determine which of the 19 FOM's correlated highest with performance. The study employed a 525 line, 60 Hz field rate television display system with 2:1 interlace of fields. Nine different display quality conditions were investigated using all combinations of three contrast ratios (50:1, 50:5 and 50:15) and three video bandwidths (6.0 MHz, 1.0 MHz, and 0.4 MHz). Noise was not varied.

To obtain further information about the 19 FOM's, they were applied to a study previously reported in the literature. This previous study investigated the effect of viewing distance on observer performance.

Three FOM's stood out as promising indicators of display quality and observer performance. The highest correlating FOM was the log band-limited modulation transfer function area (log BLMTFA) closely followed by the just-noticeable difference area-log (JNDA-log, 1/2 cpd and the JNDA-log, 2cpd.

Although these FOM's correlated very well with the performance variables used in this dissertation, the entire concept of FOM's must be approached with caution. The performance variables used for this dissertation may not be the critical performance variables for a particular application. This concern is discussed at length in Chapter 6 of this dissertation. As a result of this potential problem, a promising means of modeling the actual observer performance level was developed and is presented. A rough implementation of this model agreed well with the results of a previous study.

Two FOM's correlated significantly and consistently poorer than the others. These were the limiting resolution and the equivalent bandpass. This result provides strong evidence that these two measures should not be used as overall quality indicators of display/observer systems.

PREFACE

The research described in this dissertation was accomplished with funds provided by the Aerospace Medical Research Laboratory, Human Engineering Division, Visual Display Systems Branch of the United States Air Force as part of Project 7184 1121. This dissertation was submitted to the graduate committee on optical sciences at the University of Arizona in partial fulfillment of the requirements for the degree of Doctor of Philosophy.

There are many individuals who provided valuable assistance during the course of this research and the preparation of the final document. Mr. Alan Pinkus and Mr. Mike Poole assisted in the data collection, subject scheduling, and equipment calibration.

I would also like to express my appreciation to Prof. Sol Nudelman, my major professor and dissertation director, and Prof. James Burke of the University of Arizona Optical Sciences Center for their review and comments on the dissertation. Thanks, also, to Prof. Harry Snyder of Virginia Polytechnic Institute and State University, the third member of my dissertation committee for his constructive criticism and comments on the dissertation.

TABLE OF CONTENTS

TABLE OF CONTENTS--Continued

LIST OF TABLES

LIST OF ILLUSTRATIONS

LIST OF ILLUSTRATIONS--Continued

CHAPTER 1

INTRODUCTION

Ever since man invented the lens and thus had a means of producing an image of the real world, there has been a problem of characterizing the quality of that image. With the advent of photography and, later, television, the problem of characterizing "image quality" in a meaningful fashion has increased tremendously. The primary objective of this dissertation is to investigate and evaluate display system "figures of merit" (FOM's) that can be used to indicate the image quality of television systems.

There are two approaches that can be taken toward determining functional image quality: subjective and objective. The subjective approach compares analytically derived measures of image quality with the subjective assessment of image quality as determined by human observers. The objective approach compares the analytically derived image quality measures with a performance variable associated with a particular observer task. Typical performance variables are response time, number of correct responses, size of target at recognition, and slant range (distance) to target at recognition/detection (see Appendix A). Almost all observer tasks involve recognition, detection or identification of some type of target. Targets may be real objects such as vehicles, buildings, or faces, or they may be artificial such as tri-bar patterns, rectangles, or sine waves.

The typical objective image quality assessment study investigates the effect of two or three display variables on the image quality measure being considered and the resulting observer performance. Table 1 shows a listing of parameters used to describe a video display system.

There are two basic subcategories of objective image quality assessment studies: 1) studies which employ a method intended to predict absolute observer performance levels, 2) studies which compare the correlation of a generalized FOM with observer performance. The first type is more difficult and is typically applied to artificial targets. The second type provides a relative measure of image quality (if it is successful) but does not give information as to the absolute performance level that can be expected. This dissertation primarily addresses the second subcategory.

It is apparent from the vast number of combinations of target type, observer tasks, display variables, and display types that it is nearly impossible to make meaningful comparisons among studies found in the literature. Nevertheless, Chapter 2 of this dissertation provides a summary review of the literature and attempts to evaluate and compare the various FOM's proposed therein.

Table 1. Television display system parameters

Geometric	Electronic	Photometric
Viewing Distance	Bandwidth	Luminance
Display Size	Dynamic Range	Gray Shades
Aspect Ratio	Signal/Noise	Contrast Ratio
Number of Scan Lines	Frame Rate	Halation
Interlace Ratio	Field Rate	Ambient Illuminance
Scan Line Spacing		Color
Linearity		Resolution
		Spot Size
		MTF
		Luminance Uniformity
		Gamma

To define an area that can be reasonably investigated in this dissertation, only display systems operating under relatively low noise level conditions are considered. Even within this defined area it is found that no investigation has attempted to apply more than three FOM's to the same observer performance data to determine which one yields the best correlation. Chapter 3 provides a brief discussion on each of the FOM's under consideration. Chapter 4 describes a target detection and target recognition study that was done to provide baseline performance data for comparing the FOM's. Chapter 5 describes a previous target recognition study that compares the performance of subjects in that experiment to the calculated values of each of 18 FOM's. A discussion of the concept of FOM's and a target recognition model are provided in Chapter 6. The conclusions are given in Chapter 7.

There are several terms with which the reader may not be familiar or that may have multiple meanings. To minimize the possibility of confusion, the following list of terms and definitions is provided:

Area-type FOM: If the FOM is calculated by finding the area under a curve, it is referred to as an "area-type" FOM. The most common of these is the modulation transfer function area (MTFA) which is defined as the area between the MTF of the display system and the visual contrast threshold function.

Bandwidth: Bandwidth is defined as the width of the band of frequencies that a system is capable of transmitting. For display systems this can be defined in either electronic temporal frequencies or the corresponding spatial frequencies. Since the television image is produced by a single scanning spot of light, the temporal frequency bandwidth and the spatial frequency bandwidth are directly related. If the MTF is Gaussian, then the bandwidth can be specified by a single number. This number is the frequency at which the modulation transfer factor is 0.5. This corresponds to the point at which the output signal is reduced by 3 dB, or 50 percent, with respect to the input signal (see definition of Gaussian MTF).

Contrast: There are many definitions of contrast; only one is used throughout this dissertation. Contrast is defined as the maximum luminance minus the minimum luminance divided by the sum of the two. This term is used interchangeably with the terms, "modulation" and "modulation contrast" and is denoted by the symbol M.

Contrast ratio: This is defined as the ratio of the maximum luminance to the minimum luminance. It is not the same as contrast but is related to contrast by the following equation:

$$C_r = \frac{1 + M}{1 - M} \tag{1}$$

where

C_r = contrast ratio

M = contrast (or modulation)

Contrast sensitivity function: The reciprocal of the contrast threshold function.

Contrast threshold function: The eye requires a certain minimum level of contrast before it is able to detect the presence of a spatially varying sine-wave pattern. This level depends on the spatial frequency of the sine-wave pattern. The level of contrast required for an observer to detect the presence of the pattern with a 50 percent probability level, described as a function of angular spatial frequency, is defined as the contrast threshold function.

Correlation: The correlation coefficient, r, ranges in value from $r = 0$, indicating no relationship between the two variables to $r = \pm 1$, indicating a perfect linear relationship between the two variables. The negative sign corresponds to a negative sloping line and the positive sign to a positive sloping line. The equation used to calculate r, is discussed in <u>Mathematical Statistics</u> by J. E. Freund (1962).

Frame rate: This is the rapidity with which the video picture is fully updated. For standard commercial television this is 30 frames (or pictures) per second.

Modulation: see contrast

Modulation contrast: see contrast

Modulation factor: see modulation transfer factor

Modulation transfer factor: The modulation transfer factor is the ratio of the modulation at the output to the modulation at the input of a system for a particular spatial frequency sine-wave pattern. This is denoted by the symbol M.

Modulation transfer function: If a sine-wave pattern is imaged through a linear display system, then the resulting image is a sine-wave pattern that may have a different modulation from the original.

The ratio of the modulation of the output sine-wave pattern to the modulation of the input sine-wave pattern is the modulation transfer factor. The curve describing this factor as a function of spatial frequency is the modulation transfer function, or MTF. This function is identified by the symbol $M(\omega)$. The MTF is strictly defined only if the display system is linear. However, for systems that depart only slightly from linearity, the concept of MTF is still useful. Such is the case for the application of the MTF concept to video displays. A Gaussian MTF is defined by the following equation:

$$M_g(\omega) = e^{-0.693 \left(\frac{\omega}{\omega_0}\right)^2} \tag{2}$$

where

$M_g(\omega)$ = modulation transfer factor

ω = spatial frequency variable

ω_0 = bandwidth

Defined in this manner the value of $M_g(\omega)$ is 0.5 for $\omega = \omega_0$. Thus ω_0 is the bandwidth of the display.

Scan line: A video picture is typically made up of a number of horizontal lines that are "painted" on the phosphor of the television display. This is done by an electron beam inside the cathode-ray tube that scans across the display. Each of these lines of picture information is called a scan line. This is not the same as the number of TV lines, which is a measure of resolution.

Sine-wave pattern: This is a two-dimensional pattern with a luminance distribution in one dimension that varies as the sine of the coordinate of that dimension plus an average luminance value. There is no luminance variation in the orthogonal dimension.

Spatial frequency: There are three distinctly different spatial frequency parameters. The distinction is sufficiently important that each of these is represented by a different symbol to avoid confusion. Each has its appropriate use in describing display systems.

Angular spatial frequency, ω. This quantity is measured in units of cycles per degree. This indicates the number of cycles of a periodic pattern that subtend an angle of one degree as measured from a particular viewing distance. It is typically used when one is interested in relating to vision or visual characteristics. The contrast sensitivity function and the contrast threshold function are expressed in terms of this variable.

Linear spatial frequency. There are two ways of characterizing linear spatial frequency: in units of cycles per unit length or cycles per display width. The first indicates the number of cycles of a target pattern that are contained in a specified unit of length such as an inch or centimeter. This is denoted by the symbol "f", and is commonly used in optics and photography. This type of measure corresponds to the density of information that can be transmitted through the display system. The second is generally used in television and denotes twice the total number of cycles (number of TV lines counting black and white lines) that are contained along a raster line, across the full width of the display, regardless of the actual display size. This variable is indicated by N, defined as the number of half-cycles across the display width.. This measure is appropriate for relating to the total information the display is capable of transmitting.

These three spatial frequencies are related according to the following equations:

$$f = \frac{N}{2W}$$

$$\omega = \frac{1}{2}\left\{\text{arc tan }\left(\frac{1}{2fD}\right)\right\}^{-1}$$

where

f = linear spatial frequency (cycles/unit length)

N = linear spatial frequency (half-cycles/display width)

ω = angular spatial frequency (cycles/degree)

W = display width

D = viewing distance

The equation for ω gives the angular spatial frequency for the center of the display only if the display surface is perpendicular to the observer's line of sight.

Square-wave pattern: This is a two-dimensional pattern in which the luminance distribution varies as a square wave in one dimension. It appears as a series of equal width, alternating bright and dark bars.

Transfer factor: see modulation transfer factor.

TV lines per picture height: This is a linear spatial frequency measure developed by Schade (1953) that corresponds to the maximum number of square-wave half cycles (black or white bars) that can be resolved along a distance on a display equal to the height of the display. Also, referred to as TV lines resolution. It is denoted by N_h.

CHAPTER 2

LITERATURE REVIEW

The most widely used measure of display quality is limiting resolution. Even with the advent of more elegant display measurements such as the modulation transfer function (MTF), display users still resort to limiting resolution as a means of specifying the required or actual display quality (Brock, 1967). Several test patterns have been developed to directly determine the limiting resolution of an imaging system. Figures 2.1 and 2.2 show two such patterns. Figure 2.1 is the Electronic Industries Association (EIA) Resolution Chart (formerly RETMA chart) developed specifically for use with television systems, and Figure. 2.2 is the 1951 standard U.S. Air Force tri-bar target pattern.

The wedge shaped patterns of the EIA chart are used to directly determine the limiting resolution of the display system in units of TV lines per picture height. Two TV lines correspond to one line pair or cycle of the bars making up the wedge pattern. The point at which the bars of the wedge pattern are no longer individually distinguishable is the limiting resolution of the display system. Normally the procedure requires that the observer making the resolution determination is sufficiently close to the display that he is not vision limited. Thus, the resolution measure is strictly a characteristic of the display

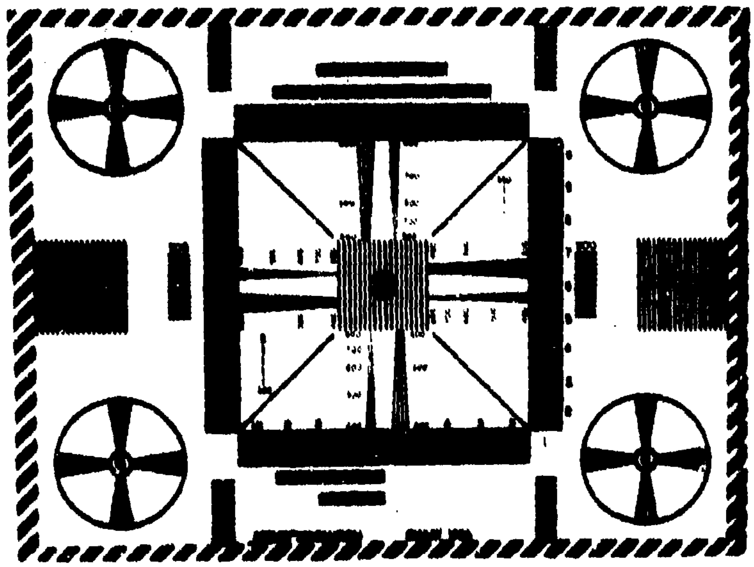

Fig. 2.1. EIA resolution chart

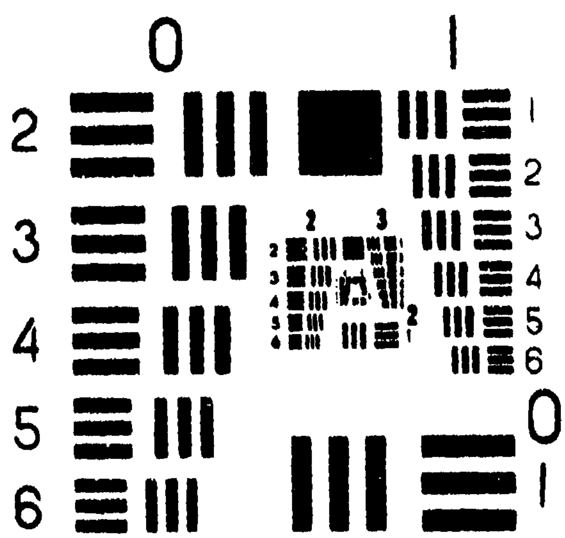

Fig. 2.2. U.S. Air Force 1951 tri-bar resolution target

system. However, if the observer is required to view the display from the same distance at which the display will be used operationally, then the resolution measure is determined by a combination of the display system capability and the observer's visual system. This second method is seldom used but it should provide a more reasonable resolution value since it is a result of the complete display/observer system.

The Air Force tri-bar target pattern is divided into seven groups of six elements. Each spatial frequency is represented by a three-bar pattern oriented vertically and a three-bar pattern oriented horizontally. The resolution of the imaging system is determined by the smallest tri-bar pattern that can be resolved into its three bars. This limiting resolution is then specified in terms of the group and element of the "just resolvable" tri-bar.

Both of these methods of determining limiting resolution require a subjective assessment from the observer as to whether or not a pattern is "resolved." This is not always an easy judgment and can lead to considerable variability in resolution measurements due to individual differences between observers. There is an alternative approach (Snyder, 1974a). Limiting resolution can be determined by making use of the MTF of the system in conjunction with measurements of the human visual contrast threshold curve (Campbell and Robson, 1968; Depalma and Lowry, 1962).

The MTF of the display system indicates the system's capability to transfer contrast from the input scene to the output image as a function of spatial frequency. As such, the MTF itself does not define a contrast level at the output of the display unless an input contrast has been specified. For all of the FOM's that use the MTF in conjunction with the visual threshold function, there is an implied assumption that the input contrast is 100 percent across all spatial frequencies. With this assumption, the MTF curve describes the actual expected output contrast as a function of spatial frequency. This is a subtle point but it should be noted.

Figure 2.3 shows how the display system MTF and the visual threshold function are used to determine the limiting resolution of the display system. The intersection of the display system MTF with the visual contrast threshold curve represents the highest sine-wave spatial frequency that can be produced by the display system and that can be seen by the observer. The advantage of this approach is the reduction of variability in determining the limiting resolution.

All of these resolution measures provide information about the high frequency portion of the display MTF but not about the display capability at lower spatial frequencies. One method of providing more information about the lower spatial frequency performance is to measure the suprathreshold resolution (Task, Pinkus, and Hornseth, 1978) described below.

In 1968 Campbell and Robson published the two curves shown in Fig. 2.4. The right-hand curve is the often measured contrast threshold curve for the human visual system. This curve indicates the amount of

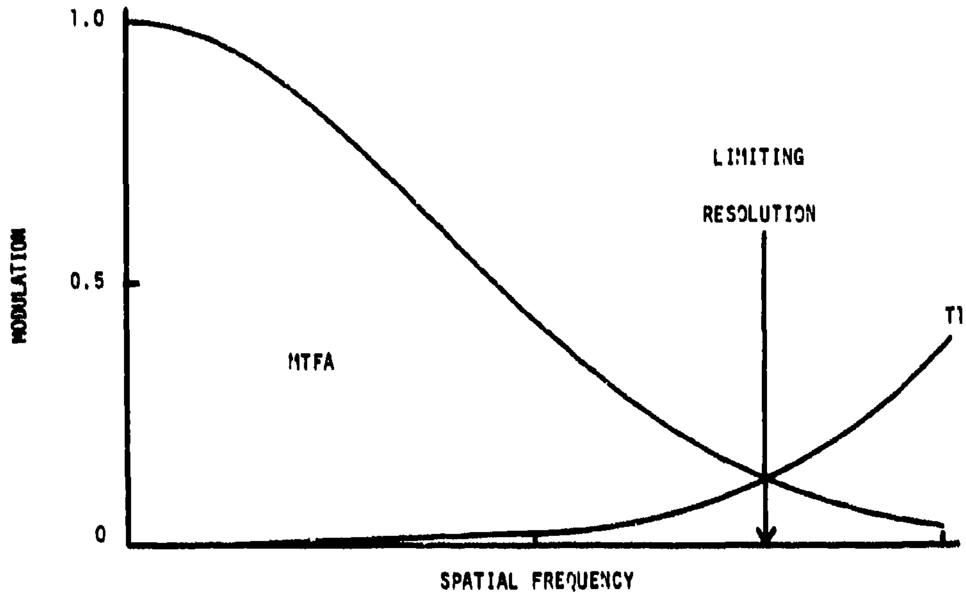

Fig. 2.3. Limiting resolution determined by the intersection of the display system MTF and the visual contrast threshold functions

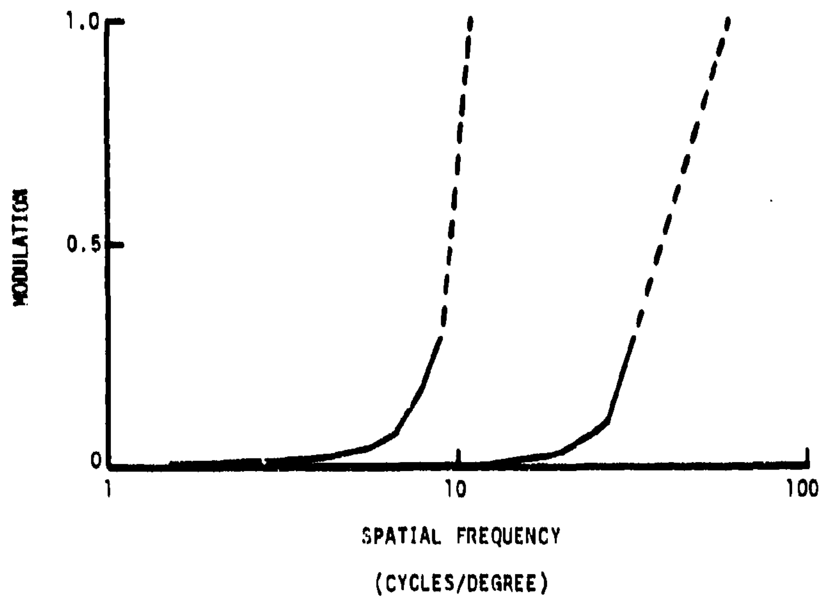

Fig. 2.4. Campbell and Robson (1968) study results showing the sine-wave threshold function (right) and the sine-wave square-wave discrimination curve (left)

The dashed line is an extrapolation.

contrast required for a sine-wave pattern to be just detectable 50 percent of the time as a function of angular spatial frequency. The left-hand curve of Fig. 2.4 indicates the amount of contrast required to determine whether the target pattern being viewed is a sine-wave or a square-wave target as a function of spatial frequency. The intersection of this sine-wave/square-wave discrimination curve with the MTF of the display system is defined as the suprathreshold resolution of the system.

All of the measures described so far provide information about only a single spatial frequency. A concept that was proposed to incorporate aspects of the MTF value for all spatial frequencies is the equivalent bandpass, N_e (Schade, 1953). The equivalent bandpass is calculated using equation 3.

$$N_e = \int_0^\infty \left\{ M(N_h) \right\}^2 dN_h \tag{3}$$

where

$M(N_h)$ = MTF of the display system

N_h = spatial frequency in units of TV lines per picture height

This measure depends only on the display system characteristics and is independent of the visual system capabilities.

Borough, Fallis, Warnock and Britt (1967) proposed an FOM for film systems designated the MTFA. Snyder (1974a) applied this measure to television systems as a potentially useful means of indicating video display image quality. The MTFA is calculated by computing the area between the MTF of the display system and the contrast threshold function of the observer. This is shown in graphic form in Fig. 2.3. In equation form the MTFA is:

$$\mathrm{MTFA} = \int_0^{\omega_\ell} \left\{M(\omega) - T(\omega)\right\} d\omega \qquad (4)$$

where

$M(\omega)$ = angular MTF of the display system

$T(\omega)$ = visual contrast threshold function

ω = angular spatial frequency (cycles/degree)

ω_ℓ = angular spatial frequency at which $M(\omega)$ intersects $T(\omega)$ (which is also the limiting resolution of the display/observer system)

Because of the difficulty of producing high quality sine-wave patterns for measuring the MTF of the display system, Snyder proposed a variation of the MTFA concept using square-wave (bar) patterns. The resulting area measure was designated MTFA_{sq} to indicate that the area measured was between the square-wave response of the television system and the square-wave contrast threshold of the observer. Using the MTFA_{sq} Snyder (1974b) was able to obtain very good correlations with reaction time and correct responses for a face recognition task. Display quality was varied by changing the video bandwidth, line rate, and noise level. Changing the line rate and bandwidth affected the vertical and horizontal resolution of the display, respectively, and the noise affected the contrast threshold curve of the observer. A total of 15 display conditions composed of different combinations of line rate, bandwidth and noise were used in the study. The results showed good correlations with $\log_{10}$ $MTFA_{sq}$. Correlation with correct response was $r = 0.87$ ($p < 0.001$) and with response time was $r = 0.92$ ($p < 0.001$). Correlations were calculated using the method described in Mathematical Statistics by Freund (1962).

One criticism of the MTFA and $MTFA_{sq}$ (and similar FOM's) is that they are based on a one-dimensional MTF (measured along the scan lines) whereas the display system provides visual information in two dimensions. For television displays the problem is compounded somewhat by the fact that the display is continuous in one dimension and discretely sampled in the other.

In a later study, Snyder (1976) attempted to measure directly the MTF of the display in the direction perpendicular to the scan lines. This measured MTF was then combined in various ways with the MTF in the perpendicular direction (along the scan lines) to obtain a two-dimensional MTFA. These combinations included the arithmetic mean, geometric mean, harmonic mean, and the quadratic mean. The resulting two-dimensional MTFA values were applied to a target acquisition task with some degree of success.

The correlations calculated for this experiment were lower than in previous experiments, but the interesting point is that most of the two-dimensional MTFA values correlated higher than the one-dimensional

MTFA values. However, many of the differences in correlation were not statistically significant. Correlations with simulated slant range (see Appendix A) to target at detection and the number of correct responses ranged from 0.16 to 0.70. Probably part of the reason for the lower correlations is that subjects were required to search the display to acquire the target. This adds to the variance due to differences in search strategies between subjects and, consequently, tends to lower the correlation.

The MTFA concept has a certain amount of appeal since it includes both characteristics of the display system and of the observer. However, some criticism has been raised as to the way in which the display characteristics and the observer characteristics should be combined. van Meeteren (1973) suggested that the MTF of the display system should be multiplied by the contrast sensitivity function (CSF) of the visual system. Since the CSF is the reciprocal of the visual contrast threshold curve previously discussed, this is equivalent to dividing the MTF by the contrast threshold function. The resulting quantity has been designated the integrated contrast sensitivity (ICS):

$$\text{ICS} = \int_0^\infty M(\omega) \cdot S(\omega)\, d\omega = \int_0^\infty \frac{M(\omega)}{T(\omega)}\, d\omega \qquad (5)$$

where

ICS = integrated contrast sensitivity

$M(\omega)$ = display system MTF

$S(\omega)$ = contrast sensitivity function

$T(\omega)$ = contrast threshold function

ω = spatial frequency (angular units)

Granger and Cupery (1972) have proposed a modified version of the MTFA concept called the subjective quality factor (SQF). Although their experiments were done using film, the SQF can easily be applied to television systems. In equation form:

$$SQF = K \int_{\ln a}^{\infty} \int_{0}^{2\pi} |M(\ln \omega, \theta)| \cdot |M_V(\ln \omega)| d\theta \; d(\ln \omega) \qquad (6)$$

where

K = normalizing factor

a = low spatial frequency integration limit

$M(\ln \omega, \theta)$ = two-dimensional optical transfer function of the display system in polar coordinates

M_V = MTF of the visual system

ω = angular spatial frequency

θ = orientation angle of the spatial frequency

Granger (1974) observed that most of the visual response occurs between 3 and 12 cycles per degree (cpd), so he suggested a simplified SQF that uses a rectangular frequency bandpass from 3 cpd to 12 cpd to approximate the visual passband, ($M_V(\ln \omega)$). The resulting equation for SQF is

$$SQF = K \int_{\ln 3}^{\ln 12} \int_{0}^{2\pi} |M(\ln \omega, \theta)| d\theta \, d(\ln) \quad (7)$$

Experiments done by Granger and Cuprey (1972) and Granger (1974) showed excellent correlation between the computed SQF and the rank order of subjectively ranked black and white photographs (correlation $r = 0.990$).

The area-type FOM provides a conceptually simple method of determining the quality of a display system. However, for the area-type FOM approach to be successful, the area enclosed must be isotropic with respect to visual effect. That is, each unit of area must contribute as much to overall visual performance as every other identically sized unit of area. If this is not the case, then it would be possible to devise display conditions that have the same MTFA but permit markedly different observer performance. It is therefore desirable to transform the two axes of the area-type FOM so that they are linear with respect to visual effect.

Task and Verona (1976) attempted to produce an isotropic area-type FOM by transforming the modulation contrast axis into the number of $\sqrt{2}$ gray shades. The resulting gray shade versus spatial frequency graph was then used to calculate the area between the visual threshold curve (converted to gray shades) and the gray-shade response of the display system. This FOM was designated the gray shade frequency product (GFP). Figure 2.5 shows the method used to convert modulation contrast to gray shades. The effect of this conversion is to weight the upper contrast levels more heavily, as can be seen by the graph in Fig. 2.6.

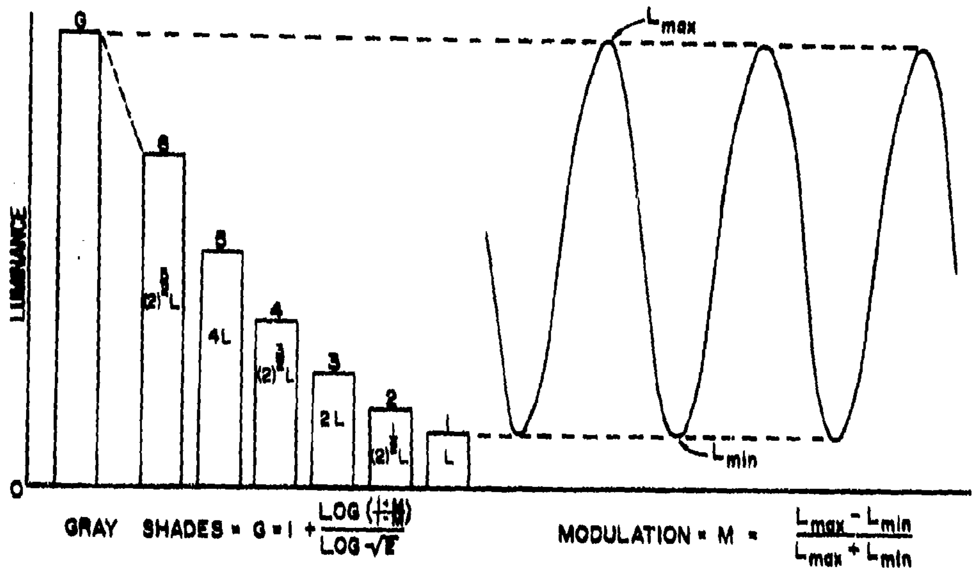

Fig. 2.5. Conversion of modulation contrast to number of $\sqrt{2}$ gray shades

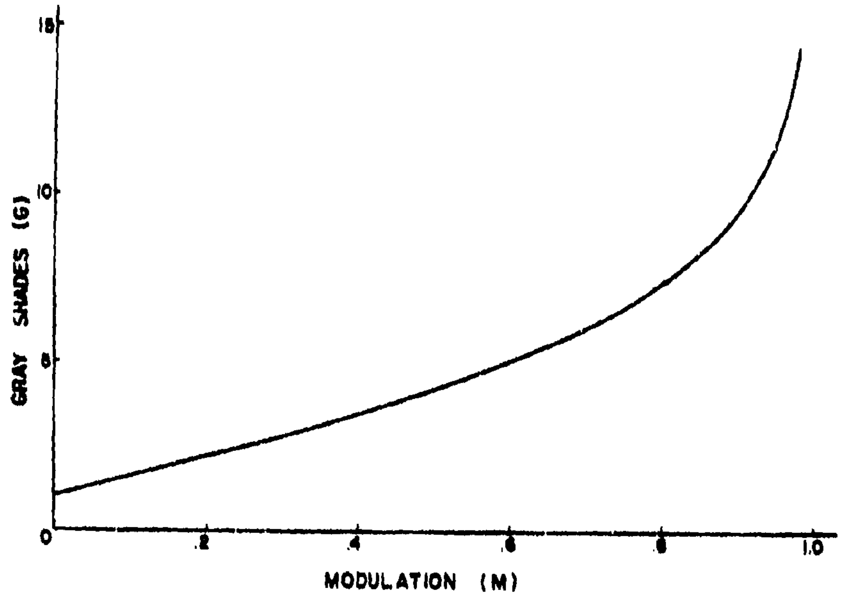

Fig. 2.6. Number of gray shades versus modulation contrast

This type of weighting is reasonable if the visual system responds logarithmically to luminance levels, which has been shown to be the case for moderate luminance levels and just-noticeable difference (JND) studies (Graham, 1965, p. 215). However, more recent experiments (Carlson and Cohen, 1978) have shown that the visual system seems to respond logarithmically to levels of modulation contrast of sine-wave gratings. This type of transformation would tend to weight the lower contrast levels more heavily than the upper contrast levels.

The work done by Carlson and Cohen (1978) was directed toward developing a means of predicting JND's in display imaging quality. To this end they developed detectable difference diagrams (DDD) to aid in determining how much of an MTF change can be tolerated in a display system before the change is noticed. Figure 2.7 shows the DDD they published in the SID (Society for Information Display) 78 Digest. One concept that is explored later in this paper is the application of the DDD to transform the area-type FOM to a quantity that may be linearly related to vision. This FOM is designated the just-noticeable difference area (JNDA). It is calculated by transforming the display system MTF curves to JND levels using the DDD of Carlson and Cohen, then intdgrating to find the area under the resulting curve. The lower limit of integration is at one-half cycle per degree since this is the lowest frequency shown on the DDD.

In the course of the literature review other FOM's for displays were found but could not be considered for evaluation and comparison due to problems of implementing the measures.

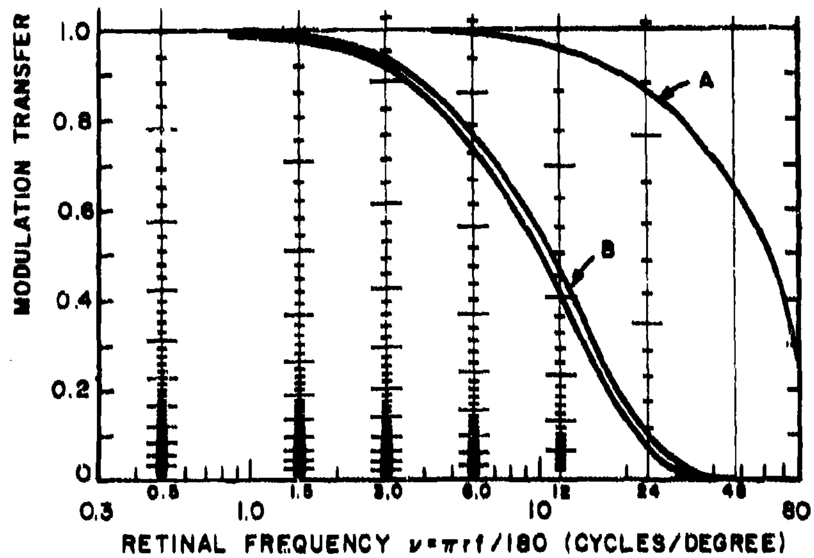

Fig. 2.7. Detectable difference diagram of Carlson and Cohen (1978)

The DDD was presented by Carlson and Cohen (1978) as a means of determining how much the MTF of two displays must differ before an observer can detect the difference. This DDD shows the MTF's of three different displays on it. The two MTF's indicated by the label B are just noticeably different because they differ by more than one just-noticeable difference (JND) level at some spatial frequency (in this case, at 12 cycles/degree). The MTF labelled A corresponds to a natural maximum MTF, i.e., distinguished as noticeably better because there are no higher JND levels to encompass. This corresponds to the limit of visual capability.

Rosell and Willson (1971, 1972, 1974) and Willson, Rosell, and Walmsley (1976) have developed and investigated the signal-to-noise ratio at the display (SNR_D). Equations describing the SNR_D for rectangular targets and periodic targets have been produced and applied to observer tasks involving the detection of rectangles or tri-bar patterns. Results from these studies have been successful within the limits of the assumptions made in deriving the SNR_D equations. Since these efforts were primarily directed toward characterizing the sensor and of the display system, the display itself was neglected. The SNR_D equations assume the display MTF to be unity. This was not the case for the studies undertaken for this dissertation, so it was not possible to apply the SNR_D concept without violating the assumption under which it was derived. The SNR_D was intended primarily to characterize effects due to noise. Since this paper is concerned with only low-noise systems and noise was not a variable in the experiments, it is not appropriate to try to force the SNR_D into the role of a display system FOM.

Schindler (1976) has proposed that information density (bits per square degree), measured in a unique fashion, be used as a display system FOM. Using information theory, Schindler derived an equation for information density:

$$D = \int_0^{F_o} 4 \log_2 \left[\left(\frac{P_s(f)}{P_{\Delta s}(f)} \right)^{1/2} + 1 \right] f \, df \qquad (8)$$

where

F_o = spatial frequency of maximum useful information

f = spatial frequency variable (linear spatial frequency)

$P_s(f)$ = signal power at frequency f

$P_{\Delta s}(f)$ = power of the just discriminable signal difference at frequency f

Using a modified version of this equation, Schindler measured the "information spectrum" obtained from a film transparency by employing optical Fourier transform techniques and a special segmented detector. The detector was located at the Fraunhofer diffraction plane of the optical Fourier transform system. It contained 32, semicircular, concentric segments which were used to measure the power as a function of spatial frequency in the transform plane. The integral of this information spectrum (bits per cycle squared) was calculated to obtain the overall information density.

A major problem with applying this technique to television displays is that a photographic transparency of the display must be obtained first before the optically measured information density can be calculated. This intermediate step requires time for developing the film and contributes to the possibility of error. There is also some problem in quantifying the relationship between exposure time and dynamic noise on the display and its effect on the optically determined information density. Also, the film MTF is implicitly assumed to be unity for the spatial frequencies of interest.

In spite of these concerns, Schindler obtained good correlations between the information density metric and performance variables for several target recognition studies ($r = -0.67$; $r = -0.82$; $r = -0.96$).

Since the equipment was not available to measure the information density in the same manner as Schindler, this FOM is not considered in later sections of this paper. However, it is possible to use the information density approach of Schindler (1976) and the DDD's of Carlson and Cohen (1978) to calculate a FOM that can be considered to be the information density capability of the display/observer system. From Schindler (1976) the information density is defined to be:

$$D = 4 \int_0^{F_x} \int_0^{F_y} \log_2 \{L\ (f_x,\ f_y)\}\ df_x\ df_y \qquad (9)$$

where

D = information density in bits per unit area

f_x = linear spatial frequency in x direction

f_y = linear spatial frequency in y direction

$L(f_x,\ f_y)$ = number of discriminable levels

F_x = upper frequency limit for x-axis

F_y = upper frequency limit for y-axis

If it is assumed that the JND levels of Carlson and Cohen can be used to replace $L(f_x,f_y)$ in equation 9, the information density could then be calculated using equation 10:

$$D = 4 \int_0^{F_x} \int_0^{F_y} \log_2 \{JND\ (f_x,\ f_y\}\ df_x\ df_y$$

A modified version of this equation is used in later sections of this dissertation to calculate an FOM value which is proportional to the information density.

Another variation of the area-type FOM is the JNDA-log. This FOM is calculated by determining the area under the JND vs. log spatial frequency curve. Two lower limits of intergration for the log spatial frequency were tried: one-half cycle per degree and two cycles per degree. These are distinguished by a notation following the abbreviations, 1/2 cpd and 2 cpd, respectively.

Table 2 shows a summary of the FOM's that are investigated in this dissertation. The GFP-log (Task and Verona, 1976) shown in Table 2 was calculated by integrating the gray-shade response curve with respect to log spacial frequency. The log after the abbreviation indicates this type of integration. Unfortunately, integrating with respect to log spatial frequency requires a choice of some arbitrary low spatial frequency limit of integration. For the GFP-log values calculated in this dissertation the lower frequency cutoff was chosen to be one cycle per degree.

Two other FOM's were investigated that are not listed in Table 2. These represent minor modifications of the FOM's listed and are explained in the appropriate sections of this dissertation.

Table 2. List of FOM's investigated and their abbreviations

Limiting Resolution	Lim. Res.
Log Limiting Resolution	Log Lim. Res.
Suprathreshold Resolution	S.T. Res.
Log Suprathreshold Resolution	Log S.T. Res.
Modulation Transfer Function Area	MTFA
Log Modulation Transfer Function Area	Log MTFA
Equivalent Bandpass	N_e
Gray Shade Frequency Product	GFP
Gray Shade Frequency Product-Log	GFP-Log
Subjective Quality Factor	SQF
Integrated Contrast Sensitivity	ICS
Just-Noticeable Difference Area	JNDA
Log Just-Noticeable Difference Area	Log JNDA
Information Density	Info. Dens.
Log Information Density	Log Info. Dens.
Just-Noticeable Difference Area-Log (1/2 cpd)	JNDA-Log (1/2 cpd)
Just-Noticeable Difference Area-Log (2 cpd)	JNDS-Log (2 cpd)

CHAPTER 3

EVALUATION OF DISPLAY SYSTEM FIGURES OF MERIT

There have been countless studies in the past to determine the effect of several parameters on vision and visual perception. Likewise many studies have been done to assess the effect of various display parameters on visual performance. In order to be useful an FOM must be sensitive to both characteristics of vision and characteristics of the display system. All of the FOM's under consideration in this paper, with the exception of one, are affected by both display and vision characteristics. The exception is the equivalent bandpass, N_e (Schade, 1953).

On close inspection it can be seen that all of the FOM's under consideration fall into two basic categories. Limiting resolution and suprathreshold resolution are single-number quantities (angular spatial frequencies) which characterize the display/observer system for a single spatial frequency. The remaining FOM's are area-type measures. That is, each one depends on the MTF of the display system (or some transformation of the MTF) and the human visual contrast threshold function. The different variations of the area measures are essentially attempts to transform the axes into dimensions that are properly weighted in terms of visual information content.

The remainder of this chapter contains a discussion of each of the FOM's and an evaluation of the relationship of each FOM with known characteristics of vision and displays.

Equivalent Bandpass

This measure does not include any characteristics of the visual system. Therefore, there are several parameters that can be changed in the display/observer system that would affect visual performance but would not affect N_e. For example, performance is affected by the angular size of the display with respect to the observer (Martin, Task, Woodruff, and Pinkus, 1976) but this parameter does not affect the value of N_e. For this reason it is not expected that N_e will perform well as a display system FOM.

Limiting Resolution

This FOM incorporates characteristics of both the visual system and the display system as indicated in Fig. 2.3. A loss of bandwidth or a loss of contrast will cause the contrast threshold function to intersect the MTF of the display system at a lower spatial frequency. Any parameter which affects vision will cause a change to the contrast threshold function, resulting in a different spatial frequency for the limiting resolution. Parameters such as luminance level and noise level are thus indirectly incorporated into the limiting resolution concept by their effect on the contrast threshold function. These effects probably account for the limited success and wide use of this FOM as a means of characterizing display quality. One problem with this FOM is due to the ways in which it can be obtained. The limiting resolution value obtained for a display system depends upon the way it is determined and upon the observer making the determination.

A major problem with this FOM stems from the fact that it is a "limit-type" measure. That is, it provides information concerning only a single spatial frequency and this spatial frequency is, by definition, at the limit of vision. Figure 3.1 shows the MTF of two display systems which have identical limiting resolution values, but much different contrast capabilities at the lower spatial frequencies. The display with the upper MTF will appear to have a better image quality due to the increased contrast, and if the contrast difference is great enough, it will also permit better visual performance. It is this type of problem that motivated the creation of the suprathreshold resolution FOM discussed in the next section.

Suprathreshold Resolution

The suprathreshold resolution is a single frequency type FOM, but it provides information about the display/observer system in the middle range of spatial frequencies rather than in the high range. This partially alleviates the problem depicted in Fig. 3.1 concerning the limiting resolution. Figure 3.2 shows two display systems with identical suprathreshold resolutions but with different MTF's. Note that the display system with the higher contrast must have a lower bandwidth (equivalent to a lower limiting resolution) in order to maintain

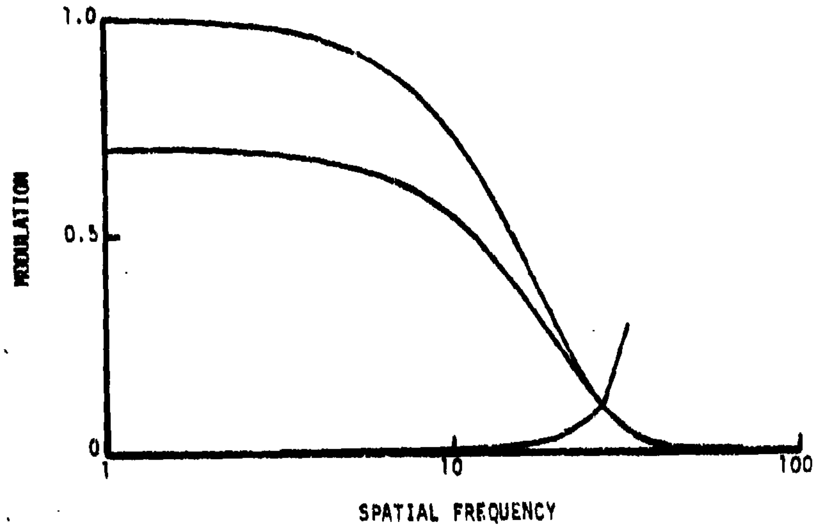

Fig. 3.1. Limiting resolution of two hypothetical displays with different MTF's but identical limiting resolutions

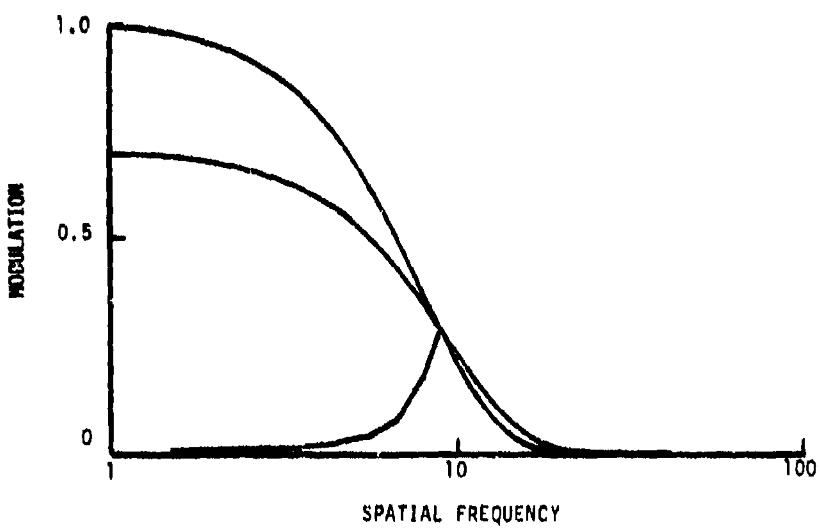

Fig. 3.2. Suprathreshold resolution of two hypothetical displays with different MTF's but identical suprathreshold resolution values.

Note that the suprathreshold resolution acts as a pivot point in the trade-off between bandwidth and contrast.

the same suprathreshold resolution. Thus, the suprathreshold resolution acts as a fulcrum point in the trade-off between contrast and bandwidth. If the way in which suprathreshold resolution was defined is appropriate, then it should accurately describe the results for studies where contrast and bandwidth are both varied.

For the examples shown in Fig. 3.1 and Fig. 3.2 a Gaussian-shaped MTF was assumed. If the shape of the MTF is allowed to deviate drastically from Gaussian, then it is possible to invent hypothetical situations for the suprathreshold resolution such that the suprathreshold resolution point would not act as a proper fulcrum for trading off bandwidth and contrast. However, barring strangely shaped MTF's, the suprathreshold resolution appears to have the characteristics for a potentially useful FOM.

Modulation Transfer Function Area

The MTFA is the basis for a number of area-type FOM's that are discussed in the following sections. The major (potential) advantage of this and the following FOM's is that they incorporate the MTF of the display system and the contrast threshold function (CTF) of the observer across all spatial frequencies. However, in order to be effective, the area-type FOM must combine the display MTF and the observer CTF in the correct manner and with the correct axes transformations to produce a quantity that will linearly correlate with performance.

The MTFA is calculated using modulation contrast on one axis and linear spatial frequency on the other. Both of these quantities are probably nonlinear with respect to vision. Typically, quantities such as modulation contrast and spatial frequency follow what is called a Weber Law (Cornsweet, 1970, pp. 83, 84). The Weber Law states that a test stimulus must change by a certain percentage of the reference stimulus in order for the subject to distinguish between the test stimulus and the reference stimulus. Studies have shown that this law holds for simple luminance targets (Cornsweet and Pinsker, 1965) and for spatial frequency discrimination ability (Campbell, Nachmias, and Jukes, 1970). Evidence from Carlson and Cohen (1978) indicates that this is also true for the contrast of sine-wave targets. In light of this information, one would not expect the MTFA to be linear with respect to visual stimulation and, therefore, to visual performance. By taking the logarithm of the MTFA, it may be possible to partially compensate for the fact that the MTFA axes do not reflect the Weber Law. Therefore, it is probable that the MTFA will not correlate as well with visual performance as the log MTFA. This was the result demonstrated by Snyder (1974a).

Gray Shade Frequency Product

This measure was proposed in an attempt to linearize the modulation contrast axis of the MTFA FOM. If the human visual system reacts logarithmically to luminance levels (Cornsweet and Pinsker, 1965), then it is possible to determine the number of detectable luminance levels that are represented by a particular modulation contrast. Using this type of transformation (described in Chapter 2), it is possible to covert modulation contrast into gray shades. The conversion uses $\sqrt{2}$ as a criterion for defining a gray shade. This is an "engineering" definition of gray shade and does not represent a true JND of luminance. However, the resulting transformation is proportional to what would be obtained if a different JND level were chosen.

This transformation should improve correlations with performance (over MTFA) only if the luminance level capability of the display is the characteristic important to vision. The effect of this transformation is to weight the higher contrast levels more heavily than lower contrast levels, as can be seen by the graph in Fig. 2.6. However, if <u>contrast</u> is the important parameter with respect to vision (which seems more likely), then the Weber Law indicates that the transformation should be the logorithm of <u>contrast</u>. This type of transformation weights the lower contrast levels more heavily than the higher contrast levels.

Since it is necessary to linearize both axes with respect to vision, the GFP-log is an attempt to linearize both the contrast axis and the spatial frequency axis. The problem with converting the spatial frequency axis (or the contrast axis) to a logorithm before integrating the area is that the lower limits of integration are no longer easily defined. Therefore, some arbitrary low spatial frequency cutoff must be used. Since this low frequency cutoff can have a large effect on the FOM value, it is difficult to determine *a priori* what is optimum. For the GFP-log the value was chosen to be one cycle per degree as a convenient, relatively low, cutoff value.

Subjective Quality Factor

The SQF does not incorporate any transformation on the contrast axis. It does transform the spatial frequency axis to natural logarithm and limits the integration to the central area of the visual contrast sensitivity function. The limits of integration are from ln 3 to ln 12 where the 3 and 12 are in units of cycles per degree. The logarithm transformation makes sense from the standpoint of the Weber Law and the limits of integration are a rough acknowledgment of the contrast threshold function. It should be noted that it might be possible to improve the log MTFA FOM (or others) by selecting an appropriate spatial frequency bandpass as was done for the SQF.

Integrated Contrast Sensitivity

The SQF is a special case (and approximation) of the ICS. The main difference between the ICS and the MTFA is their relative sensitivity to changes in the CTF. van Meeteren (1973) argued that the MTFA value would change negligibly if the CTF were raised (due to noise or some similar factor) from 0.01 to 0.10. However, the ICS would change considerably since the CTF is divided into the display MTF instead of being subtracted. It remains to be seen whether or not this difference in sensitivity to changes in the CTF improves correlation with performance.

Just-Noticeable Difference Area

This FOM is proposed in this dissertation as a possible means of linearizing the contrast axis of the MTFA FOM. The basis for the JNDA is the work done by Carlson and Cohen (1978) on detectable difference diagrams (DDD's). Figure 2.7 in Chapter 2 showed an example of a DDD. The JNDA is defined as the area under the MTF after it has been transformed into JND levels using the DDD. If vision responds primarily to contrast levels, then this transformation is more appropriate than the GFP. Note that the effect of the JND transformation is to weight the lower contrast levels more heavily than the higher contrast levels. Figure 3.3 shows the JND data of the DDD of Fig. 2.7 regraphed as a function of modulation contrast.

Just-Noticeable Difference Area-Log

This FOM is proposed in an effort to transform both axes of the area-type FOM to quantities that are theoretically linear with respect to vision based on fundamental vision studies. The JNDA-log is the same as the JNDA except the integration of the area is with respect to the log of the spatial frequency as indicated by the Weber Law. The lower limit of integration is arbitrarily set at log 1/2 cpd as the lowest frequency measured by Carlson and Cohen (1978) and shown in the DDD of Fig. 2.7.

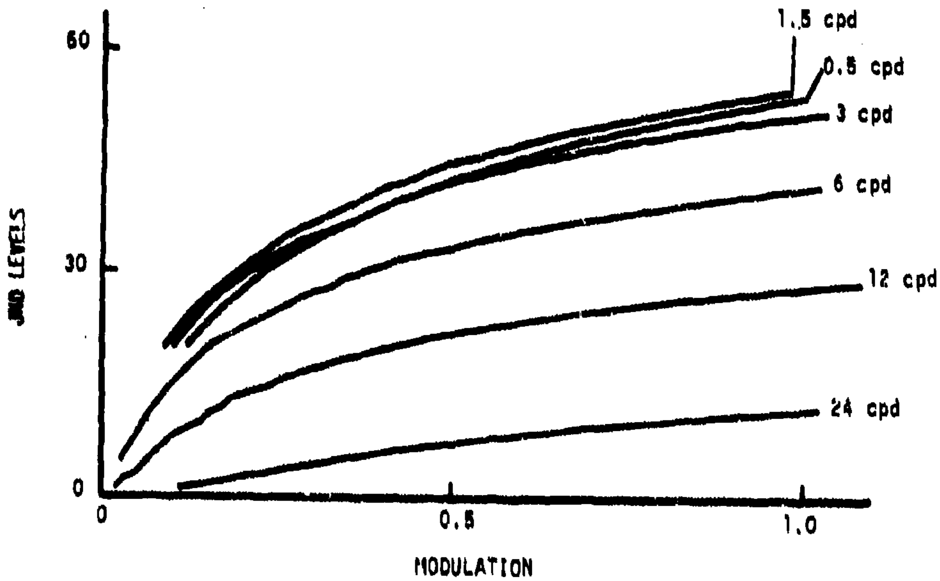

Fig. 3.3. Just-noticeable difference levels as a function of modulation contrast for several spatial frequencies

(From Carlson and Cohen, 1978)

Information Density

Information theory provides a theoretical structure for such technical areas as computers and data transmission. Many studies have investigated human decision processes and thought processes in terms of information theory (Fitts, 1954; Sperling, 1960). However, all of these have been extremely simple when compared to the problem of quantitatively determining the useful or required information content of a pictorial image. The information density approach suggested by Schindler (1976), described in Chapter 2, does not consider the characteristics of the human visual system. It is a measure only of the display system. As such it roughly corresponds to the capability of a display system to present detail. It is possible to increase the information density (amount of detail) to a point where an observer can no longer resolve the detail due to vision limitations. Thus, a point is reached at which performance can no longer improve due to vision limits, but the information density metric can increase further as detail is increased. This is not a desirable characteristic of an FOM.

The modified version of information density presented in Chapter 2 does not have this shortcoming. The JND levels approach zero as the angular spatial frequency reaches vision limits. Therefore, the modified information density shows promise in terms of a maximum upper limit that corresponds to the vision limit. However, there is no fundamental reason why one would expect the information density transformation of the modulation contrast axis to correlate well with performance.

It is very difficult to predict which of the FOM's discussed herein is best in terms of correlating with performance. The literature search did not provide any studies that had been done which compared more than two or three FOM's. Almost all studies were concerned with determining the effect of several display parameters on a single FOM and how the results correlated with performance. The following chapters will quantitatively compare all of the previously described FOM's in terms of their correlation with performance for the same experiments. This is the first known attempt to critically compare several FOM's for the identical experimental conditions.

CHAPTER 4

EXPERIMENTAL COMPARISON OF FOM'S FOR TARGET DETECTION AND TARGET RECOGNITION TASKS

The experiment described in this chapter was undertaken to provide a common basis of empirically comparing all of the previously described FOM's. Two experiments were conducted simultaneously: one a target recognition task and the other a target detection task. It was expected that the target recognition task would provide better correlations with the FOM's than the target detection task due to the increased variability of the target detection task.

Method

Subjects

Seventy-two subjects were used in the study (36 males) with ages ranging from 18 to 30 years. All subjects were prescreened for corrected or uncorrected 20/20 visual acuity, using the Armed Forces Vision Tester.

Apparatus

Two sets of equipment were used: one set to generate the appropriate display condition, and the other to adjust and measure the display characteristics (Task and Verona, 1976).

Figure 4.1 shows a picture of the apparatus used to generate the stimulus material. The primary source of imagery was recorded on black and white 16mm motion picture film and converted to video format using the apparatus of Fig. 4.1. The film was run at 24 frames per second. All experimental conditions were obtained using a standard 525 line, 60 Hz field rate display with 2:1 interlace of fields. The television monitor shown in the equipment rack of Fig. 4.1 was used by the experimenter to score the subject's responses. This monitor was not visible to the subject. The experimenter had control of an electronic cross hair which was displayed on this monitor. The cross hair was used to measure the diagonal of the target at recognition for the target recognition task, and the position of the target on the screen for the target detection task. The diagonal size of the target was converted to the angle subtended by the target at recognition for the recognition task. For the target detection task the position of the target on the display was converted to slant range at detection. The slant range to the target is defined as the direct distance from the sensor to the target. The term slant range is used to differentiate it from ground range, which is the distance from the target to a point on the ground directly below the sensor (aircraft). These calculations are described in Appendix A. The subtended angle of the target at recognition and the slant range to the target at detection served as the dependent variables for the target recognition task and the target detection task, respectively.

The display quality conditions for this study were obtained using all combinations of three levels of contrast ratio and three video

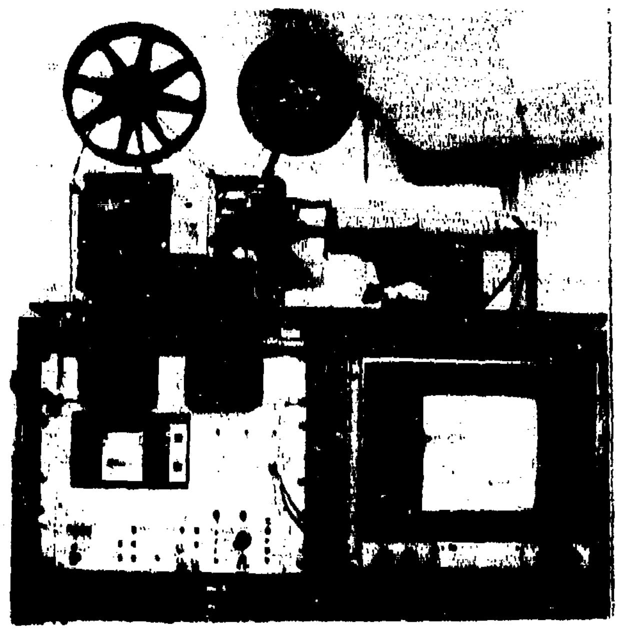

Fig. 4.1. Equipment used to generate the video stimulus material

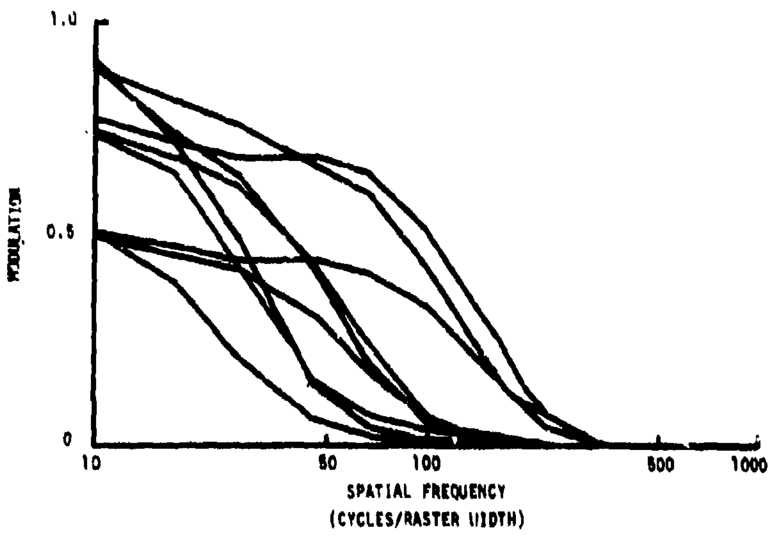

Fig. 4.2. The MTFs for the nine display system conditions

bandwidths for a total of nine conditions. The contrast ratio is defined as the ratio of the maximum display luminance to the minimum display luminance. The contrast ratio levels were obtained by adjusting the brightness and contrast controls of the subjects' monitor, and the bandwidths were obtained using a passive, low pass, variable filter. Figure 4.2 shows the resulting display system MTF's determined for these nine conditions.

The display system MTF's were calculated by multiplying together the measured MTF's of the film, the television camera, and the television monitor. It should be noted that the system MTF's calculated in this fashion represent an approximation to the actual system response. In a rigorous mathematical sense, the MTF is not defined for any of these three components (film, camera, and display) since each of these is nonlinear. However, the concept of a transfer function is sufficiently useful to warrant its use even when a system departs somewhat from linearity. This departure means that a sine-wave pattern output will not be obtained if a sine-wave pattern is provided as an input to a nonlinear system. If the nonlinearity is relatively small and well behaved (gradual curvature), the output still bears a reasonable resemblance to a sine-wave pattern. Thus the transfer function is not really an MTF but it serves the same function.

A problem can arise if one attempts to multiply a number of these "nonlinear MTF's" together without regard to the severity or direction of the nonlinearities. In the case of the TV camera and the monitor, the nonlinearity (or gamma) is in the opposite direction with respect to each other. In fact, the coupling of the camera and monitor almost perfectly compensates for the nonlinearity, resulting in an almost linear camera/display system. The film gamma was measured to be approximately one by the organization that processed and printed the film. Thus the display system was close to linear.

To insure that minimum error was introduced by multiplying the TV camera and monitor MTF's together, a short experiment was done. The camera/monitor system square-wave response was measured directly using a set of square-wave targets and a scanning photometer. This was converted to a sine-wave response, then compared to the MTF that was obtained by multiplying the camera MTF times the display MTF. The two curves were close, indicating that a relatively small error resulted from the MTF component multiplication method; thus justifying this approach for the system used. Figure 4.3 shows these two curves.

The film MTF was determined by making microdensitometer scans of high contrast edges and converting these data to an MTF using Fourier techniques. The actual microdensitometer scans and MTF calculations were done by the Dynamics and Environmental Evaluation Branch, Reconnaissance and Weapon Delivery Division of the Air Force Avionics Laboratory at Wright-Patterson Air Force Base, Ohio. The resulting MTF was sufficiently close to Gaussian in shape that a Gaussian approximation to the MTF was used for convenience of calculations. The technique used for calculating the MTF from an edge scan can be found in Gaskill (1978). The camera

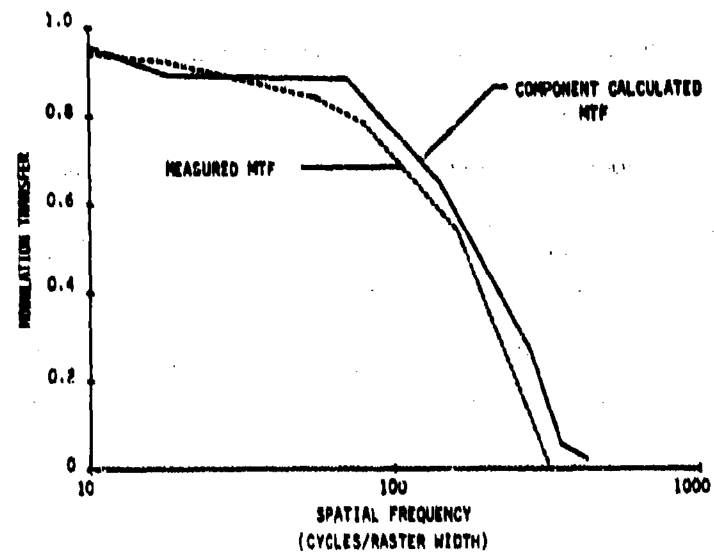

Fig. 4.3. Comparison between a system MTF calculated by multiplying the component MTF's together and a system MTF measured directly

The solid line was obtained by multiplying the directly measured television display MTF times the television camera MTF. The TV camera MTF was determined by directly measuring the square-wave amplitude response and converting it to a sine-wave response. The dotted line was obtained by measuring the total system square-wave response and then converting it to a sine-wave response.

MTF was measured by observing the electronic signal amplitude output, on an oscilloscope, as a function of the spatial frequency of square-wave targets imaged onto the photo surface. This square-wave response was then converted to a sine-wave response (Brown, Collins, and Hawkins, 1969). The television display was measured using a signal generator which produced a sine-wave electronic signal in video format. This signal was adjusted to have the same maximum and minimum signal levels as the television camera. The signal was input to the television monitor, and the resulting sine-wave pattern on the display was scanned using a telephotometer with a slit aperture as shown in Fig. 4.4. By repeating this procedure as a function of spatial frequency, the MTF of the television display was measured. The product of these was then calculated for each of the nine display conditions to determine the overall MTF of the display system for each condition.

The three levels of bandwidth used were 6 MHz, 1.0 MHz, and 0.4 MHz (measured at the 3 dB point) and the three contrast ratio levels were 50:1, 50:5 and 50:15. The contrast ratio numbers represent the maximum and minimum display luminance values (in foot-Lamberts) for a low spatial frequency (8 cycles/display width) square-wave pattern.

Appendix B provides a list of the equipment used, the model numbers and the manufacturers.

Stimulus Material

The 16mm motion picture film used for the target recognition task was produced in the following manner. Eight inch by ten inch black

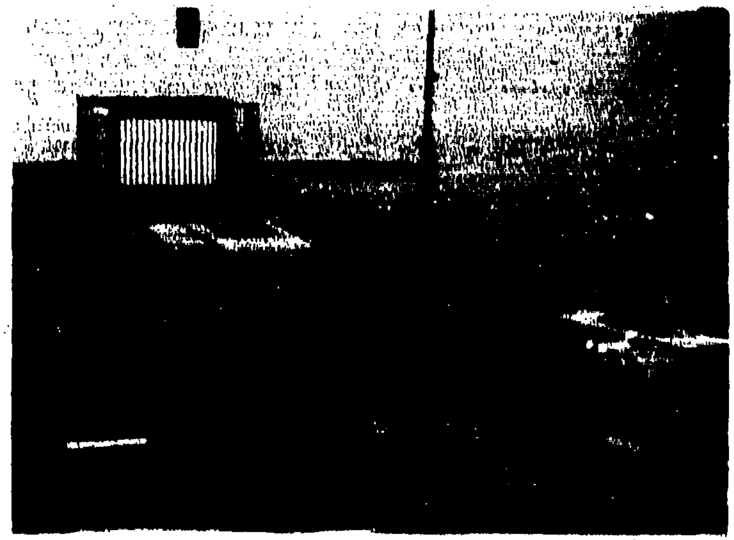

Fig. 4.3. Telephotometer with slit aperture to measure MTF of the television monitor

Fig. 4.4. The six vehicle targets used for the target recognition study

and white prints were made of six models of vehicle targets (see Fig. 4.5). Each of the targets was photographed in each of four orientations for a total of 24 target conditions. The targets were: covered truck, uncovered truck, M-60 tank, Sherman tank, mobile cannon and half-track. Each of the 8 × 10 prints was affixed to the center of a large gray backdrop. A 16mm motion picture camera with a motorized zoom lens was then used to make a "zoom-in" film of the target. The zoom sequence was about 20 seconds in duration for a 10 to 1 magnification change. This zoom sequence was done for each of the 24 target situations. When presented to the subject, the target first appeared in the center of the display for 2 to 3 seconds, then slowly increased in size until the subject could recognize which of the six targets it was.

For the target detection task the 16mm film imagery consisted of "flights" over a terrain board at simulated altitudes of 1000 and 2000 feet. The targets were prebriefed bridges and POL (petroleum, oil, and lubricant) storage tanks. Figure 4.6 shows a bridge target and Fig. 4.7 shows a POL target at relatively close range. A total of 40 "flights" over targets were presented to each subject.

Procedure

Each morning before subjects arrived and each afternoon after subjects were run, the MTF of the display monitor was measured and the signal levels from the television camera were recorded. This insured that the display quality remained constant for the duration of each experimental display condition.

Fig. 4.5. Bridge target used in target detection study

Fig. 4.6. POL (petroleum, oil, lubricant) target used in target detection study

Subjects were checked for 20/20 vision and given written instructions explaining their task. Any questions were then answered by the experimenter. Briefing materials included photographs of the targets and, for the target recognition task, the target models. Subjects were trained so that they could respond rapidly with the correct name of each of the six targets. All subjects completed the target recognition study first. They were then instructed about the target detection study and completed that second. A break period was provided between the two studies and at the midpoint of each study.

For the target recognition study, the target appeared in the center of the display and grew in size until the subject was "virtually certain" of the name of the target. At this point the subject pressed a handheld button. This action stopped the 16mm film projector and blanked the display to prevent the subject from further studying the target. The blanked screen was set to have approximately the same average luminance as the displayed imagery to prevent changes in eye luminance adaptation level. Immediately after the subject pressed the button he responded with the target name. The experimenter, observing his monitor, recorded the response and measured the diagonal of the target. This sequence was then repeated for the next target. The 24 targets were presented in a random order and were shown to each subject twice for a total of 48 target runs.

The procedure for the target detection task was slightly different. Subjects were told before each target run which target they were searching for: bridge or POL. The target was not initially visible on the display. As the "flight" progressed the target would appear on the display. The "flight" paths were arranged so that the target would appear on the center line of travel, off to the left or off to the right. When the subject detected the target he pressed the handheld button which immediately stopped the 16mm projector. The display was not blanked but remained on so that the subject could point to the location of the target. The experimenter then used the electronic cross hair to determine the x, y coordinates of the target on the screen. These data were then used to calculate the simulated slant range to the target at detection (see Appendix A).

The entire procedure for both studies, including rest breaks, required approximately three hours per subject.

Results

Table 3 summarizes the results of the target recognition study.

Table 3. Mean angle subtended by the target at recognition (in degrees) for the target recognition study

Contrast ratio	Bandwidth		
	6 MHz	1.0 MHz	0.4 MHz
50:1	1.5 deg	2.4 deg	3.4 deg
50:5	1.6 deg	1.9 deg	3.6 deg
50:15	1.9 deg	2.2 deg	3.9 deg

Each number listed in Table 3 represents the average of approximately 384 data points (eight subjects per condition times 48 target runs per subject). Some data points were missing due to subject errors in identifying the targets. These points were replaced with the average value for the display condition in which they occurred. Table 4 shows a summary of the analysis of variance done on the target recognition performance results. It is apparent from this table that bandwidth had a much greater effect on performance than contrast ratio. Table 5 shows the average percent correct responses for each of the nine display conditions. The percent correct response was approximately the same for all conditions with the exception of two of the lowest quality conditions: 50:5 and 50:15 at 0.4 MHz bandwidth. The instructions to the subject were intended to motivate the subject to recognize the target as soon as possible but with a minimum error. The subject was instructed to respond as soon as he was "virtually certain" of the correctness of his response. In previous studies (Martin et al., 1976) this provided a satisfactorily low error rate and reasonably uniform percent correct response rates across the experimental conditions. With the exceptions noted above, this technique appeared to work reasonably well for this target recognition study. The performance analysis is based on the angle subtended by the target at recognition as the performance variable of interest. Table 6 is a summary of the analysis of variance performed on the percent correct response data.

Table 4. Analysis of variance summary for the target recognition performance task*

Source	SS	DF	MS	F	p
Contrast ratio	1.1291	2	0.5645	3.1	0.05
Bandwidth	50.9949	2	25.4975	140.4	<0.001
A × B	1.2917	4	0.3229	1.8	0.14
Within cell	11.4362	63	0.1815		
Total (check)	64.8519	71	0.9134		

*A summary of the analysis of variance is provided for each performance task. The format for each of these is the same as that shown in Table 4. The SOURCE column of Table 4 indicates the item analyzed in each row. SS stands for sum of squares, DF for degrees of freedom, MS for mean square, F is the F-test number, and the p is the probability associated with accepting the null hypothesis (i.e., no difference in performance due to changes in the variable shown in the SOURCE column). A × B is the interaction of contrast ratio and bandwidth. The within cell SS value indicates the amount of unaccounted for variance. The total SS value was calculated independently of the other SS values as a check; the total value should be the same as the sum of the other SS values.

Table 5. Percent correct response for the nine display conditions of the target recognition task

Contrast ratio	Bandwidth		
	6 MHz	1.0 MHz	0.4 MHz
50:1	90.4	89.1	88.8
50:5	90.4	90.6	82.0
50:15	93.2	89.8	79.4

Table 6. Analysis of variance summary for the percent correct response data of the target recognition study

Source	SS	DF	MS	F	p
Contrast ratio	61.4444	2	30.7222	0.7745	0.465
Bandwidth	798.7778	2	399.3889	10.0686	<0.001
A × B	370.5556	4	92.6389	2.3354	0.065
Within cell	2499.0000	63	39.6667		
Total (check)	3729.7778	71	52.5321		

Table 7 shows the calculated values of the different FOM's for the nine display conditions. The values of the performance variable were correlated with the calculated values of each FOM for each condition. Table 8 shows the correlation between performance and the various FOM's. Appendix C contains the graphs of these correlations.

Table 7. Calculated FOM values for the nine display conditions

	Contrast Ratio 50:1			Contrast Ratio 50:5			Contrast Ratio 50:15			Theoretical Max.
Bandwidth (MHz)	6.0	1.0	0.4	6.0	1.0	0.4	6.0	1.0	0.4	-
N_e	53.1	25.9	19.6	55.7	22.1	14.0	23.7	10.2	5.4	-
Lim Res	14.8	8.25	8.25	15.56	9.00	9.73	15.46	10.80	6.42	61.0
Log Lim Res	1.17	0.92	0.92	1.19	0.95	0.99	1.19	1.03	0.81	1.78
FOM S.T. Res	7.90	5.63	4.25	8.40	5.78	5.09	7.80	5.73	3.56	11.25
Log S.T. Res	0.90	0.75	0.63	0.92	0.76	0.71	0.89	0.76	0.55	1.05
MTFA	4.44	2.11	1.47	4.95	2.07	1.39	3.22	1.48	0.73	40.76
Log MTFA	0.647	0.34	0.167	0.695	0.316	0.143	0.508	0.170	-0.137	1.610
GFP	31.2	15.6	11.8	32.9	13.6	9.3	19.4	9.0	4.7	-
GFP-Log	3.58	1.77	1.03	3.73	1.76	0.95	2.15	1.20	0.41	-
SQF	0.190	0.038	0.010	0.23	0.046	0.019	0.148	0.038	0.004	0.602
Bandwidth (MHz)	6.0	1.0	0.4	6.0	1.0	0.4	6.0	1.0	0.4	-
ICS	1491	743	524	1618	727	491	1049	521	263	4637
JNDA	334	179	115	365	190	141	310	172	56	868
Log JNDA	2.52	2.25	2.06	2.56	2.28	2.15	2.49	2.23	1.75	2.94
Info Dens	46.9	24.5	12.6	50.6	25.4	22.5	48.2	24.7	17.7	111.9
Log Info Dens	1.67	1.39	1.10	1.70	1.40	1.35	1.68	1.39	1.25	2.049

Table 7. Continued

	Contrast Ratio 50:1			Contrast Ratio 50:5			Contrast Ratio 50:15			Theoretical Max.
JNDA-Log 1/2 cpd	54.4	41.8	33.8	55.4	41.9	34.9	47.1	48.3	24.8	74.3
JNDA-Log 2 cpd	24.0	12.8	6.8	25.7	13.9	9.0	21.6	12.6	4.9	41.0
Log SSMTFA	0.58	0.30	0.16	0.61	0.29	0.11	0.39	0.12	-0.15	0.97
Log BLMTFA	0.35	-0.23	-0.78	0.42	-0.17	-0.66	0.20	-0.33	-1.28	0.86

Table 8. Correlations of performance with the FOM's for the target recognition study

FOM	Correlation	FOM	Correlation
N_e	-0.726	SQF	-0.781
Lim Res	-0.764	ICS	-0.818
Log Lim Res	-0.776	JNDA	-0.876
S.T. Res	-0.888	Log JNDA	-0.906
Log S.T. Res	-0.907	Info Dens	-0.795
MTFA	-0.811	Log Info Dens	-0.820
Log MTFA	-0.878	JNDA-Log (1/2 cpd)	-0.937
GFP	-0.781	JNDA-Log (2cpd)	-0.896
GFP-Log	-0.847		

After inspecting the graphs of the correlations and comparing the results with the MTF's of the nine display conditions, it became evident that higher correlations may be obtained by calculating the MTFA for a limited spatial frequency band. The arguments for doing this are similar to those that led to the band limit for the SQF FOM. Two variations of the MTFA were tried. One variation involved changing the upper spatial frequency limit of the MTFA to the sine-wave/square-wave discrimination curve instead of using the sine-wave threshold curve. This eliminates the area of the MTFA associated with the higher visual spatial frequencies. Since the sine-wave threshold used for the MTFA calculations represented a 50 percent detection probability, it can be argued that the

MTFA nearest this curve contributed relatively little to the visual information assimilated by the subject. The sine-wave/square-wave discrimination curve provides a convenient, more conservative upper limit on the spatial frequencies useful for the transfer of visual information.

The second variation included the above modification and also removed the very low spatial frequency portion of the MTFA. The SQF uses 3 cpd as the lower cutoff. Since the peak sensitivity of the visual system is somewhere between 3 cpd and 6 cpd, it was decided to lower the cutoff to 2 cpd to insure that those spatial frequencies associated with peak visual sensitivity were included.

The first variation is denoted the SSMTFA, indicating that it is calculated using the sine-wave/square-wave discrimination curve as an upper limit; and the second variation is denoted as the BLMTFA for band limited MTFA. Table 9 shows the correlations of the logarithms of these new FOM's with performance for the target recognition study.

Table 9. Correlation between the modified MTFA FOM's and target recognition performance

FOM	Correlation
Log SSMTFA	-0.869
Log BLMTFA	-0.948

The log BLMTFA produces an excellent correlation with performance. However, one must be careful when searching for quantities that correlate well with performance after the experiment is completed. Given enough degrees of freedom in creating an FOM, it is possible to achieve a perfect unity correlation with performance for a particular set of data. The real test of these modified MTFA FOM's is in the later sections of this dissertation where they are compared to performance data obtained independently from this target recognition study.

The target detection study performance analysis was limited to the slant range at which the POL targets were detected. The data for the bridge targets contained too many missed targets to use slant range as a performance variable. The POL target runs were divided into two groups: those at 1000 feet altitude and those at 2000 feet. This was necessary because of the large differences in slant range for these two conditions. Table 10 shows a summary of the slant range performance for the nine display conditions and two altitudes.

Tables 11 and 12 show the analysis of variance summary for the 1000 feet and 2000 feet altitude, respectively.

Table 10. Slant range (in feet) at detection for POL targets for the nine display conditions

Contrast Ratio	Bandwidth	1000 ft alt	2000 ft alt
	6 MHz	6998 ft	12,314 ft
50:1	1.0	6486	11,408
	0.4	5896	9986
	6	6968	12,130
50:5	1.0	6729	12,302
	0.4	6319	10,888
	6	6612	11,886
50:15	1.0	6585	11,680
	0.4	5908	10,299

Table 11. Analysis of variance summary for the target detection slant range data at 1000 feet altitude

Source	SS	DF	MS	F	p
Contrast ratio	1,162,468	2	581,234	4.5	.014
Bandwidth	8,399,907	2	4,199,954	32.7	<.001
A × B	742,405	4	185,601	1.4	.228
Within cell	8,086,816	63	128,362		
Total	18,391,596	71			

Table 12. Analysis of variance summary for the target detection slant range data at 2000 feet altitude

Source	SS	DF	MS	F	p
Contrast ratio	4,215,100	2	2,107,550	3.5	.035
Bandwidth	40,235,942	2	20,117,971	33.3	<.001
A × B	3,238,285	4	809,571	1.3	.264
Within cell	38,010,485	63	603,341		
Total	85,699,812	71			

Using the slant range as the performance variable, correlations were calculated for the 19 FOM's for both 1000 and 2000 feet. Table 13 shows these results. The correlation graphs are contained in Appendix C.

Note that the correlations in Table 6 are negative and the correlations of Table 13 are positive. This occurs because, for the target recognition study of Table 8, the smaller the target, the better the performance, whereas, for the target detection study, longer slant ranges represent better performance.

Discussion

Tables 8, 9, and 13 summarize the main results of these target recognition and target detection studies. All of the FOM's investigated correlated reasonably well with performance for all three task conditions. Correlations ranged from a high of $|r| = 0.948$ to a low of $|r| = 0.618$. Table 14 indicates the rank order of the performance correlation for each of the 19 FOM's for the three tasks. It should be noted that the three observer tasks are not independent in the sense that the nine display conditions for all three were identical. Even with this cautionary note, the consistency of the rank ordering of the FOM's across the three tasks is surprising.

Table 13. Correlations of FOM's with POL target detection performance

FOM	1000 ft alt	2000 ft alt
N_e	0.761	0.618
Lim Res	0.778	0.695
Log Lim Res	0.795	0.709
S.T. Res	0.900	0.834
Log S.T. Res	0.923	0.864
MTFA	0.829	0.717
Log MTFA	0.866	0.777
GFP	0.798	0.670
GFP-Log	0.869	0.760
SQF	0.803	0.702
ICS	0.837	0.724
JNDA	0.880	0.802
Log JNDA	0.902	0.838
Info Dens	0.824	0.766
Log Info Dens	0.880	0.842
JNDA-Log (1/2 cpd)	0.928	0.853
JNDA-Log (2 cpd)	0.902	0.835
Log SSMTFA	0.857	0.762
Log BLMTFA	0.931	0.878

Table 14. FOM's rank ordered according to their correlation with performance for the target recognition task and the two target detection conditions

FOM	Target Recognition	POL 1000 ft	POL 2000 ft
Log BLMTFA	1	1	1
JNDA-Log (1/2 cpd)	2	2	3
Log S.T. Res	3	3	2
Log JNDA	4	4	5
JNDA-Log (2 cpd)	5	5	6
S.T. Res	6	6	7
Log MTFA	7	10	9
JNDA	8	8	8
Log SSMTFA	9	11	11
GFP-Log	10	9	12
Log Info Dens	11	7	4
ICS	12	12	13
MTFA	13	13	14
Info Dens	14	14	10
Log Lim Res	15	17	15
SQF	16	15	16
GFP	17	16	18
Lim Res	18	18	17
N_e	19	19	19

It is apparent from the relatively poor showing of the limiting resolution that this quantity does not serve well as a display system FOM. Limiting resolution might be a reasonable parameter to use in conjunction with other parameters to roughly describe a television display system, but it does not provide a very good means of indicating overall display image quality. The equivalent bandpass of Schade also falls in this category, based on its rank order in Table 14.

The log BLMTFA ranked highest for all three observer tasks, followed closely by the JNDA-log (1/2 cpd). It is impossible to declare either of these as clearly superior to the other since their correlations with performance are so close. It is interesting that both are area-type measures, although the next ranked FOM is the log suprathreshold resolution which is not an area-type measure.

The failure of the gray-shade transformation to improve the area-type FOM over the MTFA and the JNDA indicates that the gray-shade concept is not appropriate as a useful display describing parameter. The work on DDD's by Carlson and Cohen (1978) and the results shown in Table 14 provide a strong indication that the gray-shade capability of a display system is not a characteristic that relates well to performance.

CHAPTER 5

APPLICATION OF FIGURES OF MERIT TO A PREVIOUS DISPLAY STUDY

The problem with applying FOM's to a previously completed study is to obtain sufficient information concerning the display conditions to calculate the value of the FOM's. Since the author was involved with the study done by Martin et al. (1976), sufficient data were available to calculate the FOM's.

The purpose of the experiment was to determine the effect of element density (number of display elements per degree visual angle) and active-to-total-area ratios on target recognition performance. The same 16mm motion picture imagery described in Chapter 4 was projected onto a rear projection screen for viewing by the subjects. In the pilot study, six viewing distances were used corresponding to six different display element density levels. The different active-to-total-area ratios were simulated by placing a grid mask over the rear projection screen. The line width of the grid mask was varied to achieve four values of active-to-total-area ratios. The results indicated no performance differences due to active-to-total-area ratios so the viewing distance data presented in this chapter is an average across this parameter.

The six viewing distances correspond to six angular MTF's at the displayed image. Figure 5.1 shows these six angular MTF's graphed with the nine display system MTF's of Chapter 4 for comparison. The two visual threshold curves of Campbell and Robson (1968) described previously are also shown.

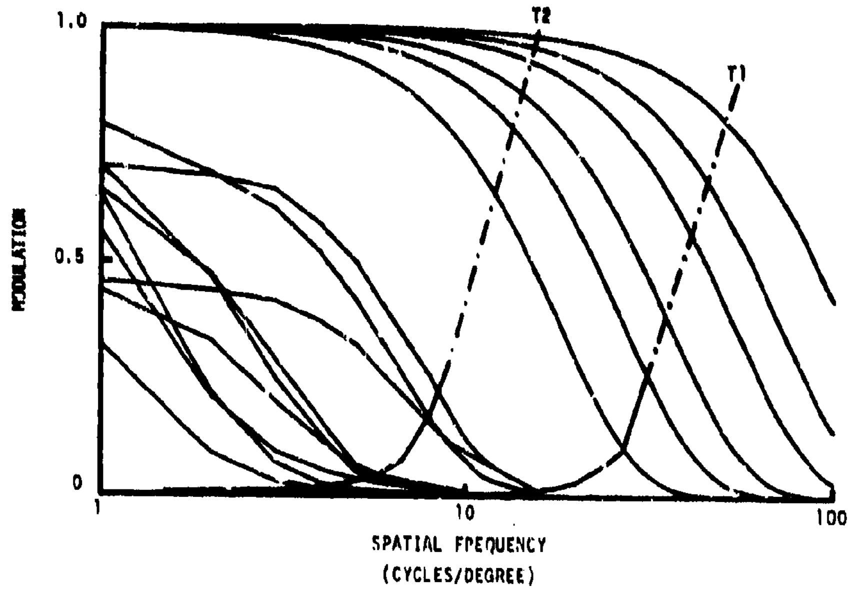

Fig. 5.1. The six angular MTF's (right) corresponding to the six viewing distances of the film display study

The nine MTF's of the study described in Chapter 4 (left) and the two visual threshold curves of Campbell and Robson (1968) are shown for reference.

The subjects for this experiment were trained for several weeks prior to participating in the experiment. All subjects were brought to an asymptotic level of performance to preclude learning effects. All conditions were presented to all subjects. Table 15 shows a summary of the performance results of the study. The performance variable was the same as that used for the study of Chapter 4, namely, the angle subtended by the target at recognition. An analysis of variance was not published for these data in the report from which they were obtained.

Table 15. Target recognition performance for different viewing distances

Viewing Distance (meters)	Angle Subtended by the Target at Recognition (deg)
4.37	0.230
2.91	0.217
2.18	0.231
1.46	0.239
1.09	0.277
0.73	0.318

Table 16 shows the calculated value of the FOM's for the six viewing distances of this experiment. The Gaussian film MTF's shown in Figure 5.1 were used to calculate the FOM values. It should be noted that these MTF's only approximate the actual display MTF for this study. Stray light and ambient room illuminance would tend to lower the MTF at the lower spatial frequencies. This display was not available to measure the actual MTF as it was projected. This approximation (using the Gaussian film MTF to be the same as the projected display MTF) is reasonable for all of the FOM's except one. The value of the GFP is very sensitive to small changes in the modulation level at high modulation levels. Since there is an uncertainty as to the exact upper modulation level of the projected image, it was decided to eliminate the GFP calculation from the list of FOM's for this study.

Table 13 shows the correlation between the FOM values and the performance variable of this study.

The most startling aspect of Table 17 is that almost all of the FOM's correlate highly (0.90 or better) with performance. In this respect the information in Table 17 does not provide any further insight into the question of which FOM is the best correlate of performance. However, the two FOM's that were ranked highest in Chapter 4 correlated very highly with performance (-0.977 and -0.983), indicating that these two are still the most promising FOM's.

Table 16. Calculated values of 18 FOM's for the six display viewing distances

	Viewing Distance (Meters) 4.37	2.91	2.18	1.46	1.09	0.73	Theoretical Max.
N_e*	67.5	44.6	33.7	22.5	17.0	11.3	∞
Lim Res	51	45	41	35	31	27	61
Log Lim Res	1.71	1.65	1.61	1.54	1.49	1.43	1.78
S.T. Res	11.1	11.0	11.0	10.8	10.6	10.2	11.25
Log S.T. Res	1.045	1.041	1.041	1.033	1.025	1.009	1.051
MTFA	35.0	31.8	28.8	23.8	20.1	14.9	40.8
Log MTFA	1.55	1.50	1.46	1.38	1.30	1.17	1.61
GFP-Log	29.2	25.3	22.6	18.9	16.4	13.1	∞
SQF	0.5995	0.5964	0.5920	0.5799	0.5635	0.5207	0.602
ICS	4381	4332	4272	4124	3951	3566	4637
JNDA	845	845	827	782	737	642	867
Log JNDA	2.927	2.927	2.918	2.893	2.867	2.808	2.938
Info Dens	111.0	111.0	110.2	107.3	104.8	94.1	111.9
Log Info Dens	2.045	2.045	2.042	2.033	2.020	1.974	2.049
JNDA-Log 1/2 cpd	73.72	73.72	73.42	72.51	71.61	69.50	74.32
JNDA-Log 2	40.97	40.97	40.57	39.76	38.86	36.75	41.76

Table 16. Continued

	Viewing Distance (Meters)						Theoretical Max
	4.37	2.91	2.18	1.46	1.09	0.73	
Log SSMTFA	0.961	0.958	0.955	0.947	0.936	0.907	0.966
Log BLMTFA	0.854	0.850	0.846	0.835	0.821	0.783	0.862

*In the original definition of N_e, there would be no change in this parameter due to viewing distance of the observer since the measure was a characteristic of the display only. The values shown here were obtained by converting the linear equivalent bandpass spatial frequency to an angular spatial frequency equivalent bandpass value. These values do change with observer viewing distance.

Table 17. Correlations between the FOM's and target recognition performance for the film study of Martin et al. (1976)

FOM	Correlation
Log BLMTFA	-0.977
JNDA-Log (1/2 cpd)	-0.983
Log S.T. Res	-0.969
Log JNDA	-0.984
JNDA-Log (2 cpd)	-0.983
S.T. Res	-0.973
Log MTFA	-0.950
JNDA	-0.983
Log SSMTFA	-0.978
GFP-Log	-0.858
Log Info Dens	-0.971
ICS	-0.978
MTFA	-0.912
Info Dens	-0.974
Log Lim Res	-0.885
SQF	-0.979
GFP	--
Lim Res	-0.851
N_e	-0.729

There are major differences between the studies of Chapter 4 and the study described in this chapter that are probably responsible for the high correlations. The most significant difference is that the film study varied only one parameter, i.e., viewing distance (angular MTF), whereas the studies of Chapter 4 varied both the contrast ratio of the display and the bandwidth. The FOM's had to account for the visual effects of only one parameter in the film study compared to the two parameters of the video study. Thus the video study of Chapter 4 represents a more critical test of the FOM's than does the film study.

Since the study described in this chapter was done with a directly viewed film display, with no intervening video system, it is difficult to make absolute performance level comparisons with the target recognition study of Chapter 4. The performance level of the film study was much higher, but it is impossible to determine how much of this was due to increased subject training and how much was due to improved image quality.

Despite the inconclusiveness of the results shown in Table 17, two significant points are evident. First, the limiting resolution and equivalent bandpass are once again found at the bottom of the list of correlations. Second, the log BLMTFA and JNDA-log (1/2 cpd) correlate very highly with performance, preserving their position as the most promising display system FOM's. Graphs of these correlations are in Appendix C.

CHAPTER 6

DISCUSSION AND MODEL DEVELOPMENT

Table 18 is a summary of the FOM's investigated and their correlation with performance for the four tasks described in Chapters 4 and 5. Table 19 shows the rank order of the FOM's for each of the four performance tasks. The last column of Table 19 is somewhat misleading due to the very high correlations that were obtained for almost all of the FOM's. To determine whether or not the differences in correlation coefficients among the FOM's were statistically significant, a statistical analysis was done using a method developed by Hotelling (Guilford, 1965, p. 191). The FOM with the highest correlation for each of the four tasks was analyzed to determine if it was statistically higher than the other FOM's. Appendix D describes the equation and procedure used to accomplish this. The log BLMTFA correlated highest with performance for the first three performance tasks of Table 18. Table 20 shows the probability level (or nonsignificance) obtained by statistically comparing the log BLMTFA with each of the other FOM's.

For the film study described in Chapter 5 the FOM that correlated highest with performance was the log JNDA. Table 21 statistically compares this FOM with the others to determine if it is statistically higher in correlation with performance.

Table 18. Summary of FOM correlations with performance for the four performance tasks

FOM	Target Recognition (Television Study)	Target Detection POL 1000 (Television Study)	Target Detection POL 2000 (Television Study)	Target Recognition (Film Study)
Log BLMTFA	-0.948	0.931	0.878	-0.977
JNDA-Log (1/2 cpd)	-0.937	0.928	0.853	-0.983
Log S.T. Res	-0.909	0.923	0.864	-0.969
Log JNDA	-0.906	0.902	0.838	-0.984
JNDA-Log (2 cpd)	-0.896	0.902	0.835	-0.983
S.T. Res	-0.888	0.900	0.834	-0.973
Log MTFA	-0.878	0.866	0.777	-0.950
JNDA	-0.876	0.880	0.802	-0.983
Log SSMTFA	-0.869	0.857	0.766	-0.978
GFP-Log	-0.847	0.869	0.760	-0.858
Log Info Dens	-0.820	0.880	0.842	-0.971
ICS	-0.818	0.837	0.724	-0.978
MTFA	-0.811	0.829	0.717	-0.912
Info Dens	-0.795	0.824	0.766	-0.974
Log Lim Res	-0.783	0.795	0.709	-0.885
SQF	-0.781	0.803	0.702	-0.979
GFP	-0.781	0.798	0.670	--
Lim Res	-0.764	0.778	0.695	-0.851
N_e	-0.726	0.761	0.618	-0.729

Table 19. Rank order of the FOM's for the four performance tasks

FOM	Target Recognition (Television Study)	Target Detection (Television Study) POL 1000	Target Detection (Television Study) POL 2000	Target Recognition (Film Study)
Log BLMTFA	1	1	1	8
JNDA-Log (1/2 cpd)	2	2	3	3
Log S.T. Res	3	3	2	12
Log JNDA	4	4	5	1
JNDA-Log (2 cpd)	5	5	6	2
S.T. Res	6	6	7	10
Log MTFA	7	10	9	13
JNDA	8	8	8	4
Log SSMTFA	9	11	11	6
GFP-Log	10	9	12	16
Log Info Dens	11	7	4	11
ICS	12	12	13	7
MTFA	13	13	14	14
Info Dens	14	14	10	9
Log Lim Res	15	17	15	15
SQF	16	15	16	5
GFP	17	16	18	--
Lim Res	18	18	17	17
N_e	19	19	19	18

Table 20. Statistical probability level that the top listed FOM is more highly correlated with performance for the performance tasks of Chapter 4 (NS means not significant at p = 0.05 level)

FOM	Performance Task: Target Recognition Probability, p<	POL 1000 Probability, p<	POL 2000 Probability, p<
Log BLMTFA	--	--	--
JNDA-Log (1/2 cpd)	NS	NS	NS
Log S.T. Res	0.05	NS	NS
Log JNDA	0.01	NS	NS
JNDA-Log (2 cpd)	NS	NS	NS
S.T. Res	0.05	NS	NS
Log MTFA	0.025	0.05	0.025
JNDA	0.025	NS	NS
Log SSMTFA	0.05	NS	0.025
GFP-Log	0.05	NS	NS
Log Info Dens	0.05	NS	NS
ICS	0.025	NS	0.05
MTFA	0.025	NS	0.05
Info Dens	0.025	NS	NS
Log Lim Res	0.01	0.05	0.05
SQF	0.025	NS	NS
GFP	0.025	NS	0.025
Lim Res	0.01	0.05	0.05
N_e	0.025	NS	0.05

Table 21. Statistical probability level that the top listed FOM is more highly correlated with performance than the other FOM's for the film study of Chapter 5 (NS means not significant at the p = 0.05 level)

FOM	Performance Task Film Study Probability, p<
Log JNDA	--
JNDA	NS
JNDA-Log (2 cpd)	NS
JNDA-Log (1/2 cpd)	NS
Log SSMTFA	NS
ICS	NS
Log BLMTFA	NS
Info Dens	NS
S.T. Res	NS
Log Info Dens	NS
Log S.T. Res	NS
Log MTFA	NS
MTFA	0.05
Log Lim Res	0.05
SQF	NS
GFP-Log	0.025
Lim Res	0.05
N_e	0.025

It is apparent from the statistical analysis shown in Tables 20 and 21 that it is impossible to confidently select one of the FOM's as clearly superior to all of the others. The three FOM's that show the most promise are the log BLMTFA, the JNDA-Log (1/2 cpd), and the JNDA-log (2 cpd). Table 20 shows that the JNDA-log (1/2 cpd) and the JNDA-log (2 cop) are the only FOM's that are not significantly lower than the log BLMTFA for all three performance tasks. None of these three had the highest correlation with performance for the film study; however, they both correlated very highly with performance, and a statistical analysis showed that there was not a significant difference between these FOM's in correlating with performance.

A cautionary note must be injected concerning the application of these FOM's to operational display systems. Performance for the target recognition studies was measured in terms of the angular size of the target at recognition. However, this may not be the important performance variable from an operational standpoint. The problem arises for display situations in which the angular size of the display is the independent variable, as in the film study of Chapter 5. The angular MTF and subjective quality of the display improve as the display is moved away from the observer. Also, the performance, in terms of the angular size of the target, improves (decreases) as the value of the FOM's increases. However, the percent of the display that the target must occupy for recognition to occur increases as the display is moved further away. This corresponds to a more inefficient sensor/display observer system in terms of the visual information transferred from the sensor to the observer.

Table 22 shows the percent of the display required for target recognition calculated from the film study of Chapter 5. The lower the percentage of the display that the target must occupy for recognition to occur, the longer the slant range to the target at recognition, if the sensor field of view (FOV) is kept constant. The important operational performance parameter is the distance at which a target can be detected or recognized. Thus, it is desirable to arrange a display system to improve this capability as much as possible. The calculated values of the FOM's do not, by themselves, provide sufficient information to determine the effect of display angular subtense on this operational performance. This inadequacy is a severe shortcoming of all the FOM's investigated and, to some extent, of the FOM concept in general. The objective of the FOM concept was to develop a means of quantifying image quality to relate to observer performance. This objective has been successfully attained for several display variables, if one is concerned about the angle subtended by the target at recognition. However, for many display applications a more meaningful measure of performance is the efficiency of the display/observer interface. This efficiency can be expressed in terms of the percent of the display that the target must occupy for target detection or recognition to occur. The smaller the percentage, the better the performance.

This approach is more in the realm of developing a model to predict absolute performance levels rather than relative performance, which was the objective of the FOM concept. However, the potential utility of a successful target detection or recognition model is sufficient to warrant a brief discussion of a possible approach. The objective of this discussion is to determine if the data shown in Table 22 can be reasonably predicted using a simple approach to a target recognition model.

Table 22. Percent of display width required for recognition for six viewing distances; from the target recognition study of Chapter 5

Viewing Distance (meters)	Angular Width of Display (degrees)	Percent of Display Width Required for Recognition
4.37	1.765	13.03
2.91	2.650	8.19
2.18	3.537	6.53
1.46	5.279	4.53
1.09	7.067	3.92
0.73	10.536	3.02

There are two easily defined extremes that can occur for a display/observer interface: 1) a severely display-limited case, and 2) a severely vision-limited case.

For the first case the display is situated very close to the observer and has a very low resolution compared to the visual acuity of the observer. Thus the observer can easily resolve all of the visual information that the display can present. The limiting factor in this case is the display/sensor capability. Therefore, the percent of the display that the target must occupy for recognition to occur is the ratio of the number of resolution elements required across the target to the total number of resolution elements across the display (times 100 for percent). As a simple example, consider a tri-bar target. There must be a minimum of five resolution elements across the target to resolve its pattern as determined by the Nyquist limit. If the display is capable of 100 resolution elements across one dimension, then the target must occupy 5 percent of that display dimension. In general, this display limit can be expressed as:

$$\text{(display limit) } \%\, D = \left(\frac{N_T}{N_D}\right) 100 \qquad (11)$$

where

$\%\, D$ = percent of the display that the target must occupy for recognition to occur

N_T = number of resolution elements required to recognize target (along one dimension)

N_D = number of resolution elements across one dimension of the display

The second extreme is the vision-limited situation. This occurs for cases where the angular size of an individual display resolution element is much smaller than the angular resolution limit of the eye (1 to 1-1/2 minutes of arc). Thus the limiting factor for this case is visual acuity. This means that the target must subtend a minimum angle for recognition to occur. For the tri-bar target example, the target must subtend 5 to 7-1/2 minutes of arc (depending on the visual resolution limit used) for the target to be resolved. This number is obtained by multiplying the number of resolution elements required to resolve the target times the angular resolution limit of the eye. The percent of the display that the target must occupy for this case is given by:

$$\text{(vision limit) } \%\ D = \left(\frac{\theta_T}{\theta_D}\right) 100 \qquad (12)$$

where

θ_T = required angular target size

θ_D = angular size of the display

% D = percent of display required for recognition to occur

Equations (11) and (12) describe the percent of the display required for display/observer extremes or limits. The problem is how does one determine the requirements for intermediate, non-extreme cases? The simplest approach is to simply add the two quantities together. Thus, combining equations (11) and (12) in this manner:

$$\text{(general case) } \%\ D = \left(\frac{\theta_T}{\theta_D} + \frac{N_T}{N_D}\right) 100 \qquad (13)$$

It should be noted that in this simple modeling approach θ_T is calculated using:

$$\theta_T = N_T \theta_V$$

where

θ_V = limiting visual acuity (in degrees)

Some assumption must be made to establish numbers for θ_V, N_T and N_D. The visual acuity limit, θ_V, is assumed to be 1-1/2 minutes of arc which is the largest value of the 1 to 1-1/2 minutes of arc typically ascribed to this parameter (Riggs, 1965). Since the targets used were somewhat similar in nature to those used by Johnson (1966) in establishing the "Johnson criteria," these criteria are employed. The Johnson criteria state that target recognition occurs for a display/observer condition wherein the observer can resolve a periodic bar target of 4.0 ± 0.8 cycles that is the same size as the target. Thus N_T is approximately eight resolution elements (assuming two samples per cycle). The useful limiting resolution of a display has been designated as the spatial frequency at which the modulation contrast drops below about two to five percent (Brock, 1967; Dyall, 1978). The number of resolution elements, N_D, is estimated to be the minimum number of samples required to resolve the spatial frequency at which the display MTF drops to 3-1/2 percent (midway between 2 and 5 percent). For the film study of Chapter 5, N_D is 680.

Using these values for θ_T, N_T, and N_D the following equation should predict the results shown in Table 22.

$$\text{(film study) } \%\ D = \left\{ \frac{0.200}{\theta_D} + \frac{8}{680} \right\} 100 \qquad (14)$$

The six viewing distances of this study correspond to six angular sizes for the display. Table 23 shows the % D values predicted by equation (14) compared to the actual % D values of the study. Figure 6.1 shows the theoretically modeled curve of % D versus θ_D. The circled points in Fig. 6.1 are the actual data points from the study of Chapter 5.

It is apparent from Table 23 and Fig. 6.1 that the agreement between the model and actual performance is excellent considering the simplicity of the model and the relative crudeness with which the critical values in the modeling equation were selected. The determination of θ_T and N_T need to be refined to be sensitive to subtle changes in target characteristics and visual acuity, but the overall model structure appears to be very promising.

Table 23. Predicted values of percent of display required for target recognition and actual values from Table 22

Display Angular Width (deg)	Predicted % D	Actual % D	Percent Difference
1.765	12.51	13.03	4.1
2.650	8.72	8.19	6.3
3.537	6.83	6.53	4.5
5.279	4.97	4.53	9.3
7.067	4.01	3.92	2.3
10.54	3.07	3.02	1.6

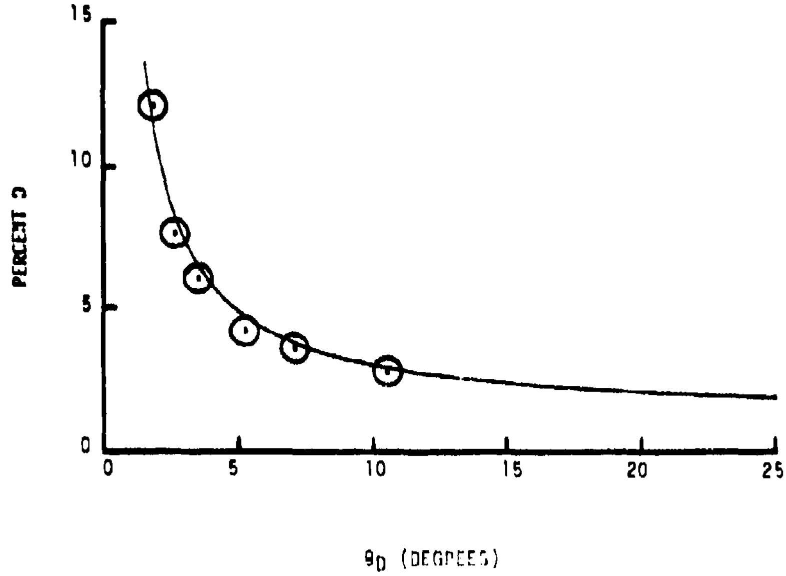

Fig. 6.1. Theoretical model of percent of display width required for target recognition versus angle subtended by the display

The circled points are experimental results of the film study described in Chapter 5.

CHAPTER 7

CONCLUSIONS

Of the 19 FOM's investigated, all showed a reasonable degree of correlation with performance, which is somewhat surprising considering the diverse assumptions and theoretical approaches of the different FOM's.

The log BLMTFA, the JNDA-log (1/2 cps), and the JNDA-log (2 cpd) showed themselves to be the most promising indicators of image quality based on the results of this dissertation. These have correlated highly with performance for target recognition and target detection tasks for studies in which the contrast ratio, bandwidth and viewing distance to the display have been varied. Also, they are affected by other display system variables such as noise, luminance, and others that were not investigated here. It remains to be seen whether or not these FOM's will still correlate well with performance for display situations in which other parameters are varied.

It may not be possible to determine which FOM is clearly superior to all of the others, but it is certainly possible to eliminate some FOM's from consideration as inferior to the more highly correlating FOM's. The limiting resolution and the equivalent bandpass are two

FOM's that are widely used that consistently correlated significantly lower with performance than the higher-ranked FOM's. This is strong evidence that these quantities should not be used as a means of describing the overall image quality of a display system.

The failure of the gray-shade transformation to correlate well with performance indicates that this type of transformation does not produce a quantity that is linear with respect to visual information. The relative success of the JNDA-log (1/2 cpd) and JNDA-log (2 cpd) indicate that the lower modulation contrast levels should probably be weighted more heavily than the higher levels, which is opposite of the gray-shade transformation effect.

The success of the modeling approach described in Chapter 6 indicates that it may be more advantageous to develop methods of predicting absolute performance levels rather than spend time and effort developing alternative FOM's for display systems.

Overall, this dissertation shows that there are several display system figures of merit that are probably adequate as quantitative indicators of image quality.

APPENDIX A

SLANT RANGE AND ANGLE SUBTENDED BY TARGET AT RECOGNITION CALCULATIONS

The slant range to the target at detection was calculated using the equation:

$$S = A \left\{ \frac{1 + \tan^2 \phi}{\sin^2 (\theta - \alpha)} \right\}^{1/2} \qquad (15)$$

where

S = slant range to target

A = altitude of sensor

α = depression angle of sensor from horizontal

ϕ = horizontal field angle to target

θ = vertical field angle to target

and

$$\phi = \arctan \left(\frac{2w \tan \left(\frac{\phi_m}{2} \right)}{W} \right) \qquad (16)$$

w = horizontal distance on display screen from center of the display to the target (horizontal coordinate)

W = width of the display screen

ϕ_m = total horizontal field of view of sensor

$$\theta = \arctan\left(\frac{2h\ \tan\left(\frac{\theta_m}{2}\right)}{H}\right)$$

h = vertical distance on display screen from center of display to the target (vertical coordinate)

H = height of display screen

θ_m = total vertical field of view of sensor

Figure A.1 was used to derive the above relationships.

From trigonometry and Fig. A.1 the following relationships are apparent:

$$\beta = 90 - \alpha + \theta \tag{18}$$

$$L = \frac{A}{\cos\beta} \tag{19}$$

$$R = L \tan\phi = \left(\frac{A}{\cos\beta}\right)\tan\phi \tag{20}$$

$$S = \left(L^2 + R^2\right)^{1/2} \tag{21}$$

Substituting (19) and (20) into (21):

$$S = A\left(\frac{1 + \tan^2\phi}{\cos^2\beta}\right)^{1/2}$$

But:

$$\cos^2 \beta = \cos^2 \left[90° + (\theta - \alpha)\right]$$

$$= \left[\cos 90 \cos (\theta - \alpha) - \sin (90°) \sin (\theta - \alpha)\right]^2$$

$$= \sin^2 (\theta - \alpha)$$

So:

$$S = A\left(\frac{1 + \tan^2 \phi}{\sin^2 (\theta - \alpha)}\right)^{1/2} \tag{22}$$

The values of ϕ and θ must be obtained from the X, Y coordinates of the target on the display screen. The derivation is the same for both vertical and horizontal dimensions so only the vertical will be considered in detail. Figure A.2 shows a plan view of a display situation. The distance labeled D is a dummy distance convenient for derivation purposes. The maximum vertical field of view of the sensor is θ_m; this must correspond to the maximum vertical display coordinate, h:

$$\tan\left(\frac{\theta_m}{2}\right) = \frac{H/2}{D} \tag{23}$$

solving for D

$$D = \frac{H}{2 \tan\left(\frac{\theta_m}{2}\right)} \tag{24}$$

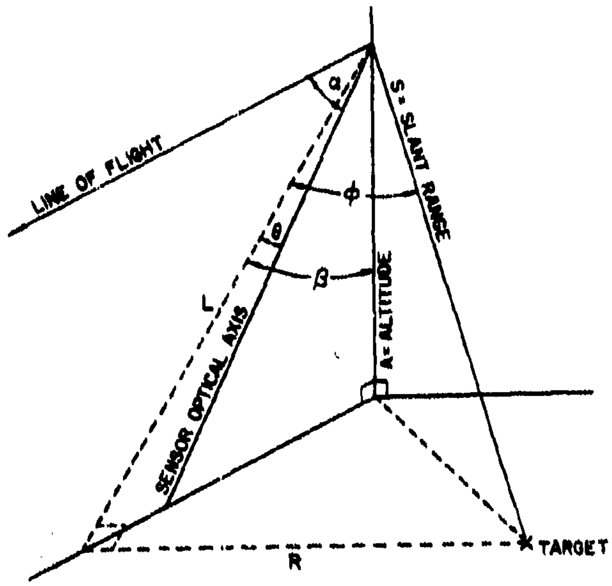

Fig. A.1. Geometry of sensor and target location for derivation of slant range equation

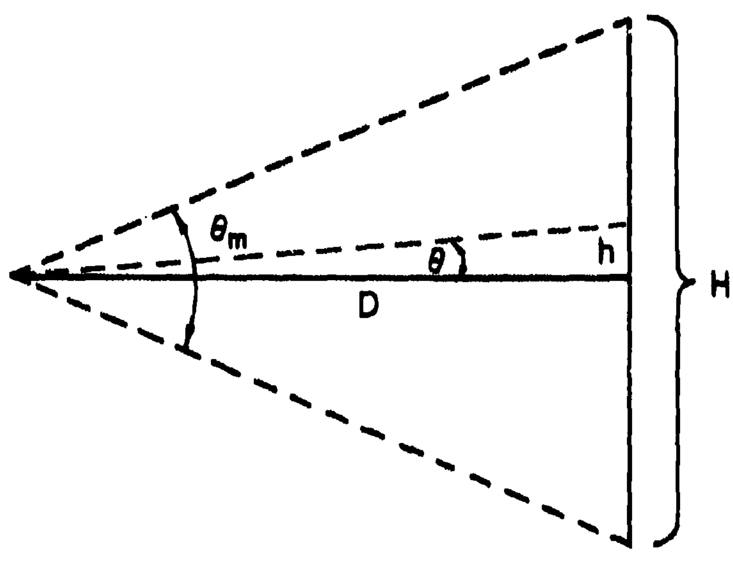

Fig. A.2. Reference diagram for calculating θ and φ

So for any vertical target position:

$$\tan(\theta) = \frac{h}{D} = \frac{2h \tan\left(\frac{\theta_m}{2}\right)}{H} \tag{25}$$

or:

$$\theta = \arctan \frac{2h \tan\left(\frac{\theta_m}{2}\right)}{H} \tag{26}$$

The linear size of the target at recognition was measured with the electronic cross hairs. Using this and the viewing distance of 28 inches the angle of the target at recognition was calculated using:

$$\theta_T = 2 \arctan\left(\frac{W}{D}\right) \tag{27}$$

where

θ_T = angle subtended by target at recognition

W = diagonal size of target on the display

D = viewing distance

APPENDIX B

EQUIPMENT USED FOR DISPLAY MEASUREMENT AND PSYCHOPHYSICAL STUDIES

Display Measurement Equipment

Strip Chart Recorder: Hewlett-Packard Model 7101B

Oscilloscope: Tektronix Model 7613

Telephotometer: Spectra Pritchard Model 1980 CDB, Serial No. 227

TV Test Signal Generator: Systems Research Laboratories Model 2550

Video Test Generator: Colorado Video Inc. Model 615

Psychophysical Study Equipment

16mm Movie Projector: L.W. Photo, Inc. Athena Model 4000 TSM

Cross Hair Generator/Video Digitizer: Systems Research Laboratories - Custom built

TV Camera: Cohu Electronics Inc. Model 2810

TV Monitor: Hewlett-Packard - Model 6946A

TV Monitor: Tektronix Model 632 Serial No. 700871

Video Filter: Systems Research Laboratories - Custom built

APPENDIX C

CORRELATION GRAPHS: PERFORMANCE VERSUS FOM'S

This section contains graphs showing the best linear fit (least squares fit) for the relationship between observer performance and the FOM's. The actual data points are shown on the graphs enclosed in small circles. The graphs are organized in rank order of their correlation coefficient for the first target recognition study (Chapter 4). The correlation coefficients and rank order are summarized in Tables 14 through 17 in Chapter 6.

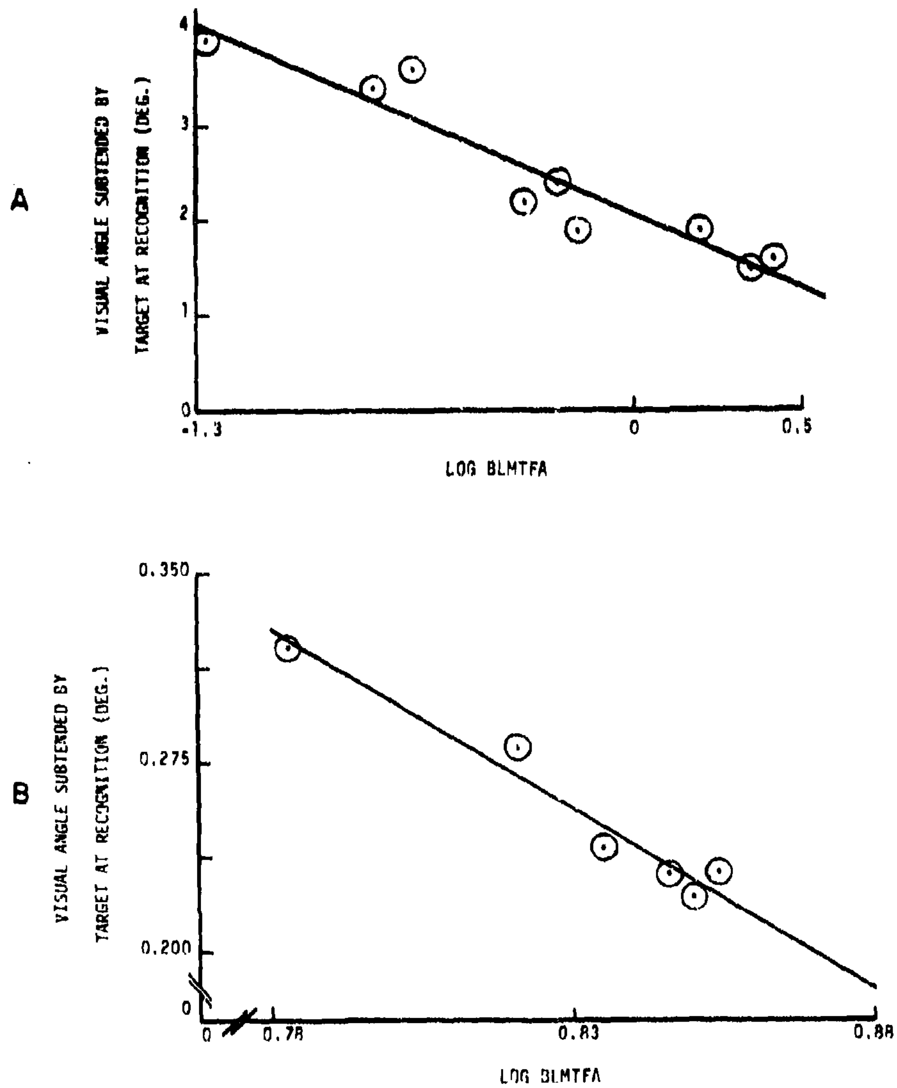

Fig. C.1. A) Graph of angle subtended by target at recognition versus log BLMTFA for the target recognition study of Chapter 4, B) graph of angle subtended by target at recognition versus log BLMTFA for the target recognition study of Chapter 5

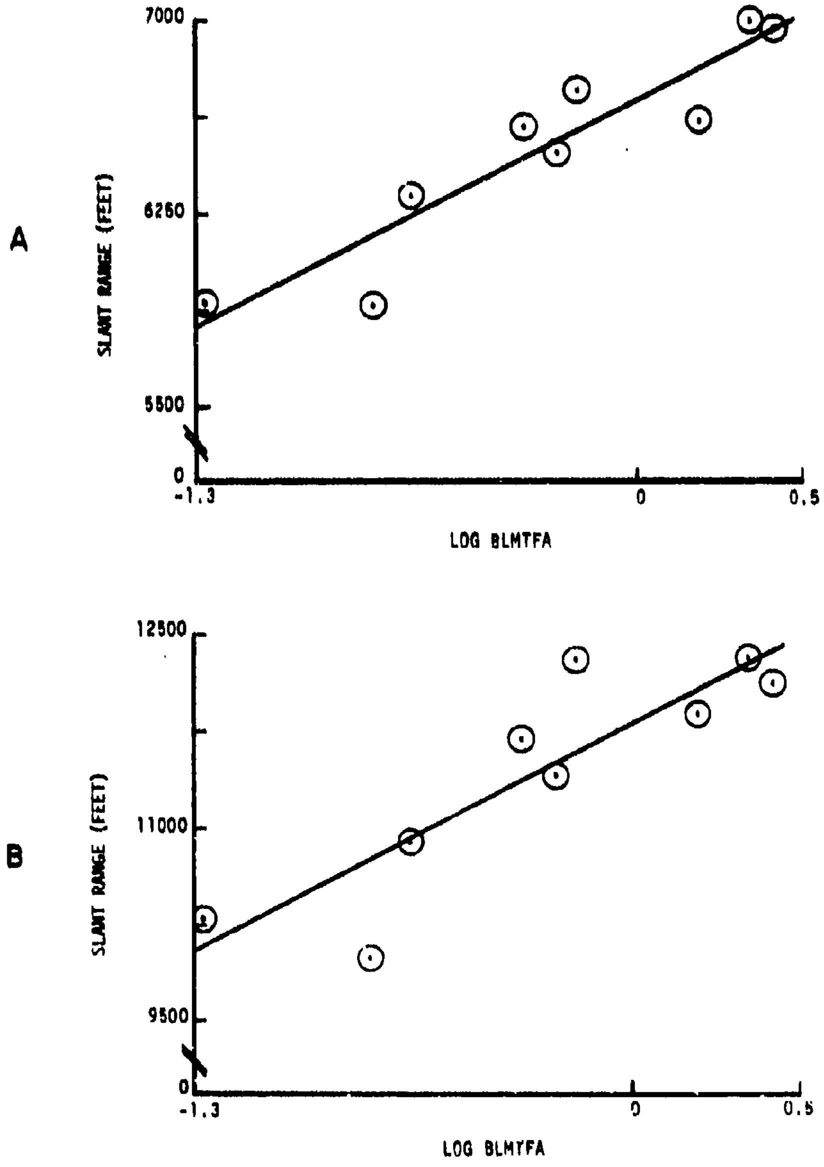

Fig. C.2. A) Graph of slant range to target at detection versus log BLMTFA for POL targets and simulated altitude of 1000 feet, B) graph of slant range to target at detection versus log BLMTFA for POL targets and simulated altitude of 2000 feet

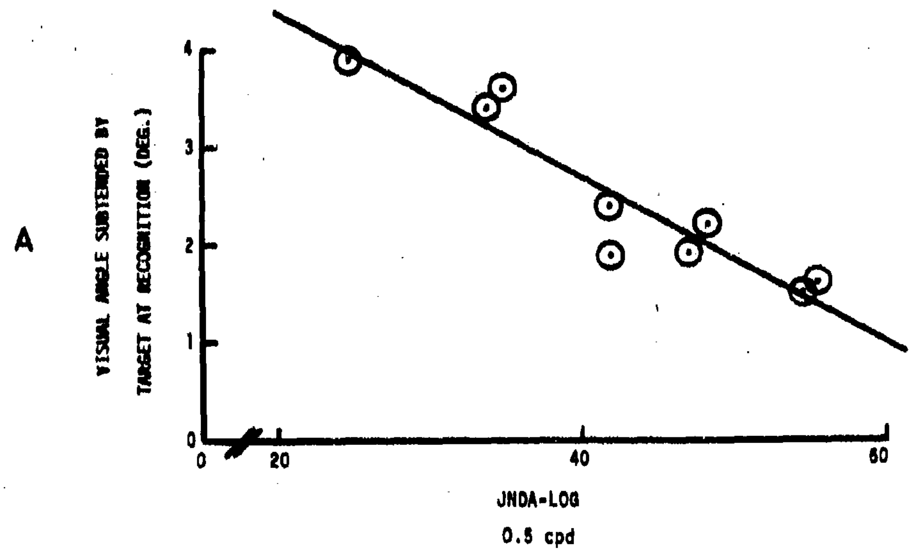

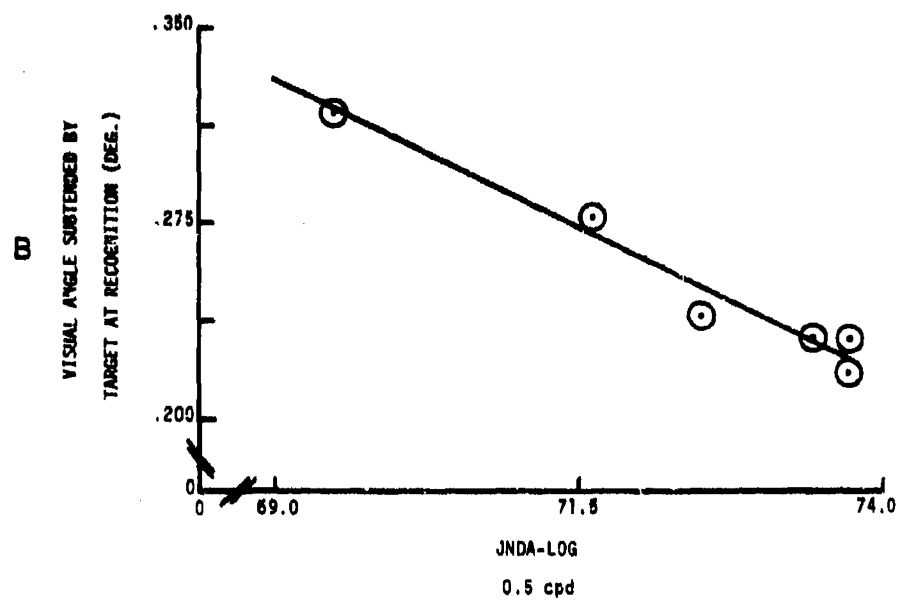

Fig. C.3. A) Graph of angle subtended by target at recognition versus JNDA-log for the target recognition study of Chapter 4, B) graph of angle subtended by target at recognition versus JNDA-log for the target recognition study of Chapter 5

A

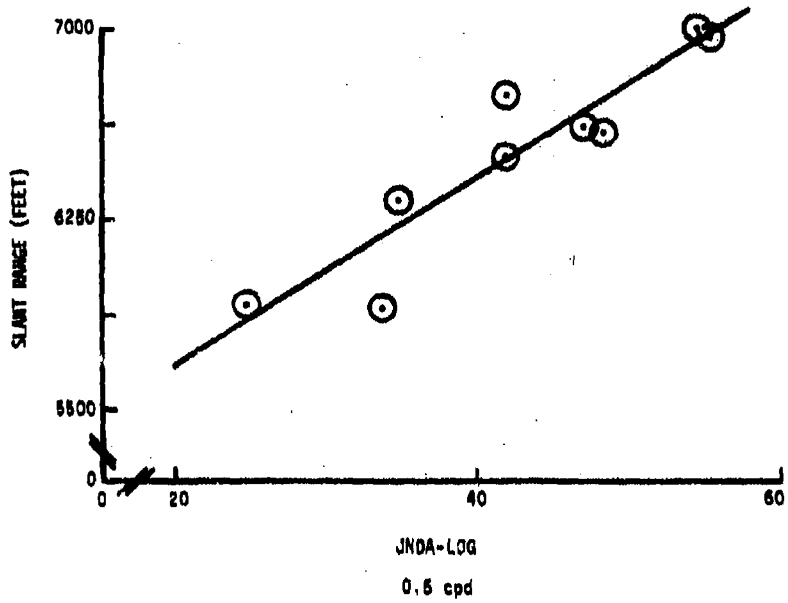

B

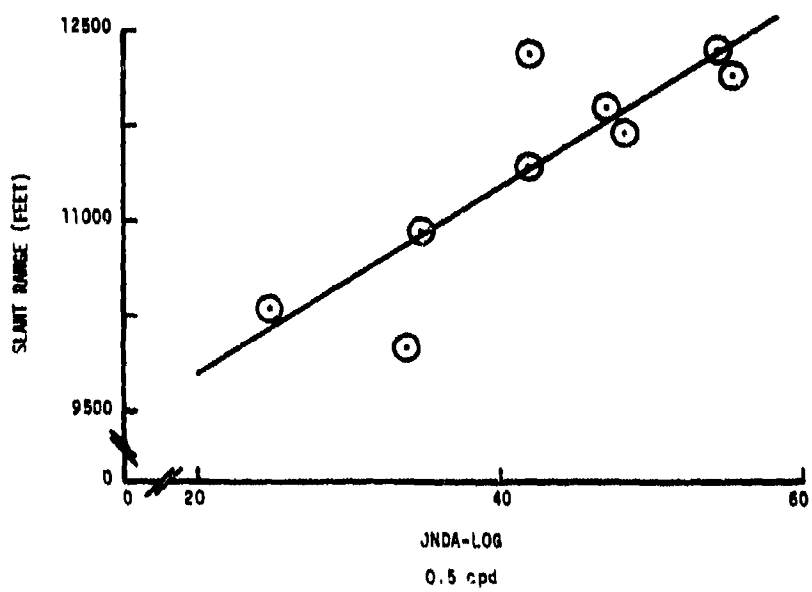

Fig. C.4. A) Graph of slant range to target at detection versus JNDA-log for POL targets and simulated altitude of 1000 feet, B) graph of slant range to target at detection versus JNDA-log for POL targets and simulated altitude of 2000 feet

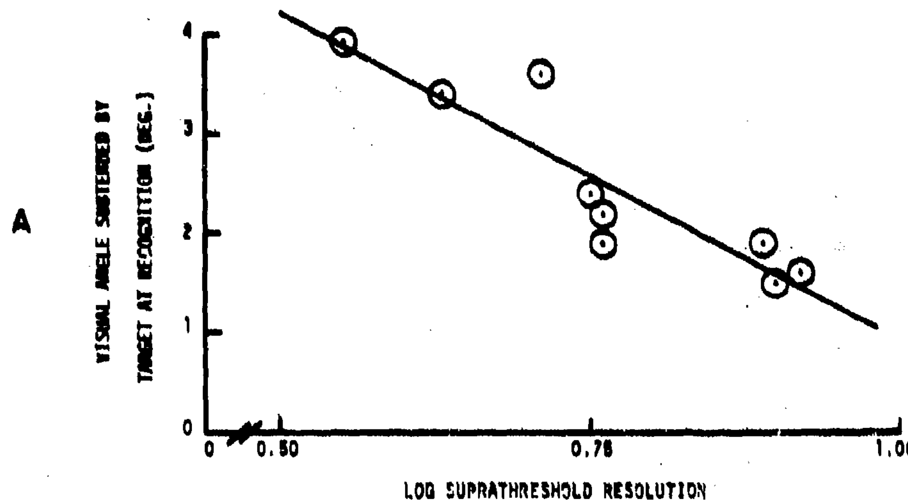

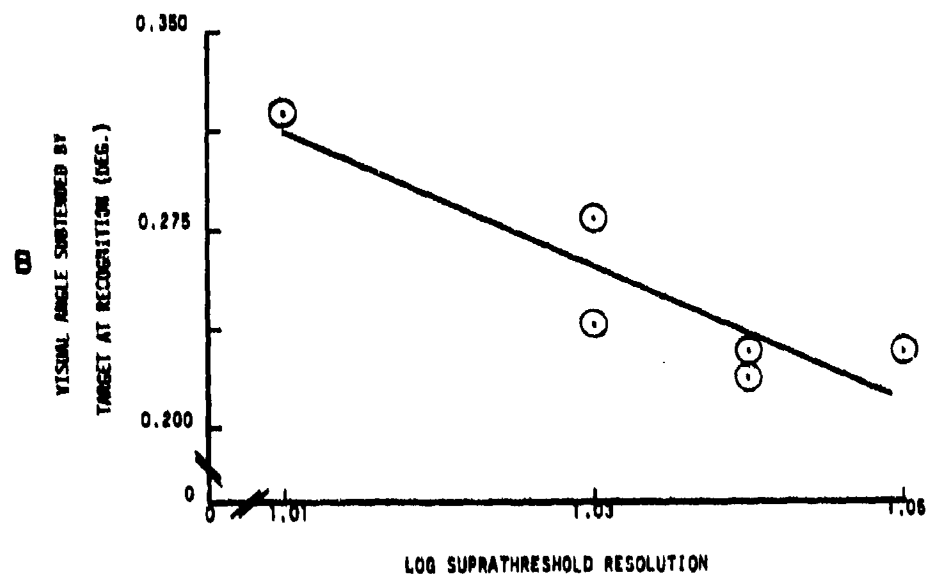

Fig. C.5. A) Graph of angle subtended by target at recognition versus log Suprathreshold Resolution for the target recognition study of Chapter 4, B) graph of angle subtended by target at recognition versus log Suprathreshold Resolution for the target recognition study of Chapter 5

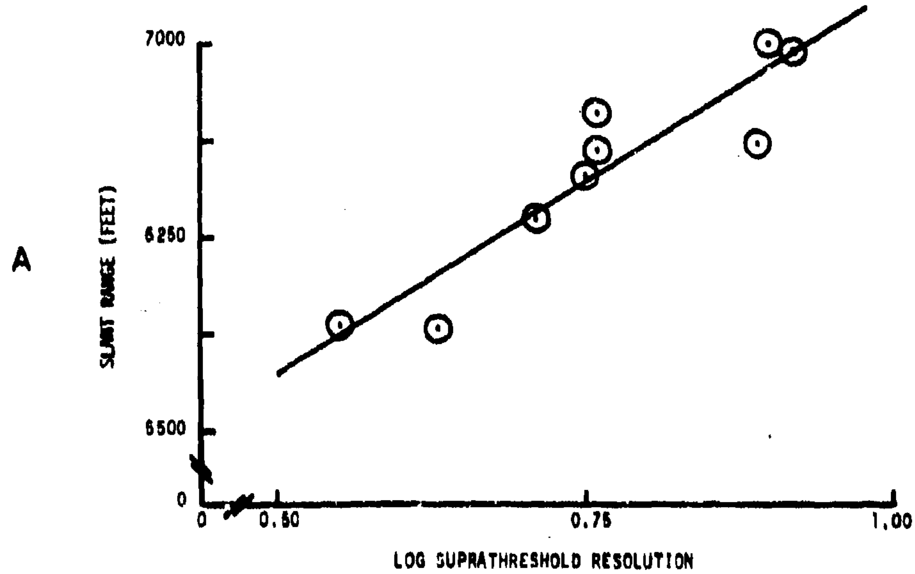

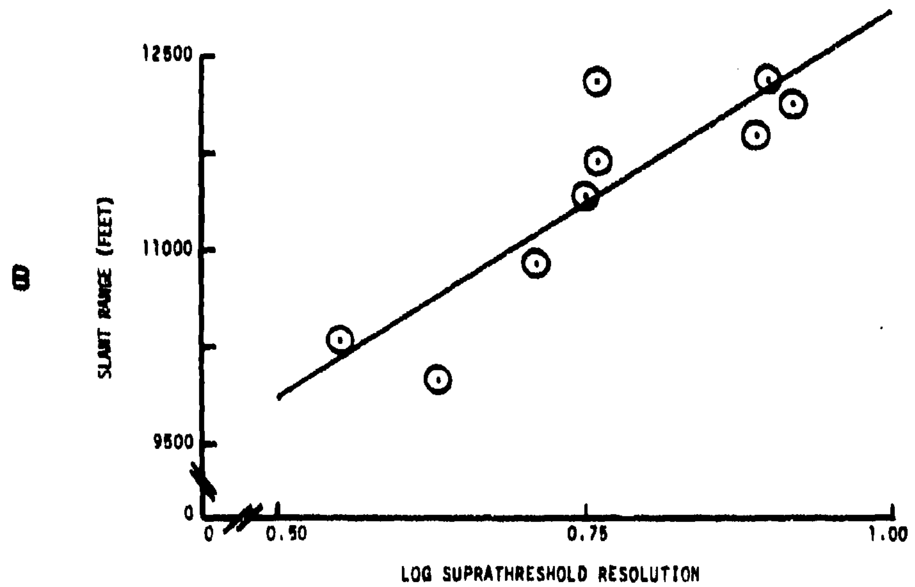

Fig. C.6. A) Graph of slant range to target at detection versus log Suprathreshold Resolution for POL targets and simulated altitude of 1000 feet, B) graph of slant range to target at detection versus log Suprathreshold Resolution for POL targets and simulated altitude of 2000 feet

A

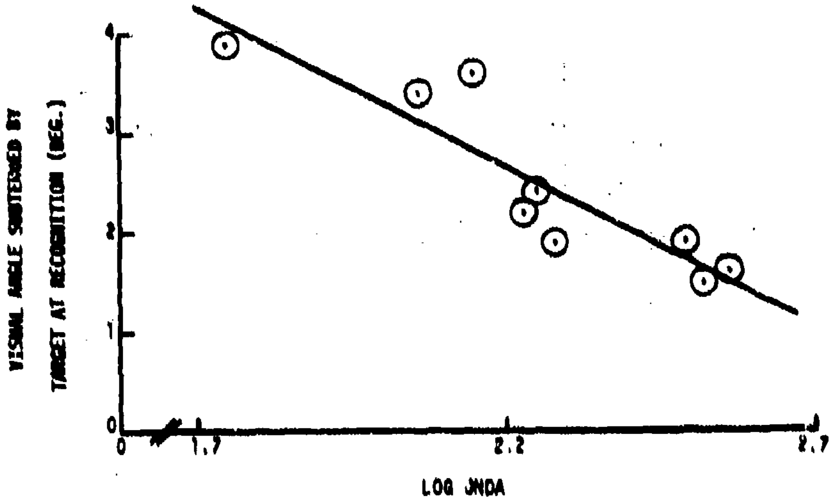

B

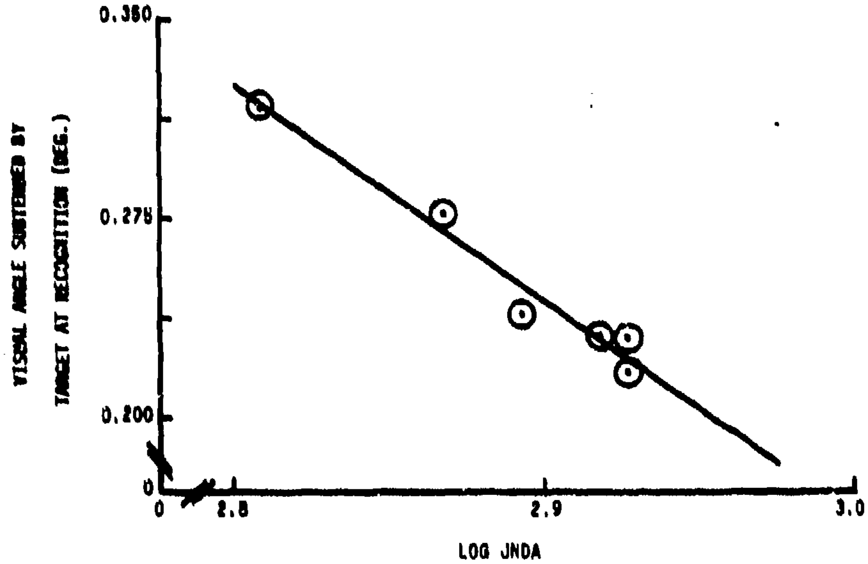

Fig. C.7. A) Graph of angle subtended by target at recognition versus log JNDA for the target recognition study of Chapter 4, B) graph of angle subtended by target at recognition versus log JNDA for the target recognition study of Chapter 5

A

B

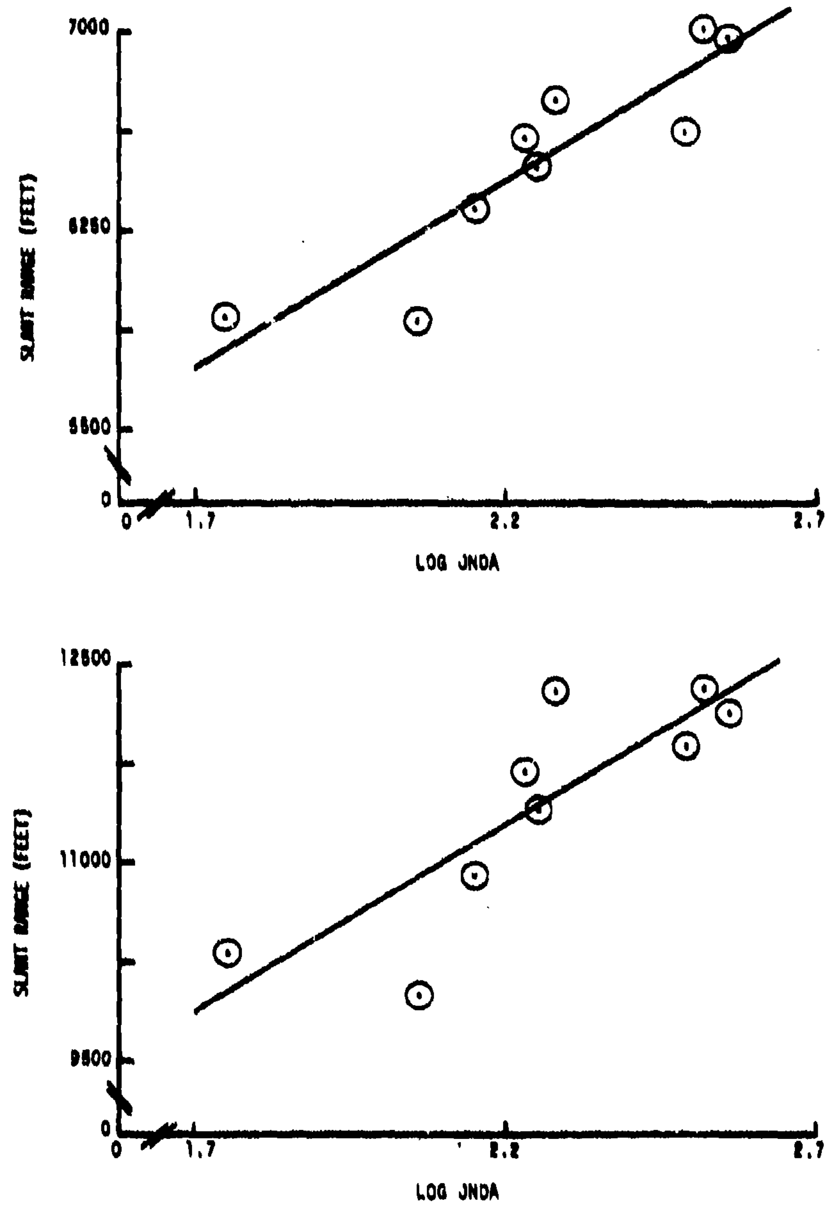

Fig. C.8. A) Graph of slant range to target at detection versus log JNDA for POL targets and simulated altitude of 1000 feet, B) graph of slant range to target at detection versus log JNDA for POL targets and simulated altitude of 2000 feet

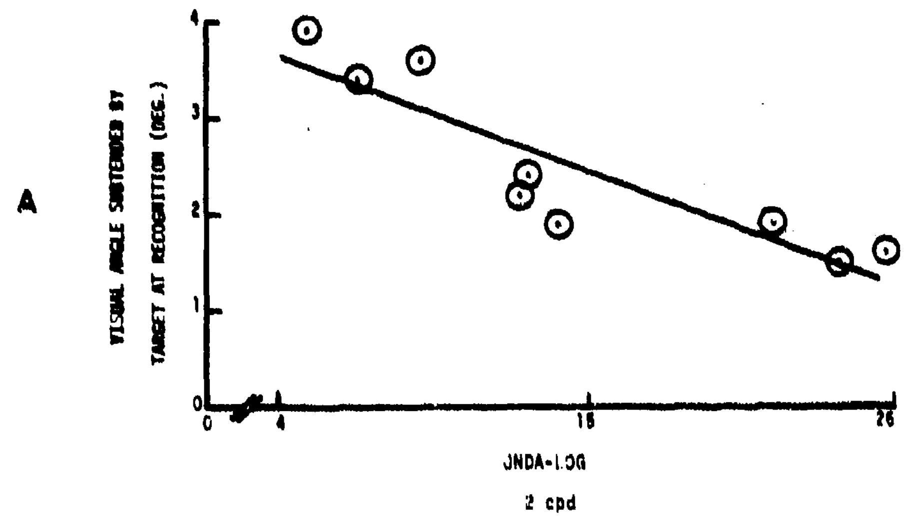

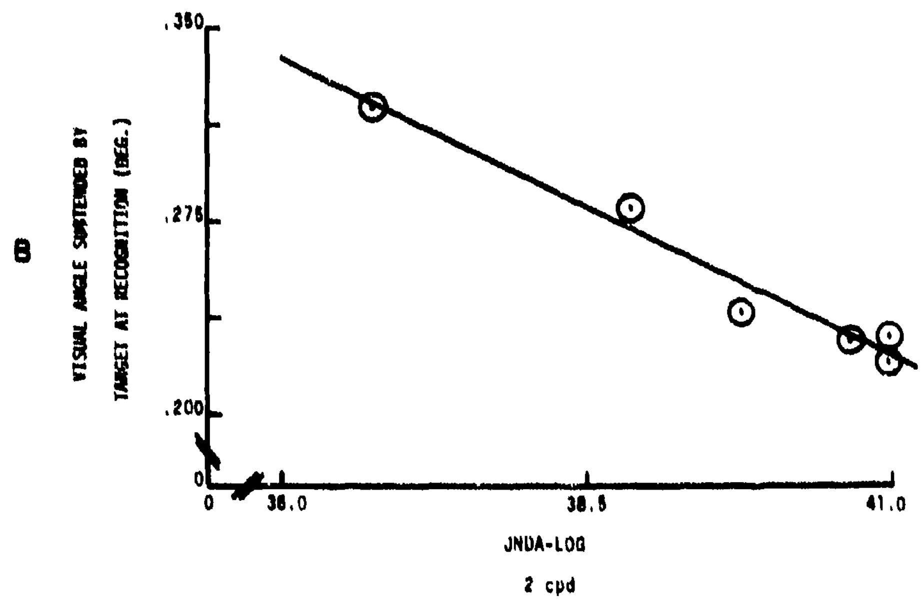

Fig. C.9. A) Graph of angle subtended by target at recognition versus JNDA-log (2 cpd) for the target recognition study of Chapter 4, B) graph of angle subtended by target at recognition versus JNDA-log (2 cpd) for the target recognition study of Chapter 5

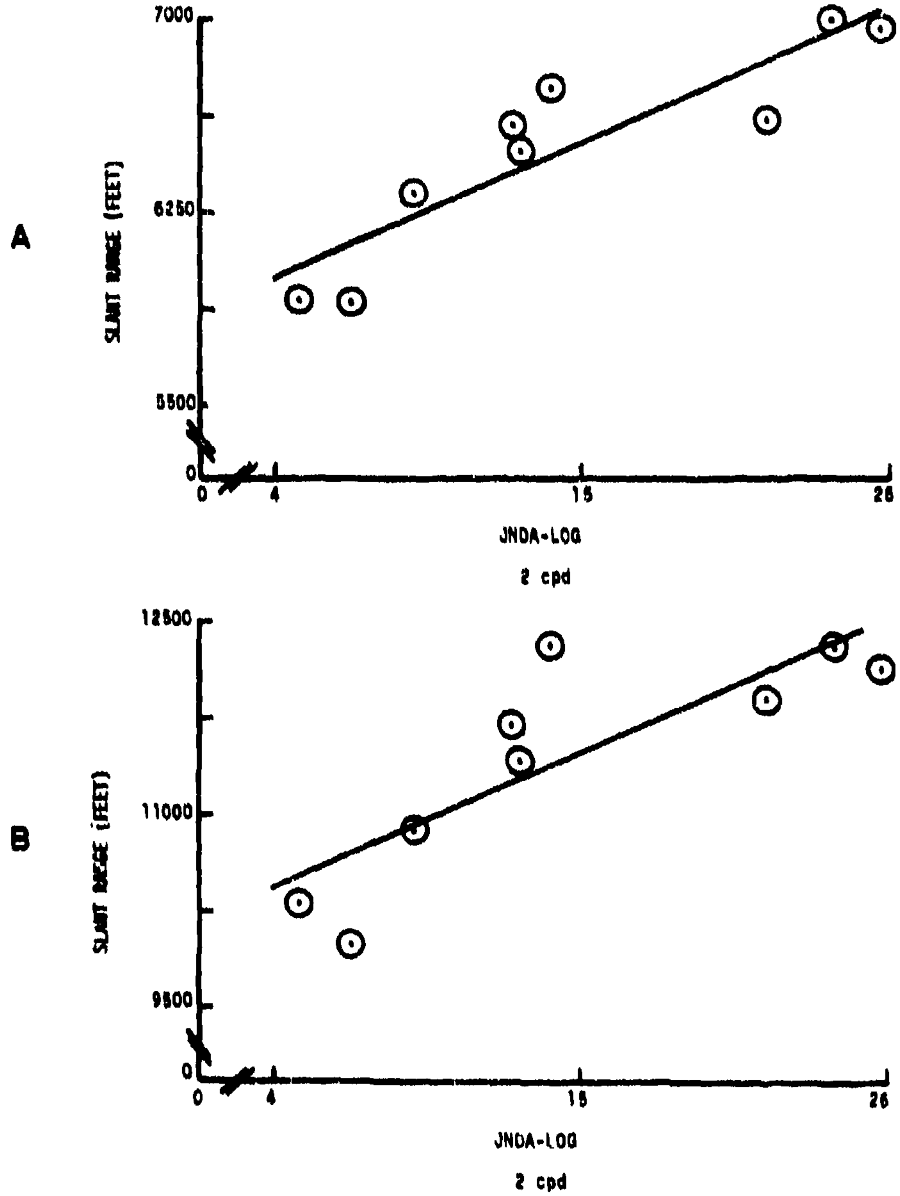

Fig. C.10. A) Graph of slant range to target at detection versus JNDA-log (2 cpd) for POL targets and simulated altitude of 1000 feet, B) graph of slant range to target at detection versus JNDA-log (2 cpd) for POL targets and simulated altitude of 2000 feet

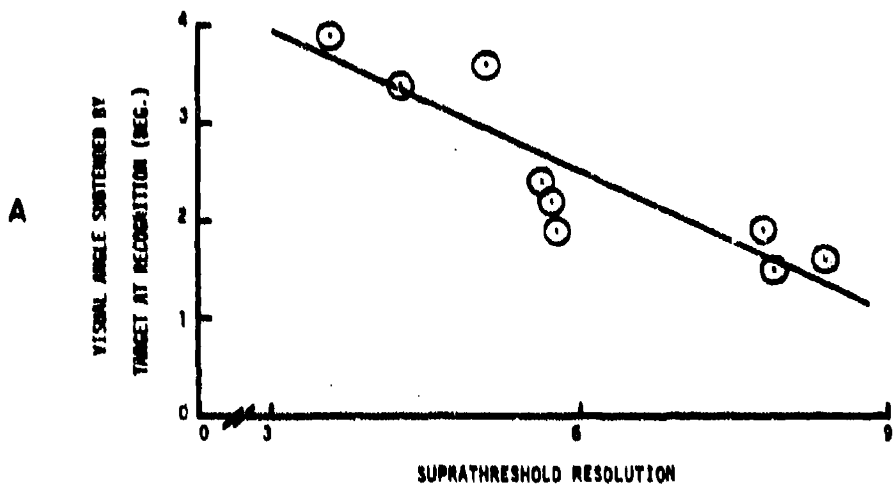

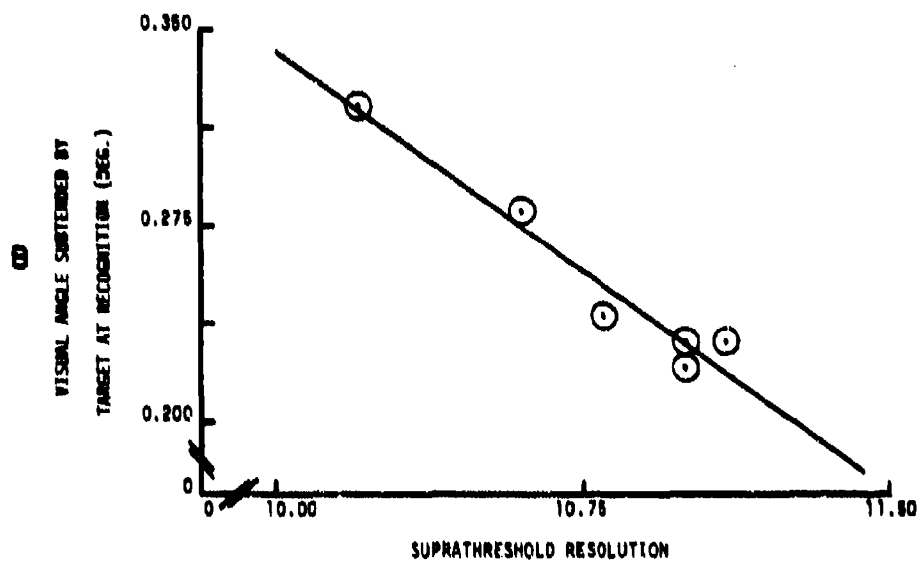

Fig. C.11. A) Graph of angle subtended by target at recognition versus Suprathreshold Resolution for the target recognition study of Chapter 4, B) graph of angle subtended by target at recognition versus Suprathreshold Resolution for the target recognition study of Chapter 5

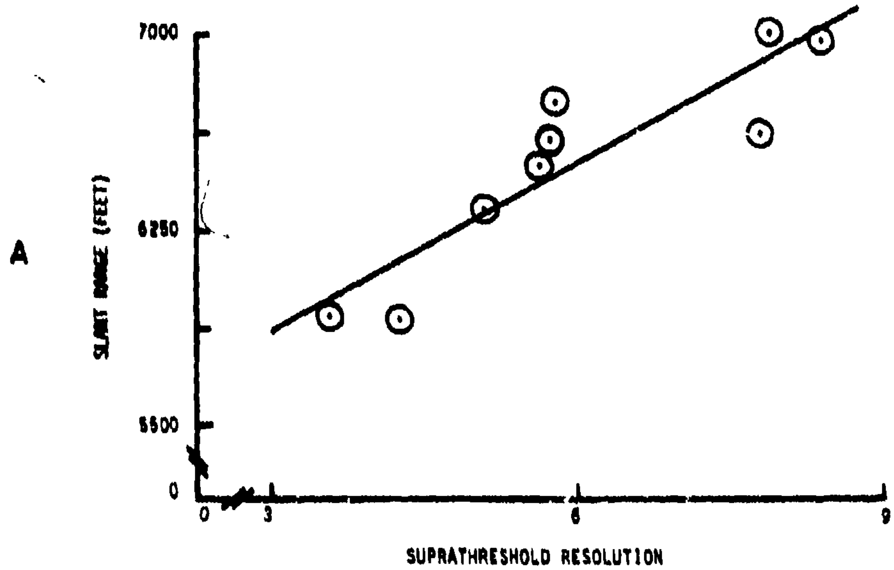

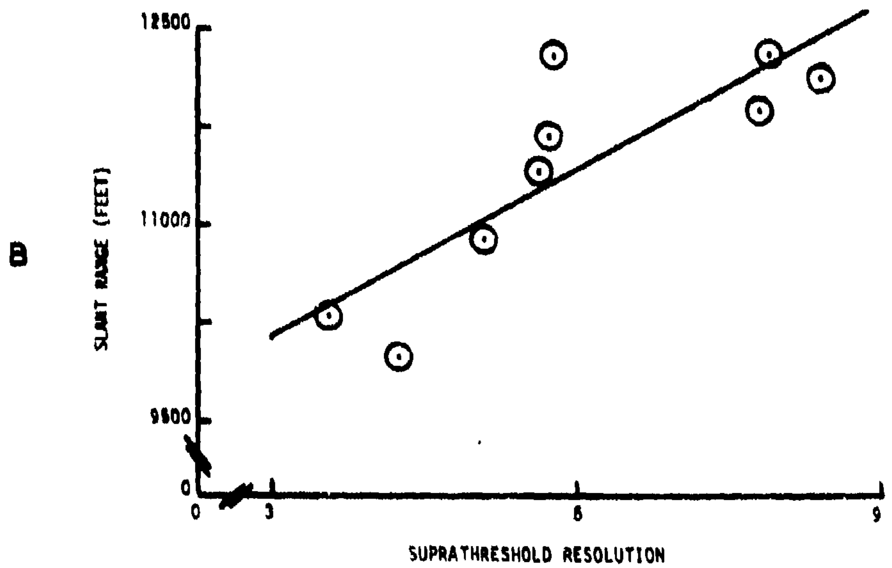

Fig. C.12. A) Graph of slant range to target at detection versus Suprathreshold Resolution for POL targets and simulated altitude of 1000 feet, B) graph of slant range to target at detection versus Suprathreshold Resolution for POL targets and simulated altitude of 2000 feet

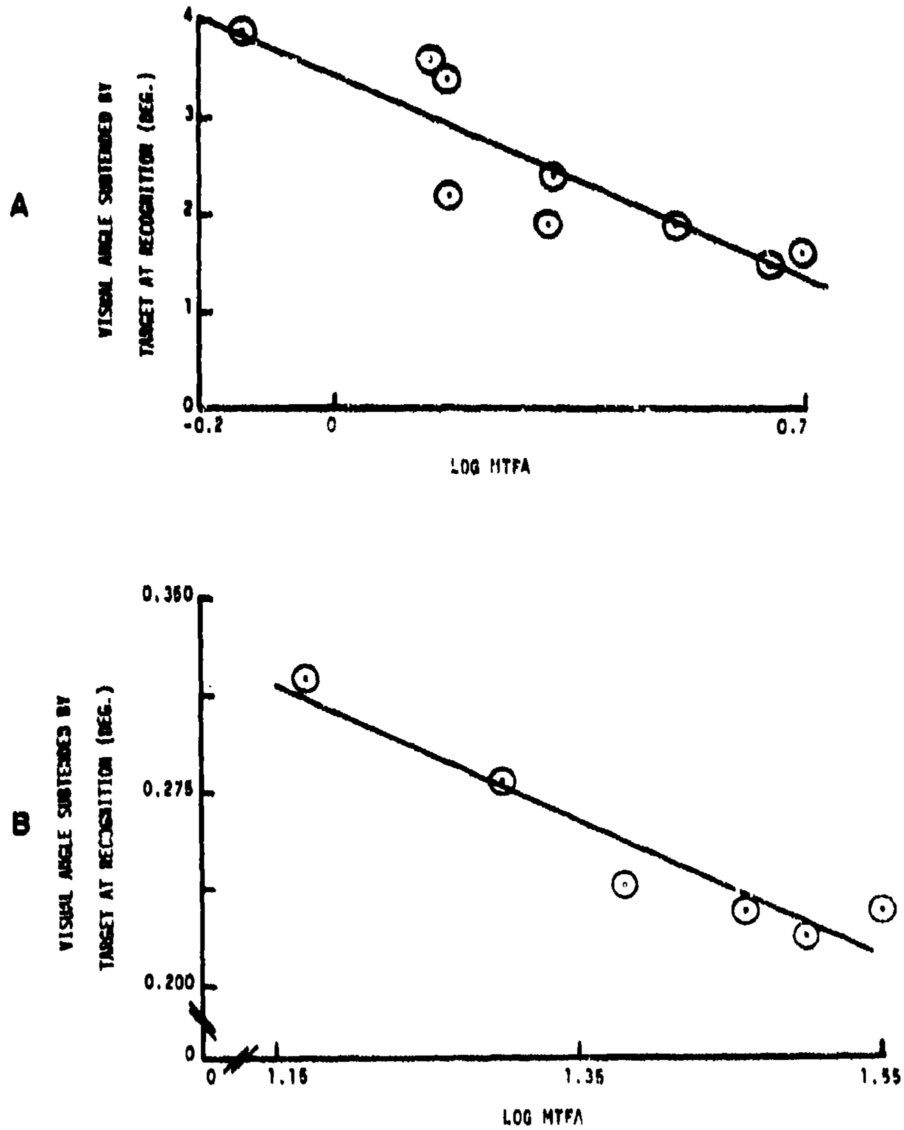

Fig. C.13. A) Graph of angle subtended by target at recognition versus log MTFA for the target recognition study of Chapter 4, B) graph of angle subtended by target at recognition versus log MTFA for the target recognition study of Chapter 5

A

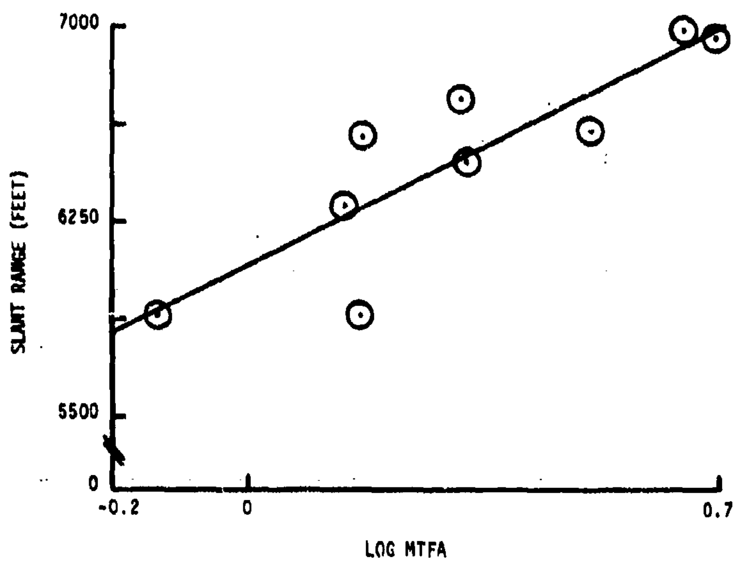

B

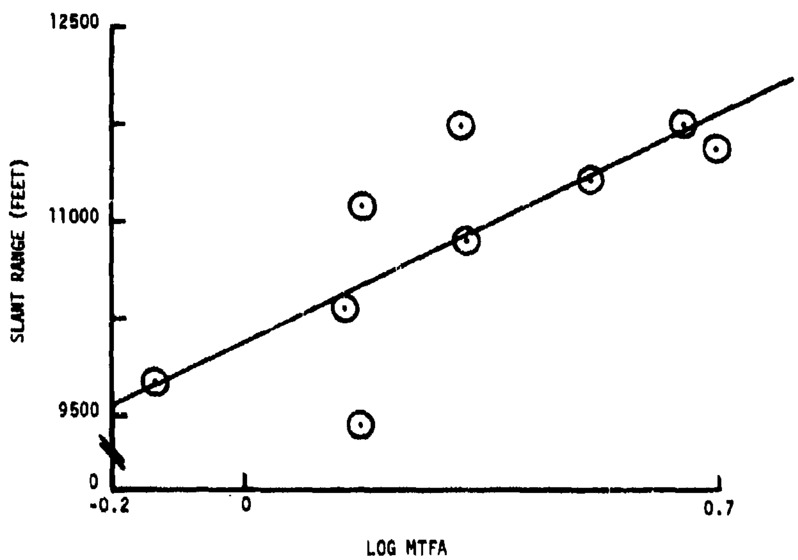

Fig. C.14. A) Graph of slant range to target at detection versus log MTFA for POL targets and simulated altitude of 1000 feet, B) graph of slant range to target at detection versus log MTFA for POL targets and simulated altitude of 2000 feet

A

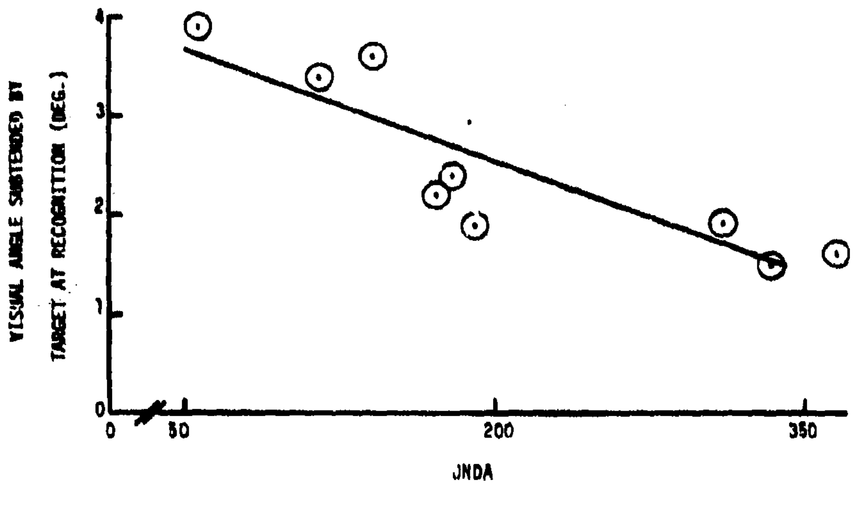

B

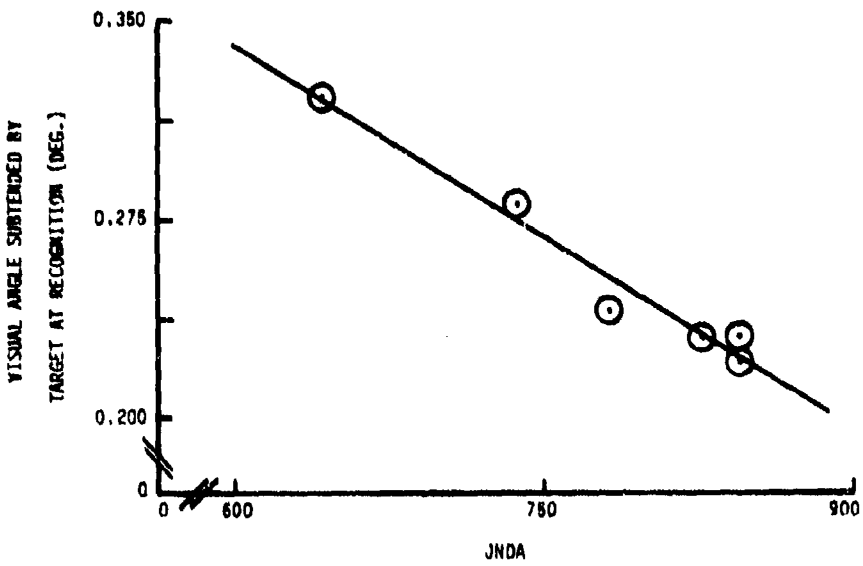

Fig. C.15. A) Graph of angle subtended by target at recognition versus JNDA for the target recognition study of Chapter 4, B) graph of angle subtended by target at recognition versus JNDA for the target recognition study of Chapter 5

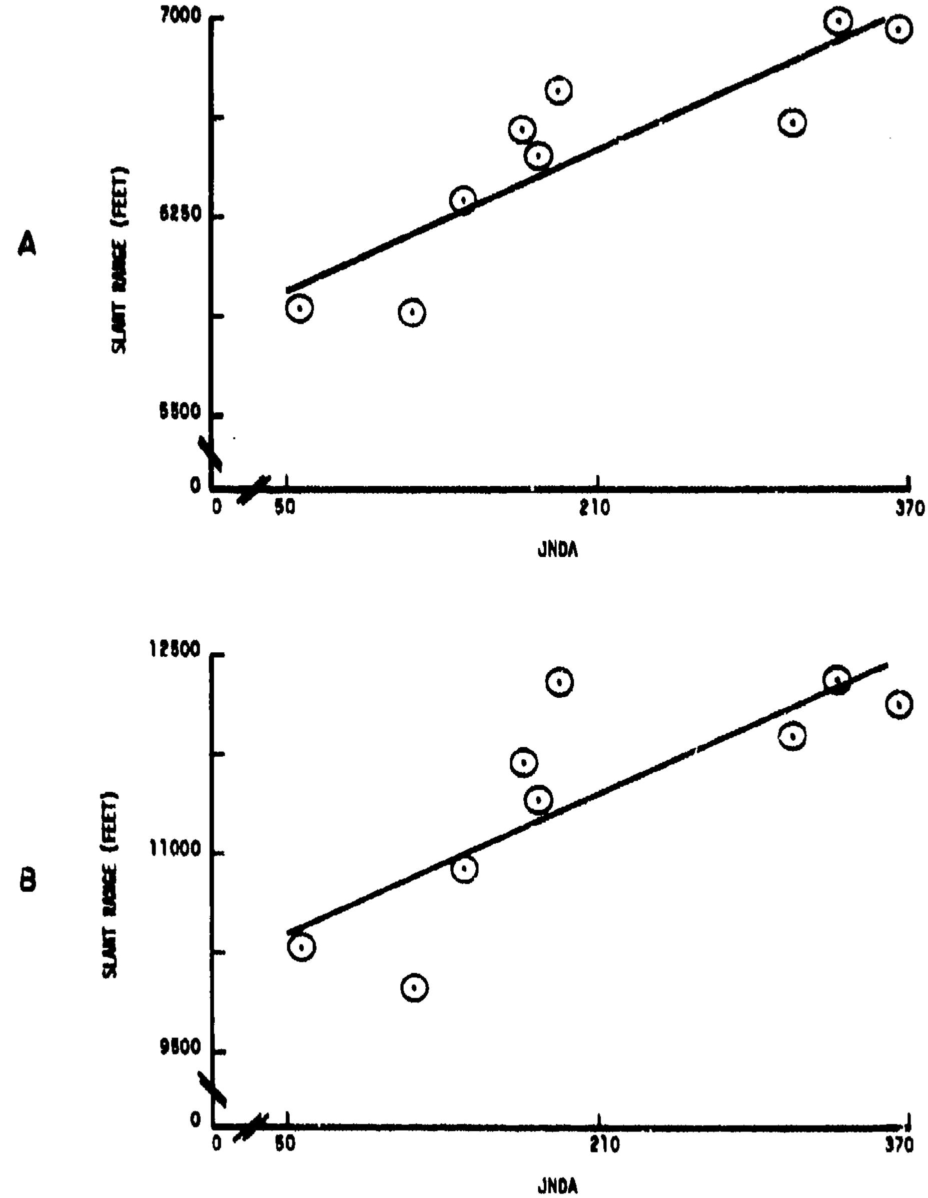

Fig. C.16. A) Graph of slant range to target at detection versus JNDA for POL targets and simulated altitude of 1000 feet, B) graph of slant range to target at detection versus JNDA for POL targets and simulated altitude of 2000 feet

A

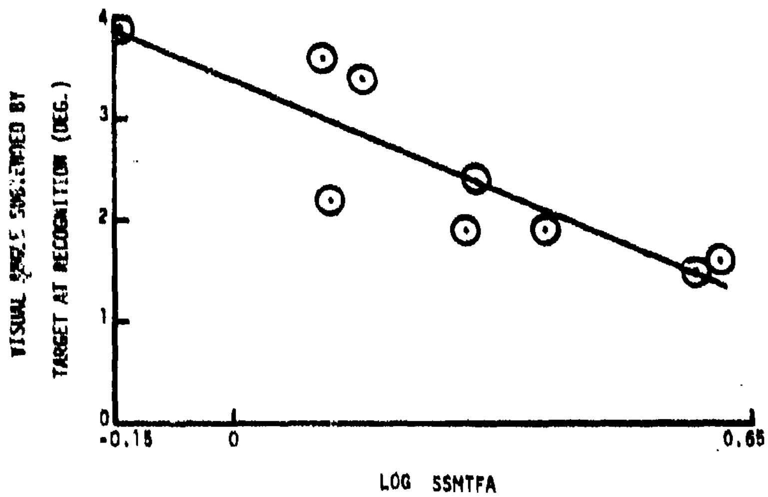

B

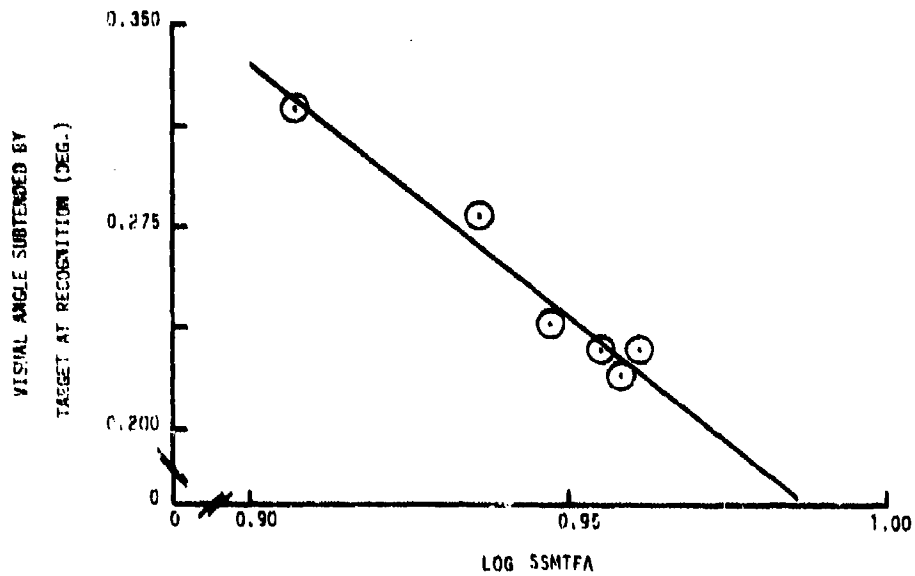

Fig. C.17. A) Graph of angle subtended by target at recognition versus log SSMTFA for the target recognition study of Chapter 4, B) graph of angle subtended by target at recognition versus log SSMTFA for the target recognition study of Chapter 5

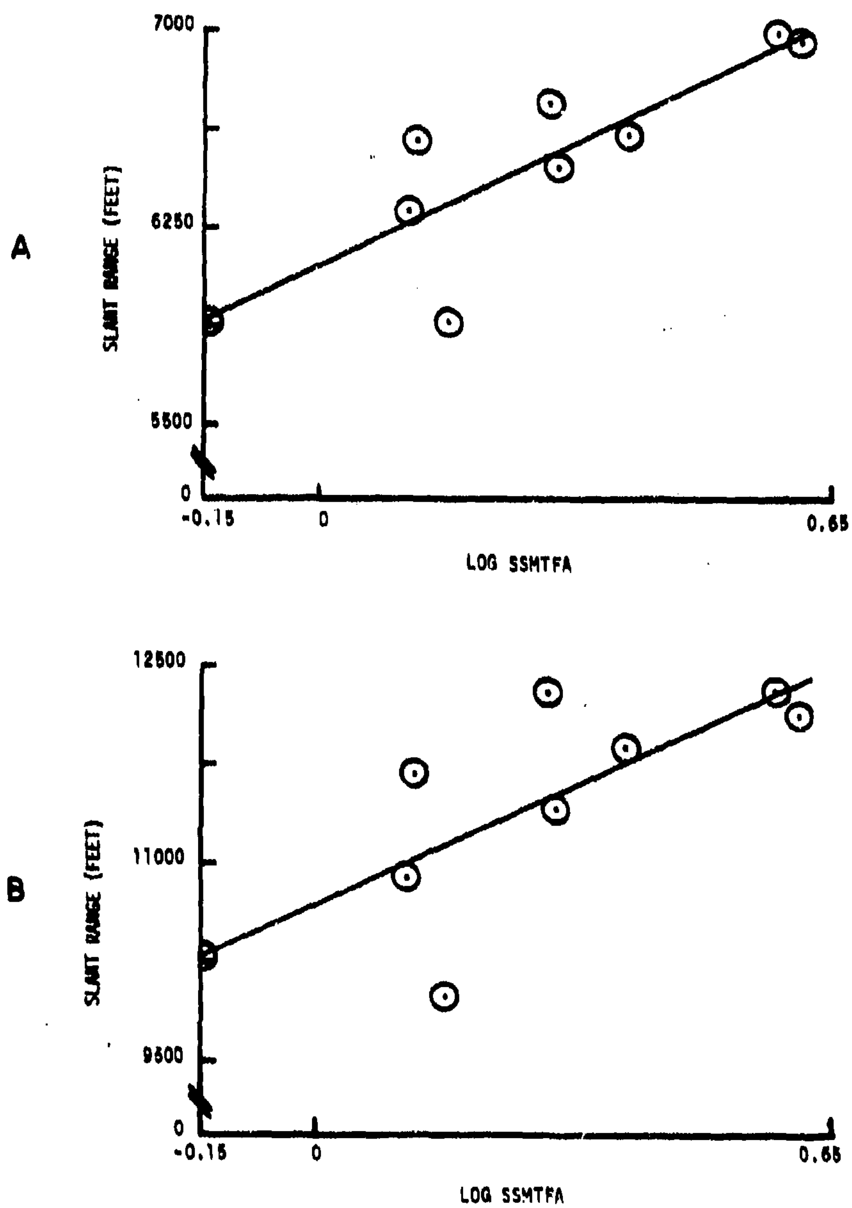

Fig. C.18. A) Graph of slant range to target at detection versus log SSMTFA for POL targets and simulated altitude of 1000 feet, B) graph of slant range to target at detection versus log SSMTFA for POL targets and simulated altitude of 2000 feet

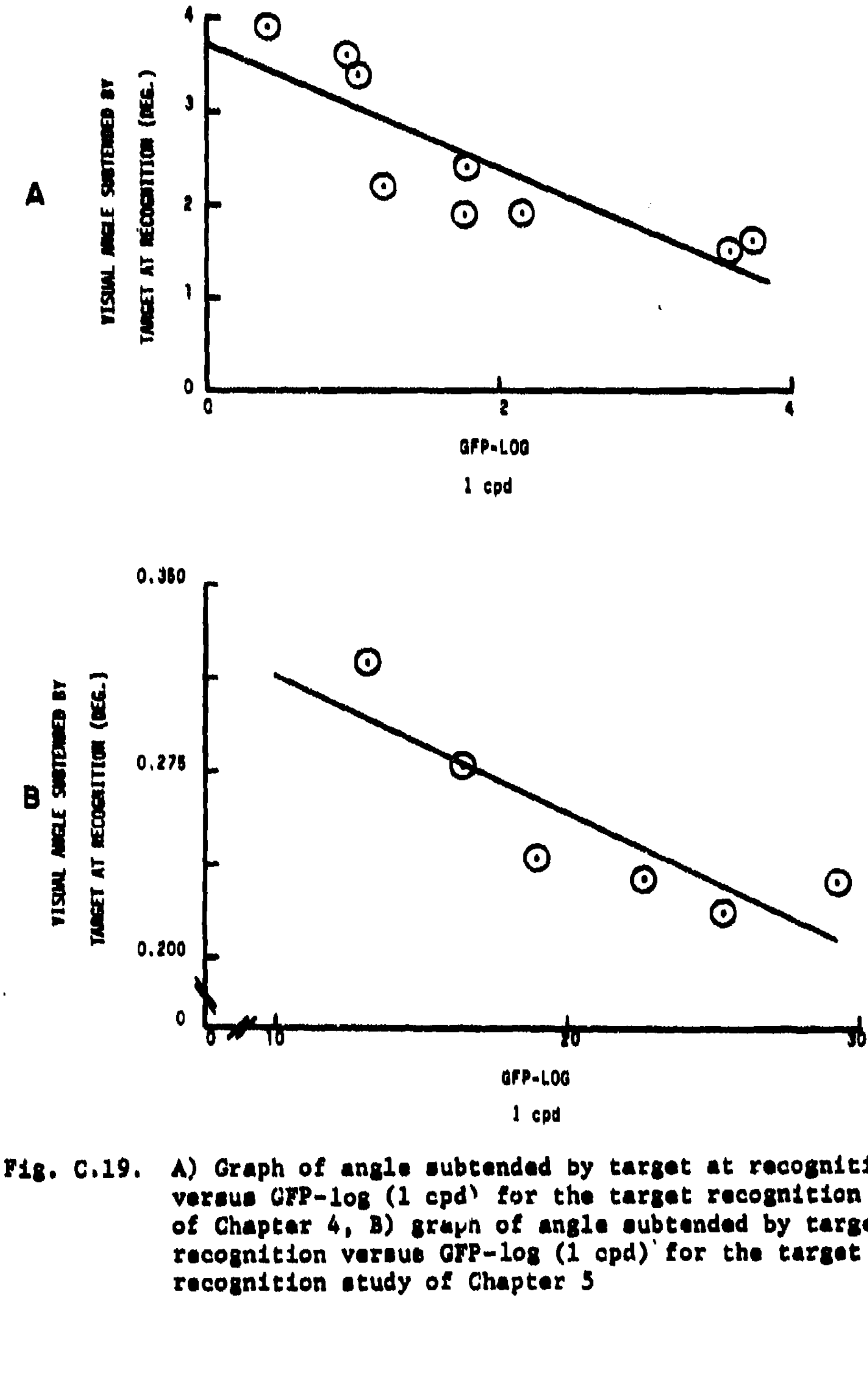

Fig. C.19. A) Graph of angle subtended by target at recognition versus GFP-log (1 cpd) for the target recognition study of Chapter 4, B) graph of angle subtended by target at recognition versus GFP-log (1 cpd) for the target recognition study of Chapter 5

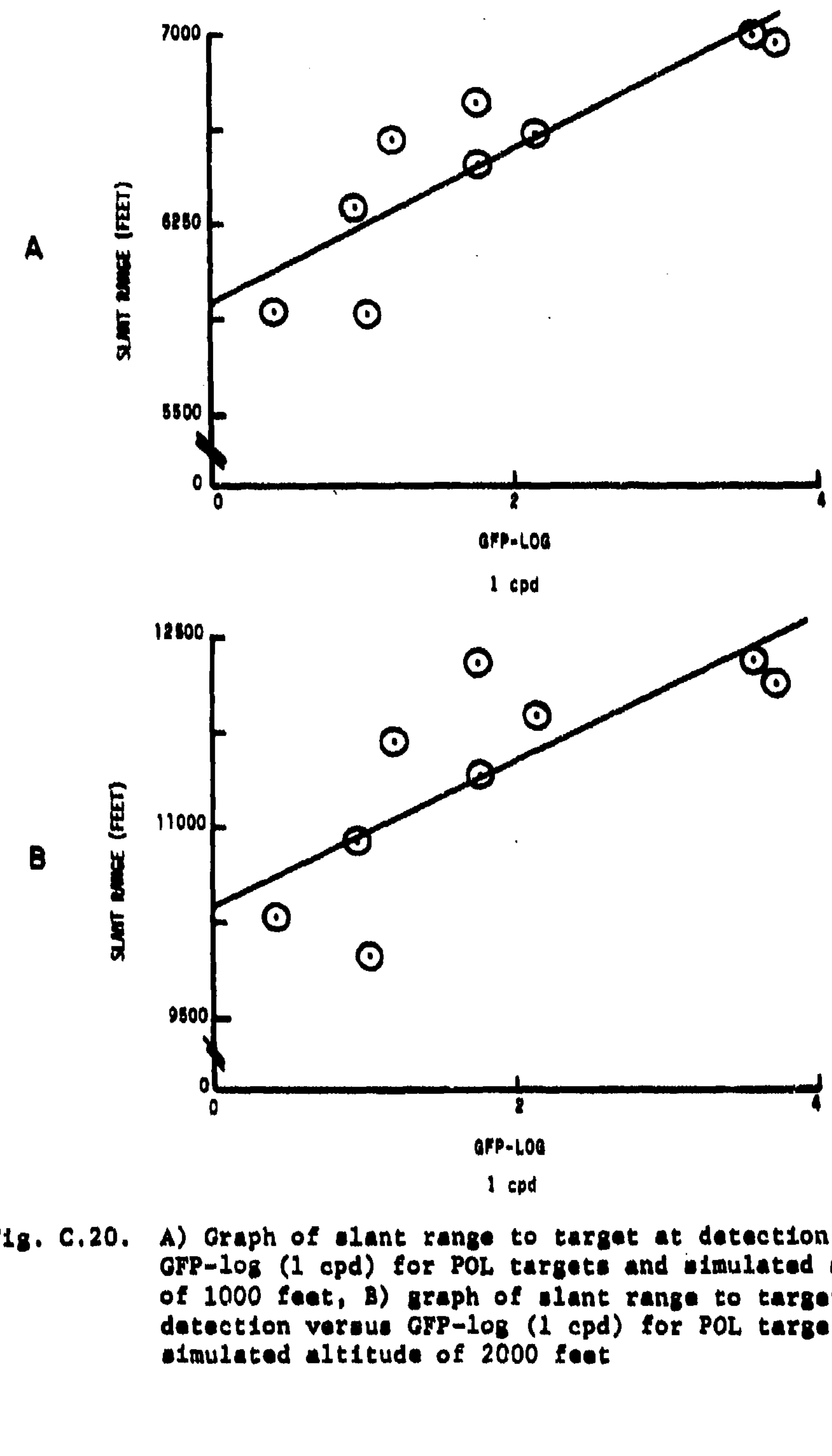

Fig. C.20. A) Graph of slant range to target at detection versus GFP-log (1 cpd) for POL targets and simulated altitude of 1000 feet, B) graph of slant range to target at detection versus GFP-log (1 cpd) for POL targets and simulated altitude of 2000 feet

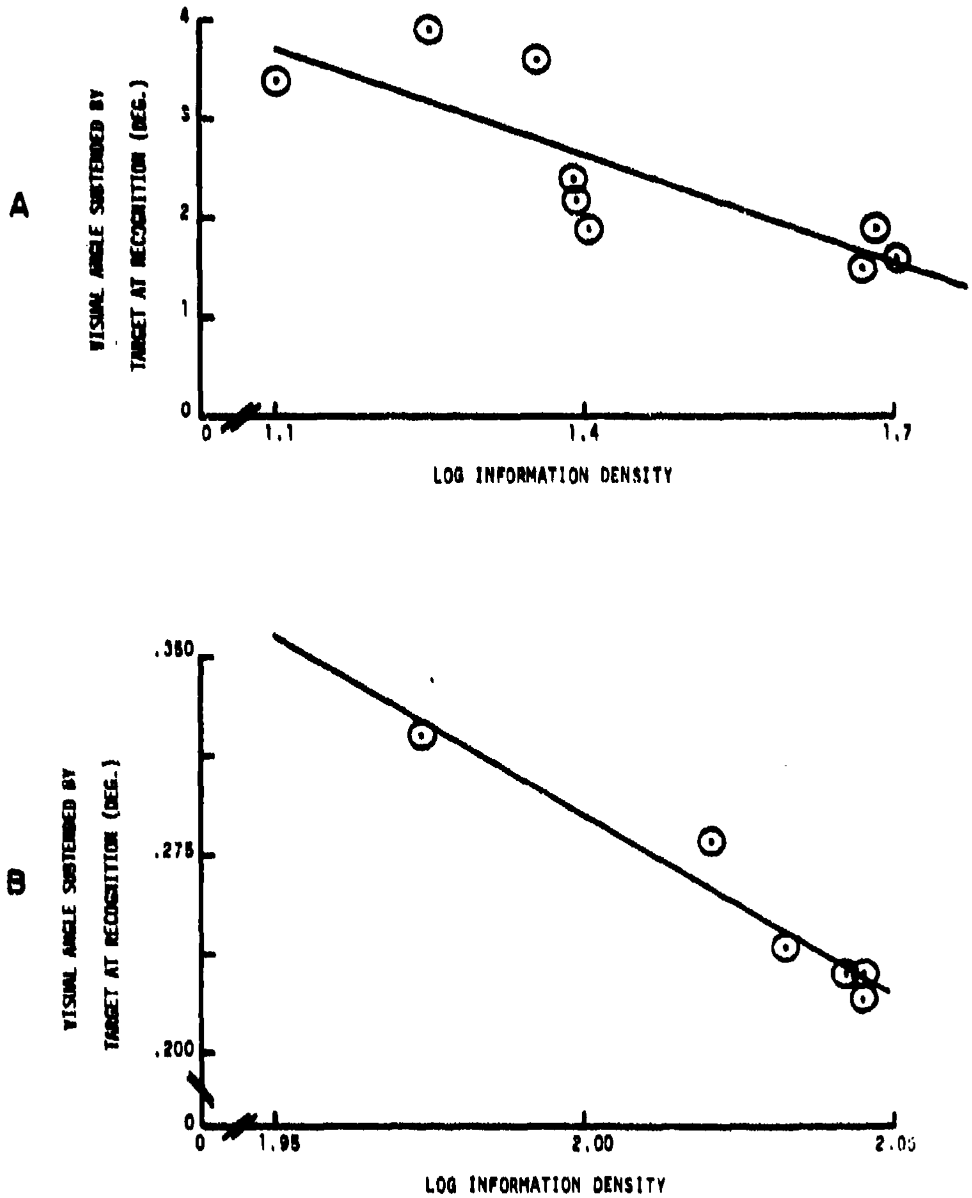

Fig. C.21. A) Graph of angle subtended by target at recognition versus log Information Density for the target recognition study of Chapter 4, B) graph of angle subtended by target at recognition versus log Information Density for the target recognition study of Chapter 5

A

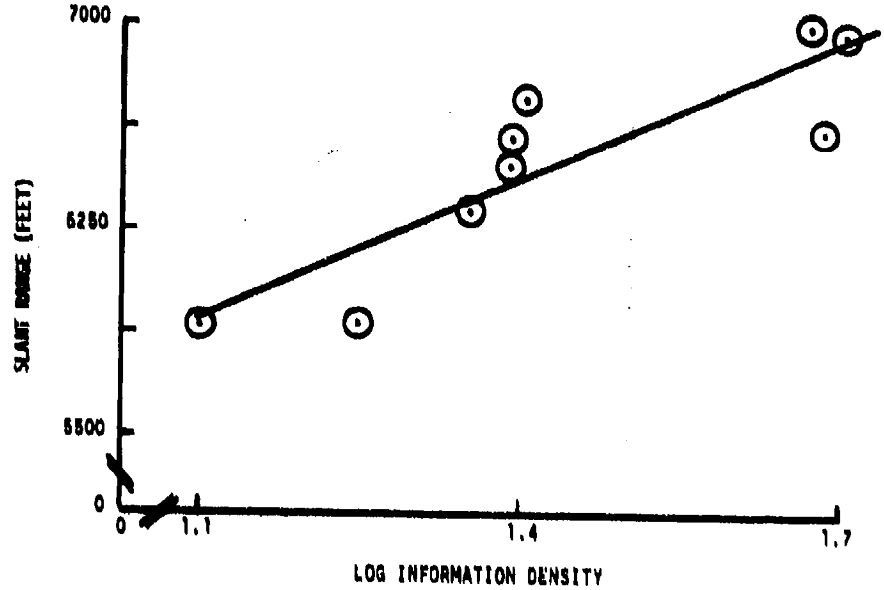

B

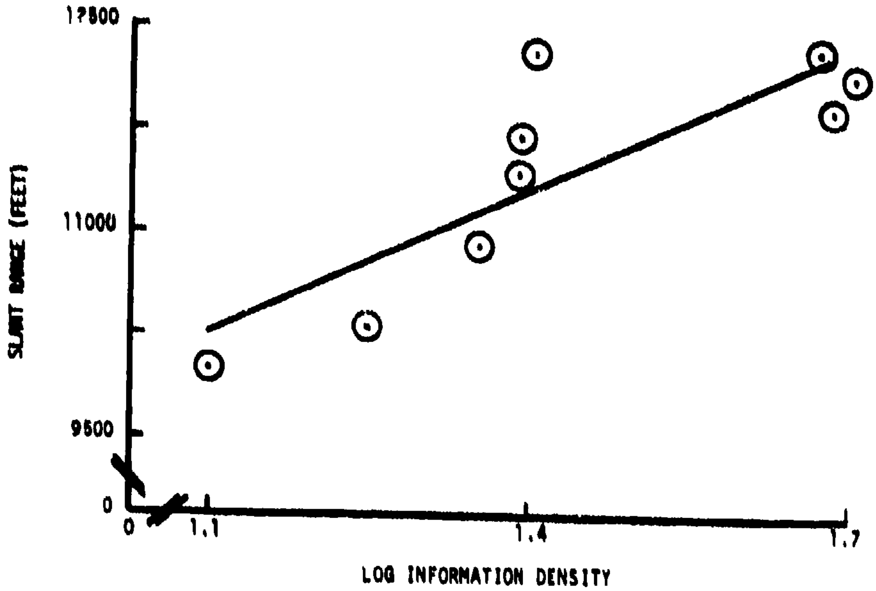

Fig. C.22. A) Graph of slant range to target at detection versus log Information Density for POL targets and simulated altitude of 1000 feet, B) graph of slant range to target at detection versus log Information Density for POL targets and simulated altitude of 2000 feet

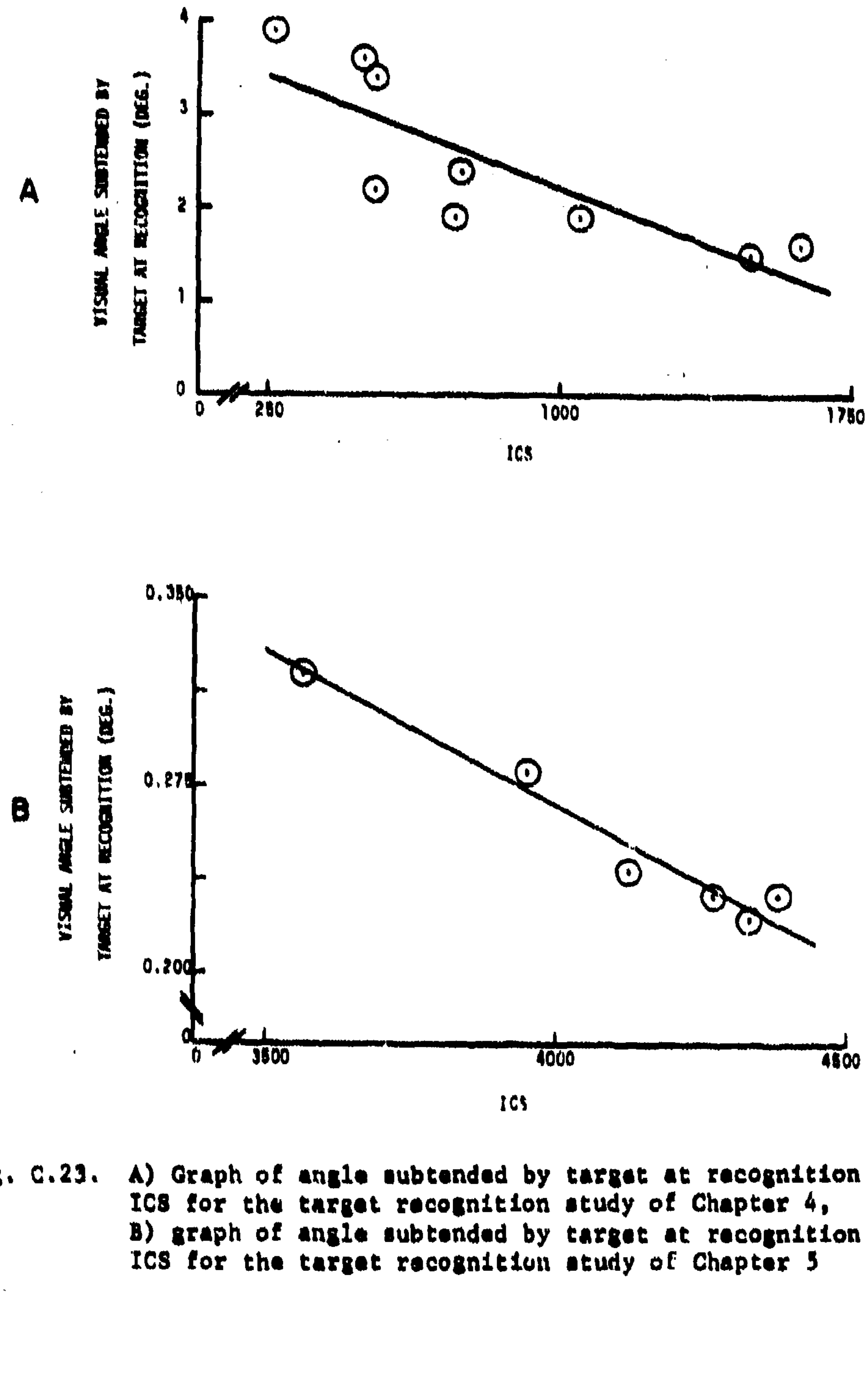

Fig. C.23. A) Graph of angle subtended by target at recognition versus ICS for the target recognition study of Chapter 4, B) graph of angle subtended by target at recognition versus ICS for the target recognition study of Chapter 5

A

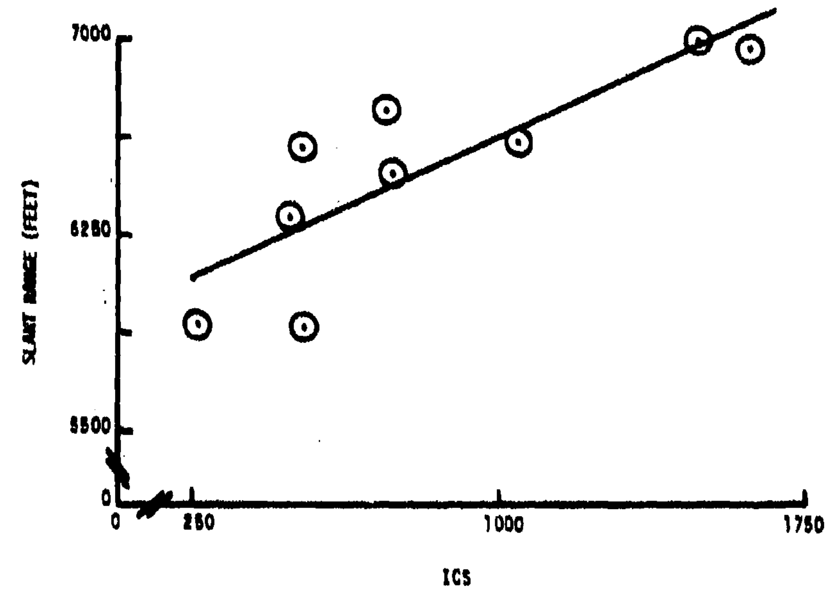

B

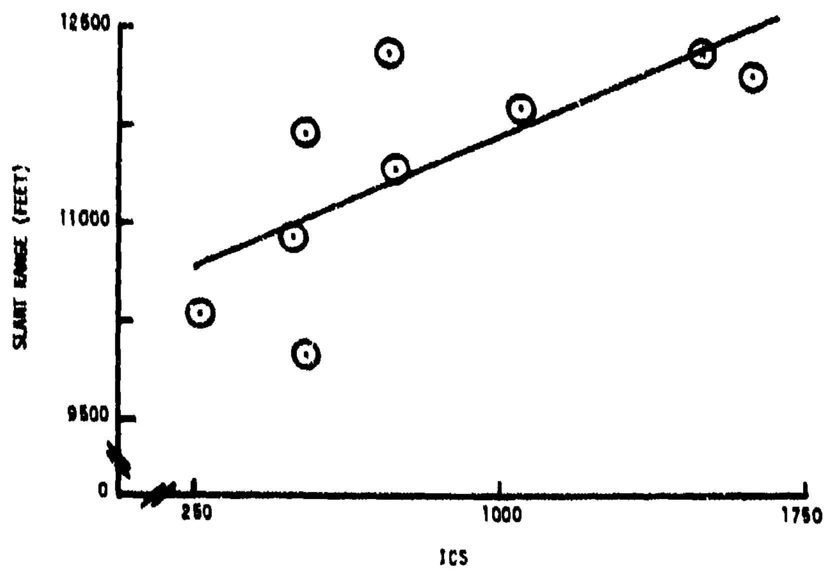

Fig. C.24. A) Graph of slant range to target at detection versus ICS for POL targets and simulated altitude of 1000 feet, B) graph of slant range to target at detection versus ICS for POL targets and simulated altitude of 2000 feet

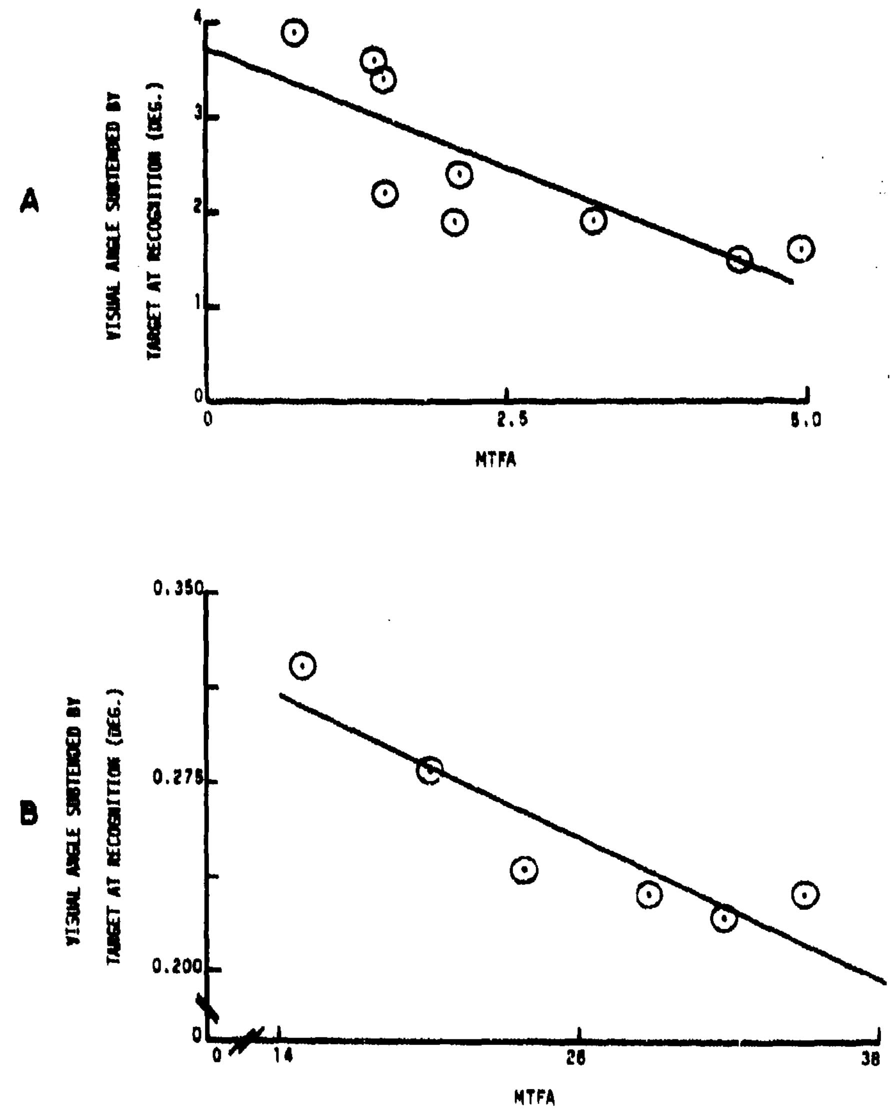

Fig. C.25. A) Graph of angle subtended by target at recognition versus MTFA for the target recognition study of Chapter 4, B) graph of angle subtended by target at recognition versus MTFA for the target recognition study of Chapter 5

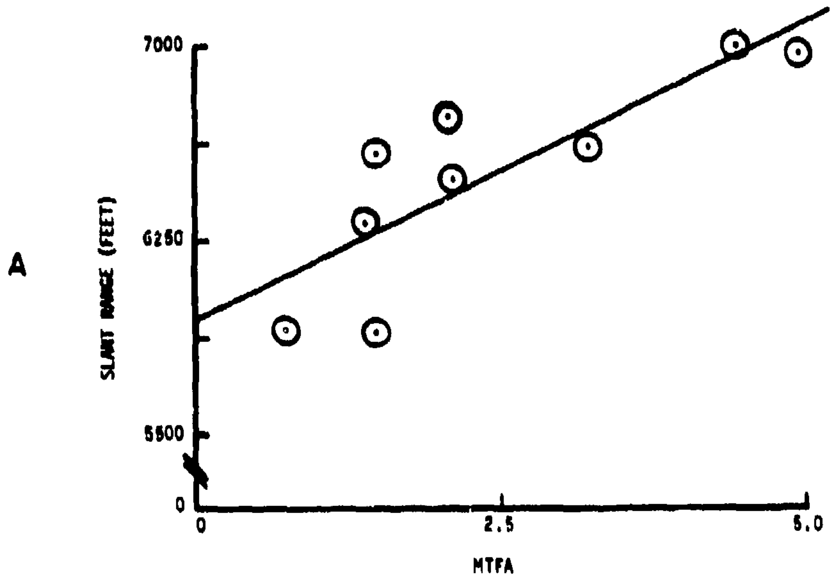

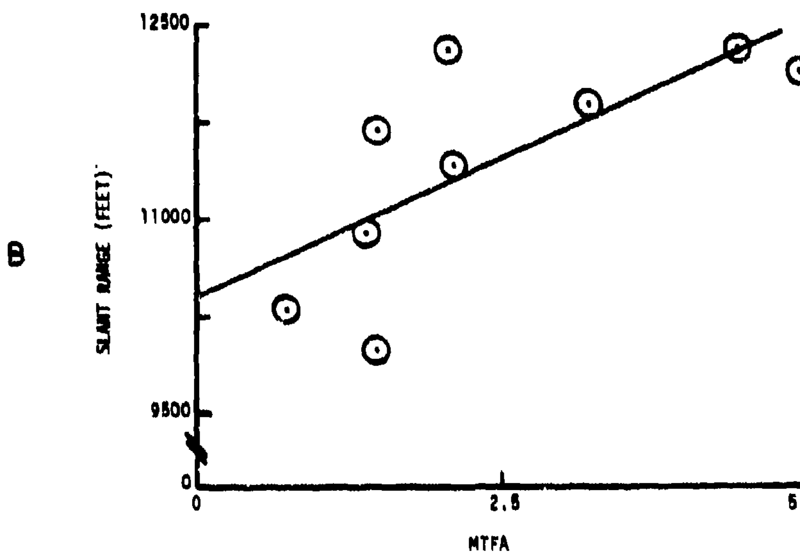

Fig. C.26. A) Graph of slant range to target at detection versus MTFA for POL targets and simulated altitude of 1000 feet, B) graph of slant range to target at detection versus MTFA for POL targets and simulated altitude of 2000 feet

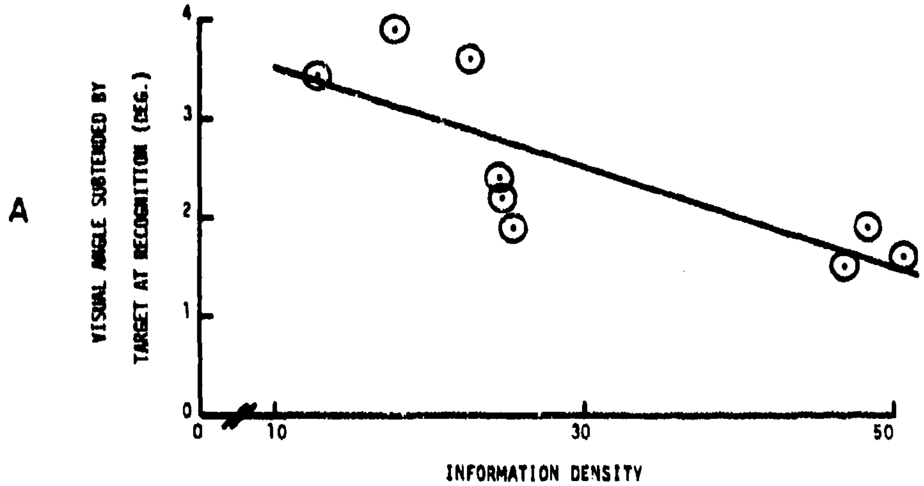

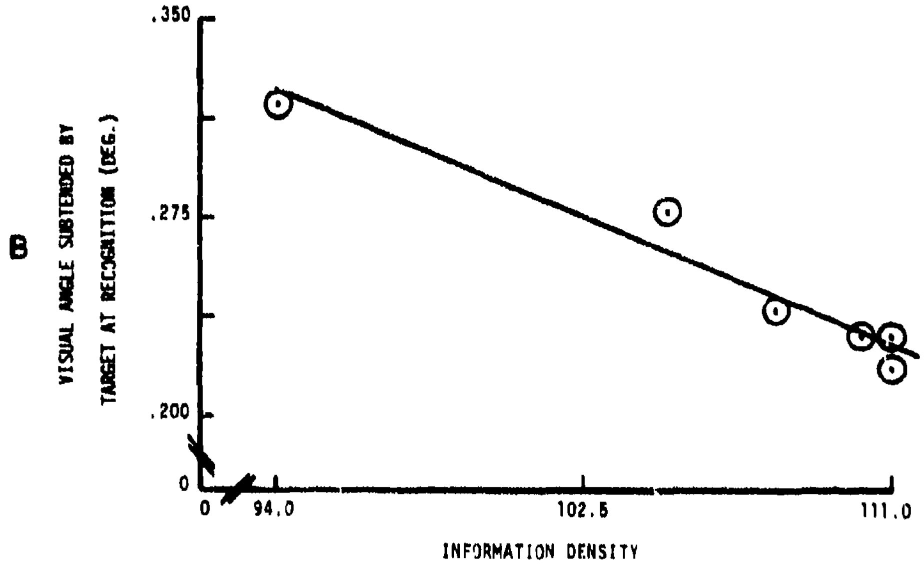

Fig. C.27. A) Graph of angle subtended by target at recognition versus Information Density for the target recognition study of Chapter 4, B) graph of angle subtended by target at recognition versus Information Density for the target recognition study of Chapter 5

A

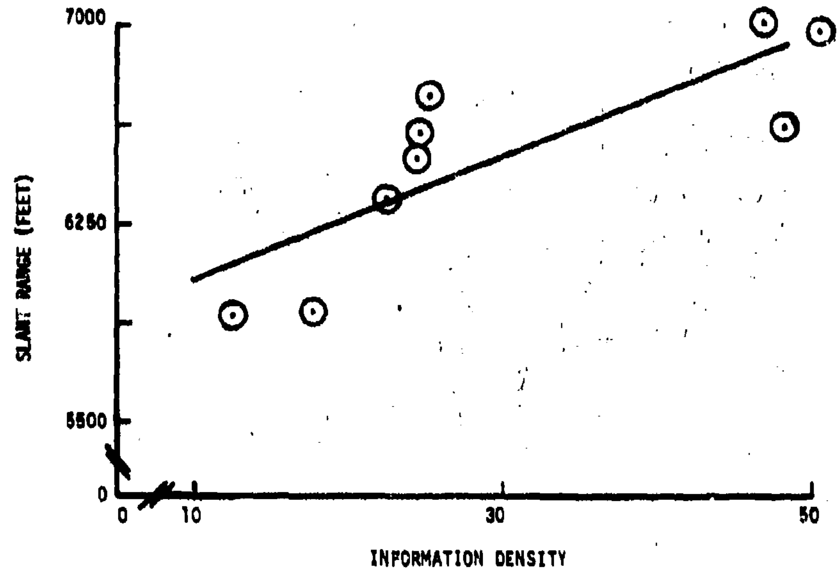

B

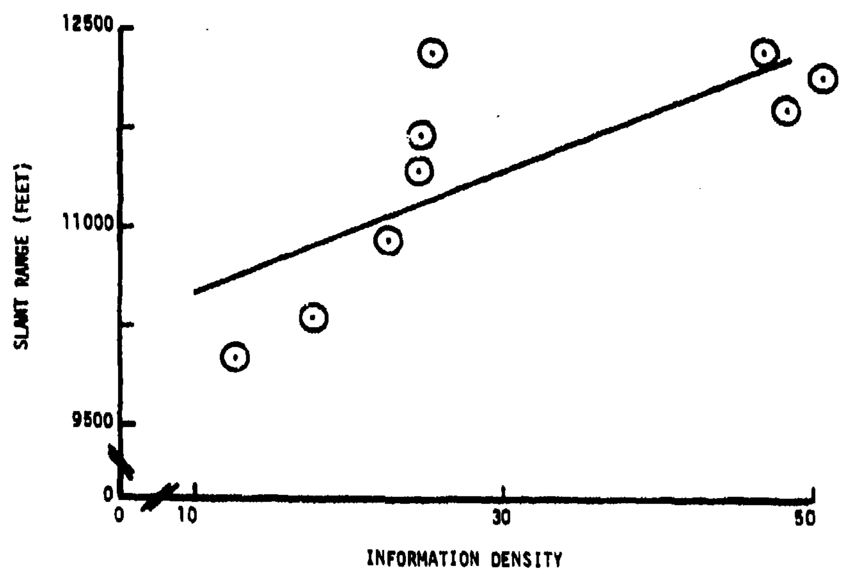

Fig. C.28. A) Graph of slant range to target at detection versus Information Density for POL targets and simulated altitude of 1000 feet, B) graph of slant range to target at detection versus Information Density for POL targets and simulated altitude of 2000 feet

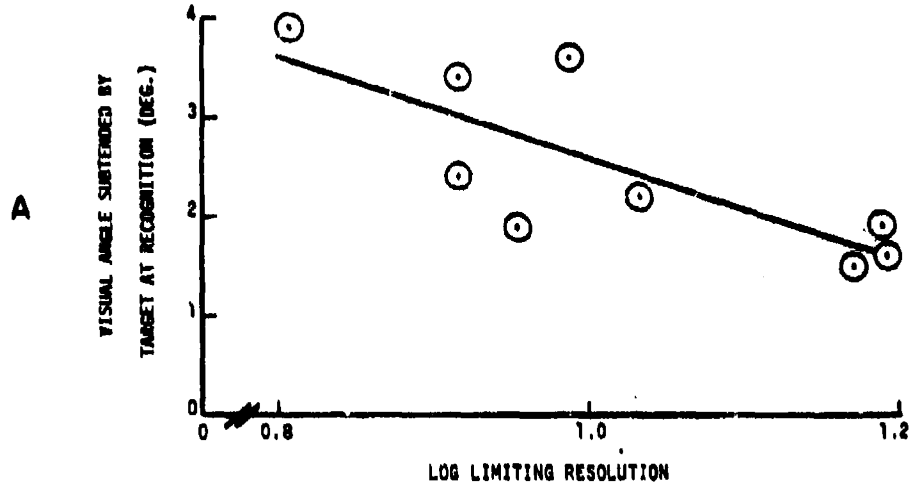

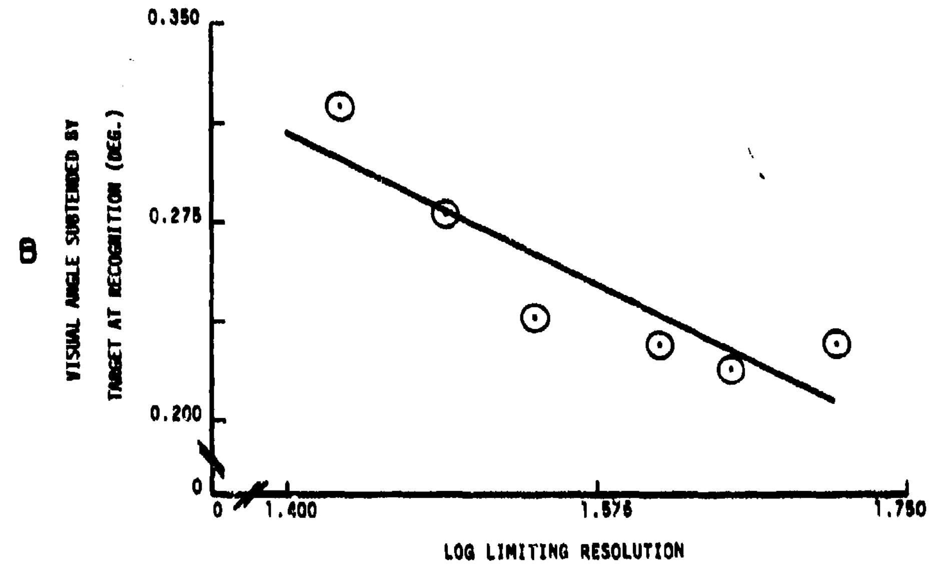

Fig. C.29. A) Graph of angle subtended by target at recognition versus log Limiting Resolution for the target recognition study of Chapter 4, B) graph of angle subtended by target at recognition versus log Limiting Resolution for the target recognition study of Chapter 5

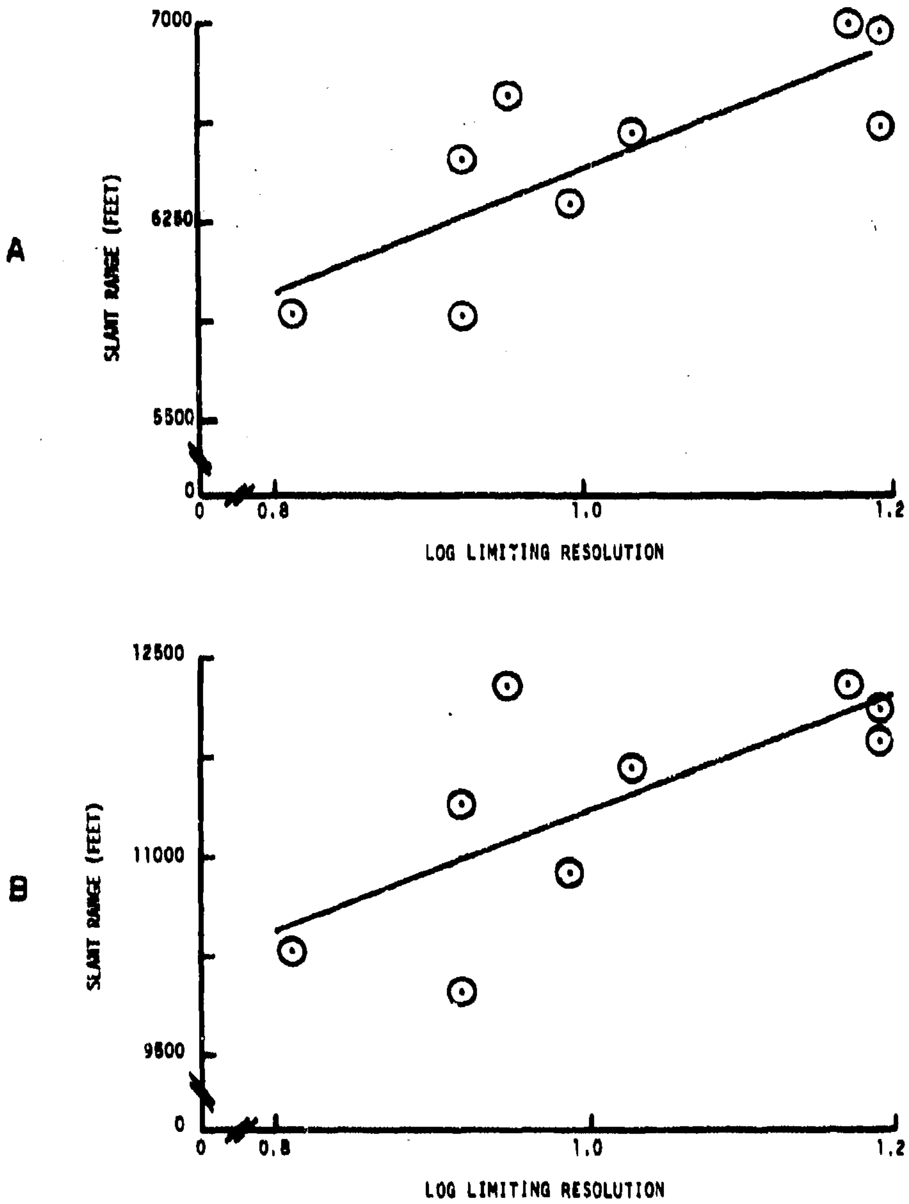

Fig. C.30. A) Graph of slant range to target at detection versus log Limiting Resolution for POL targets and simulated altitude of 1000 feet, B) graph of slant range to target at detection versus log Limiting Resolution for POL targets and simulated altitude of 2000 feet

A

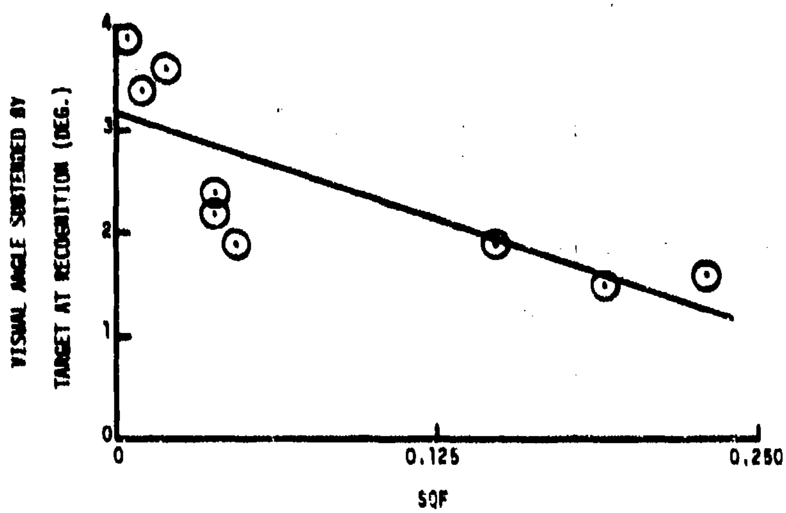

B

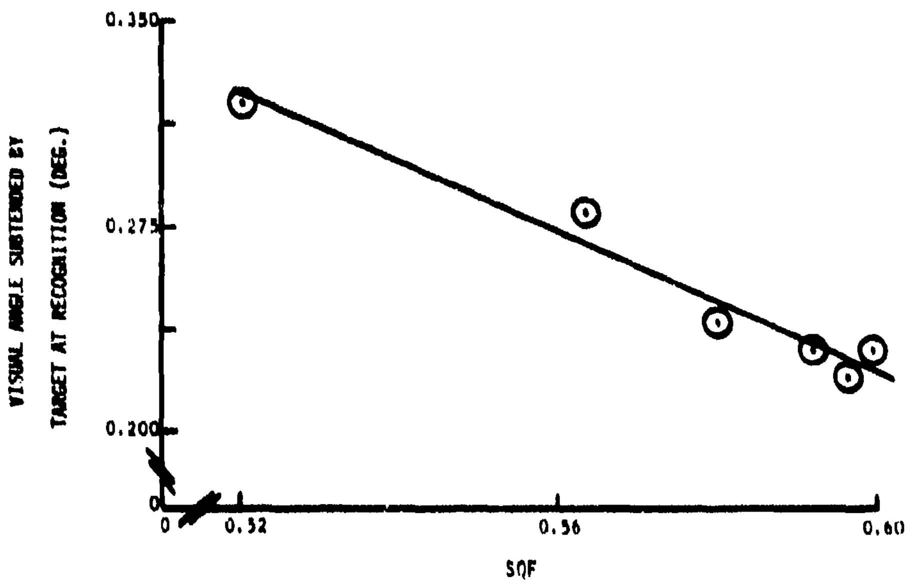

Fig. C.31. A) Graph of angle subtended by target at recognition versus SQF for the target recognition study of Chapter 4, B) graph of angle subtended by target at recognition versus SQF for the target recognition study of Chapter 5

A

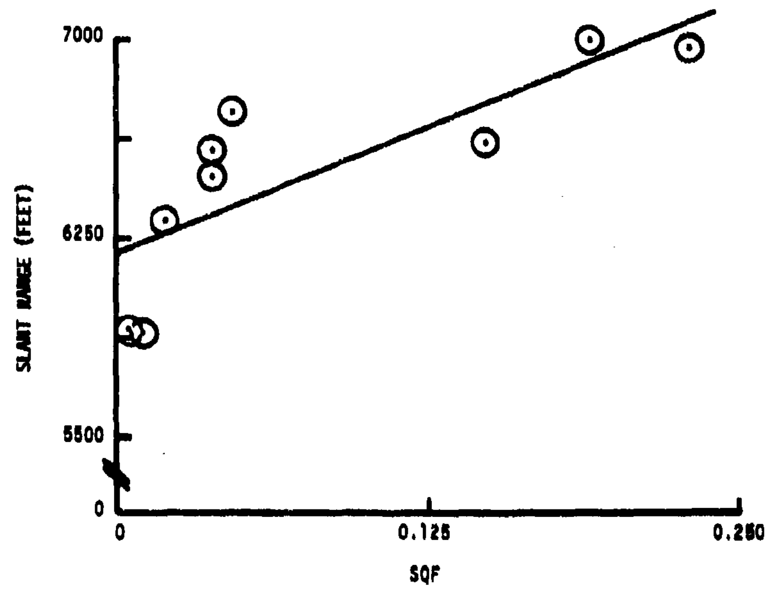

B

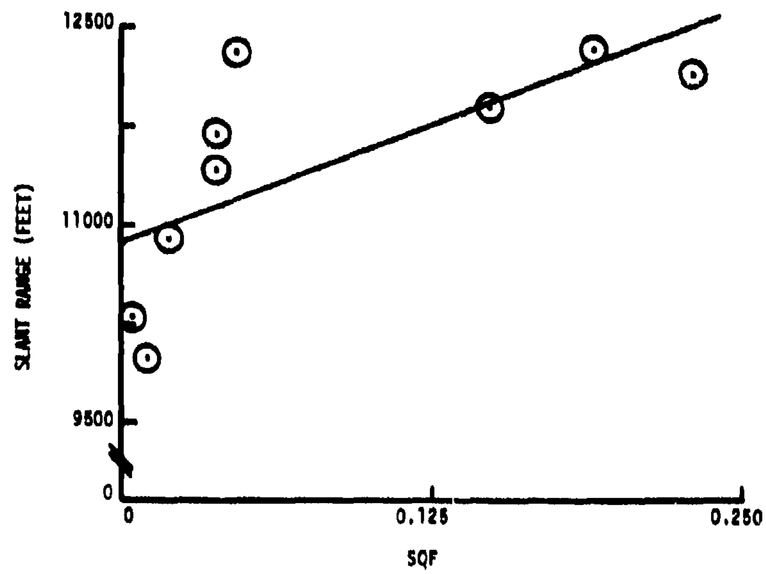

Fig. C.32. A) Graph of slant range to target at detection versus SQF for POL targets and simulated altitude of 1000 feet, B) graph of slant range to target at detection versus SQF for POL targets and simulated altitude of 2000 feet

A

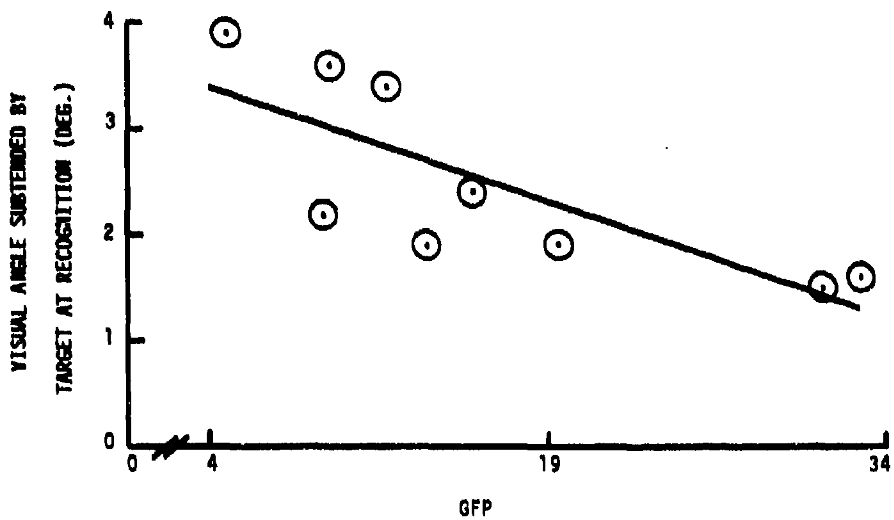

Fig. C.33. A) Graph of angle subtended by target at recognition versus GFP for the target recognition study of Chapter 4

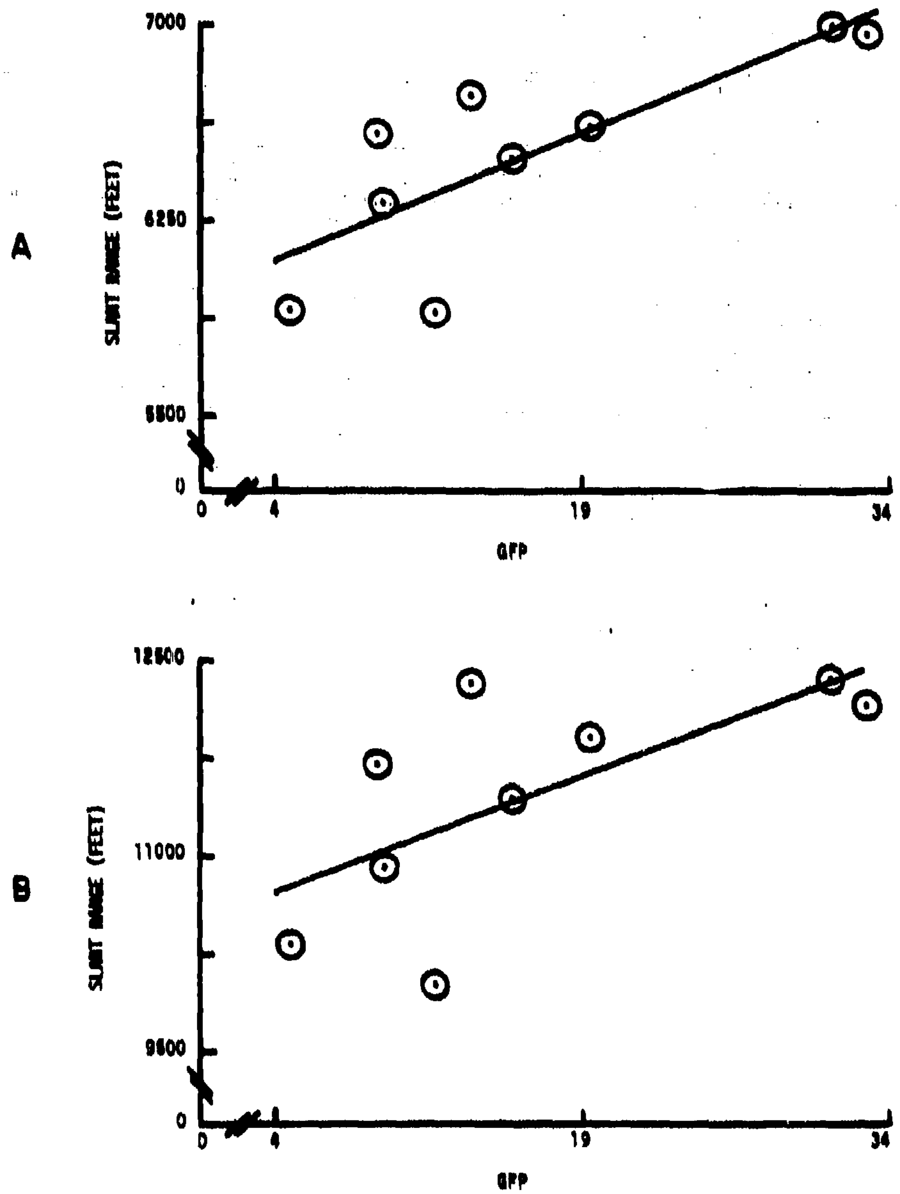

Fig. C.34. A) Graph of slant range to target at detection versus GFP for POL targets and simulated altitude of 1000 feet, B) graph of slant range to target at detection versus GFP for POL targets and simulated altitude of 2000 feet

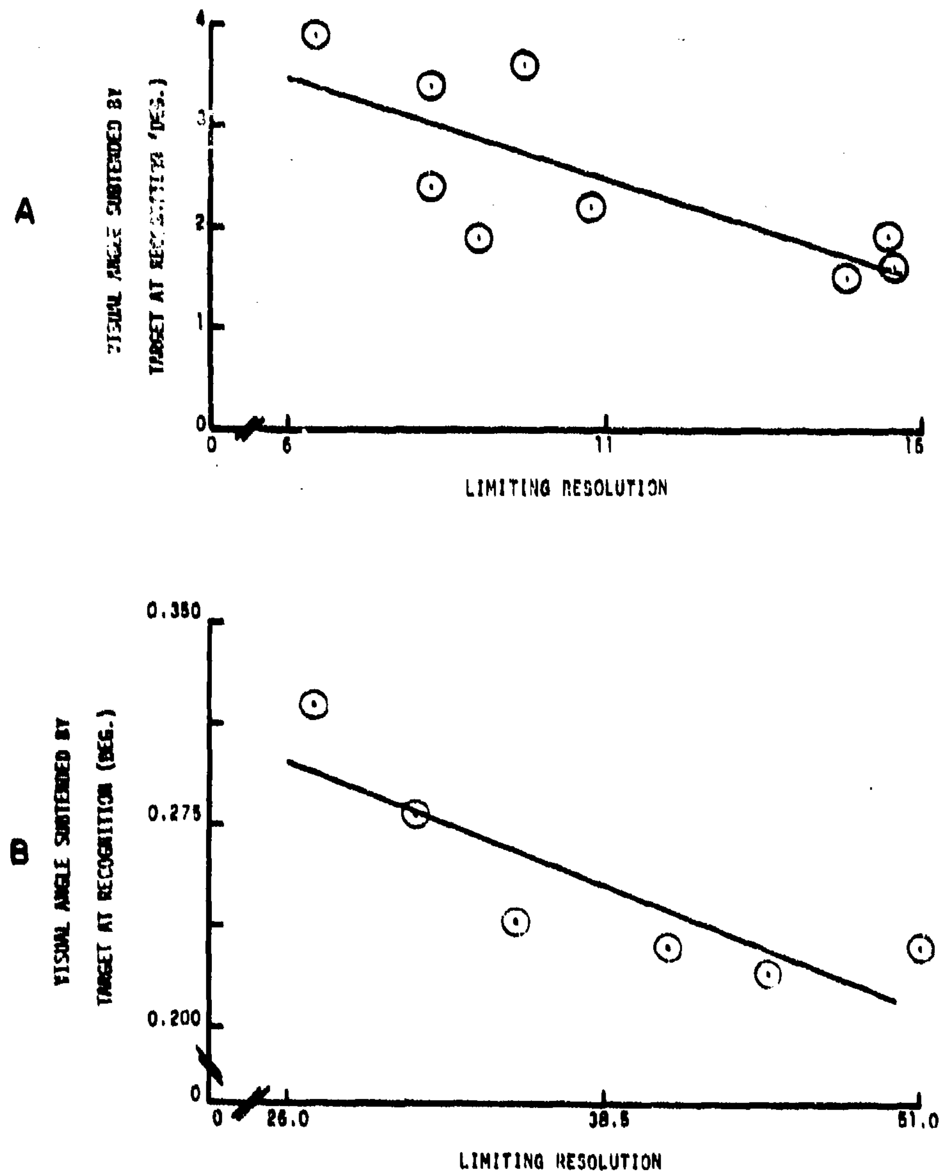

Fig. C.35. A) Graph of angle subtended by target at recognition versus Limiting Resolution for the target recognition study of Chapter 4, B) graph of angle subtended by target at recognition versus Limiting Resolution for the target recognition study of Chapter 5

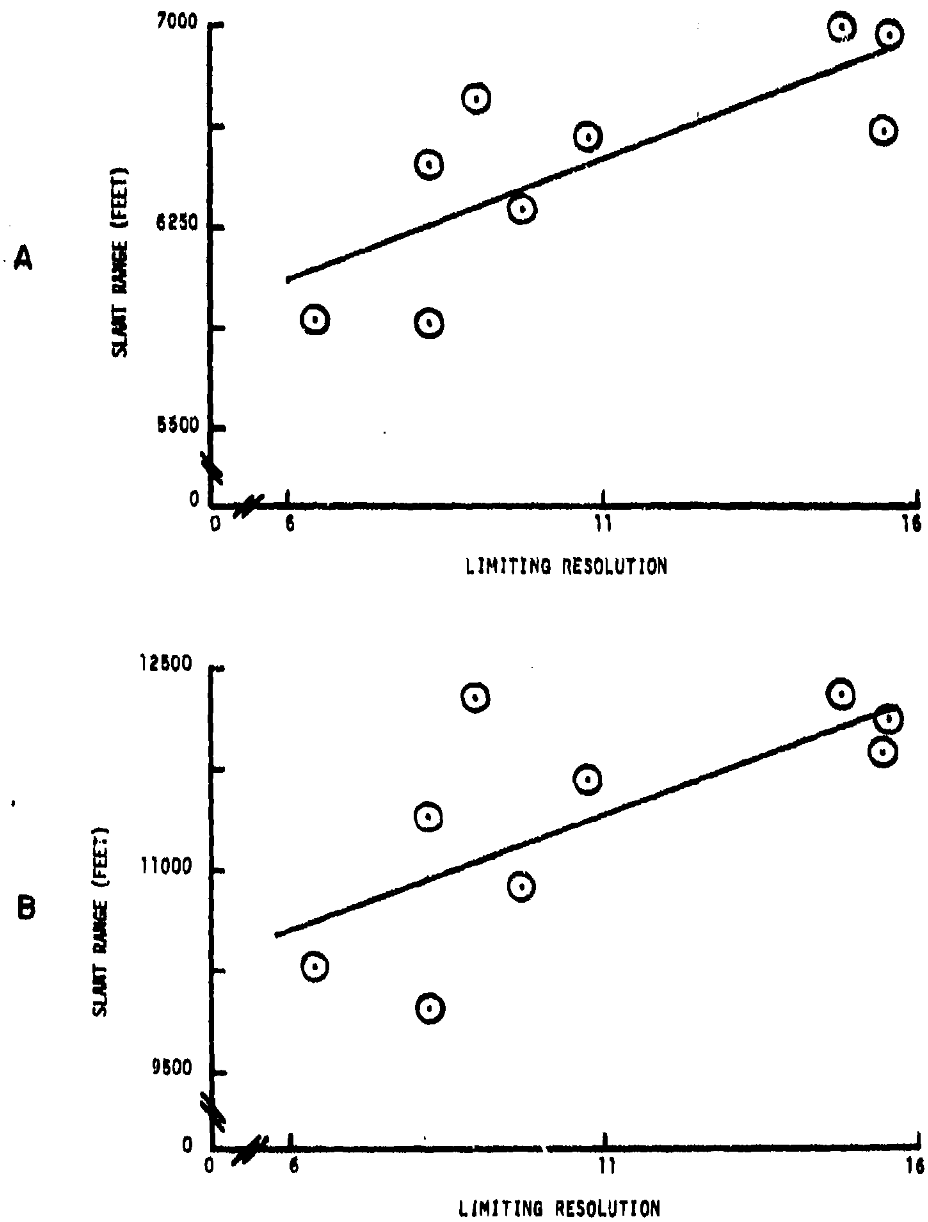

Fig. C.36. A) Graph of slant range to target at detection versus Limiting Resolution for POL targets and simulated altitude of 1000 feet, B) graph of slant range to target at detection versus Limiting Resolution for POL targets and simulated altitude of 2000 feet

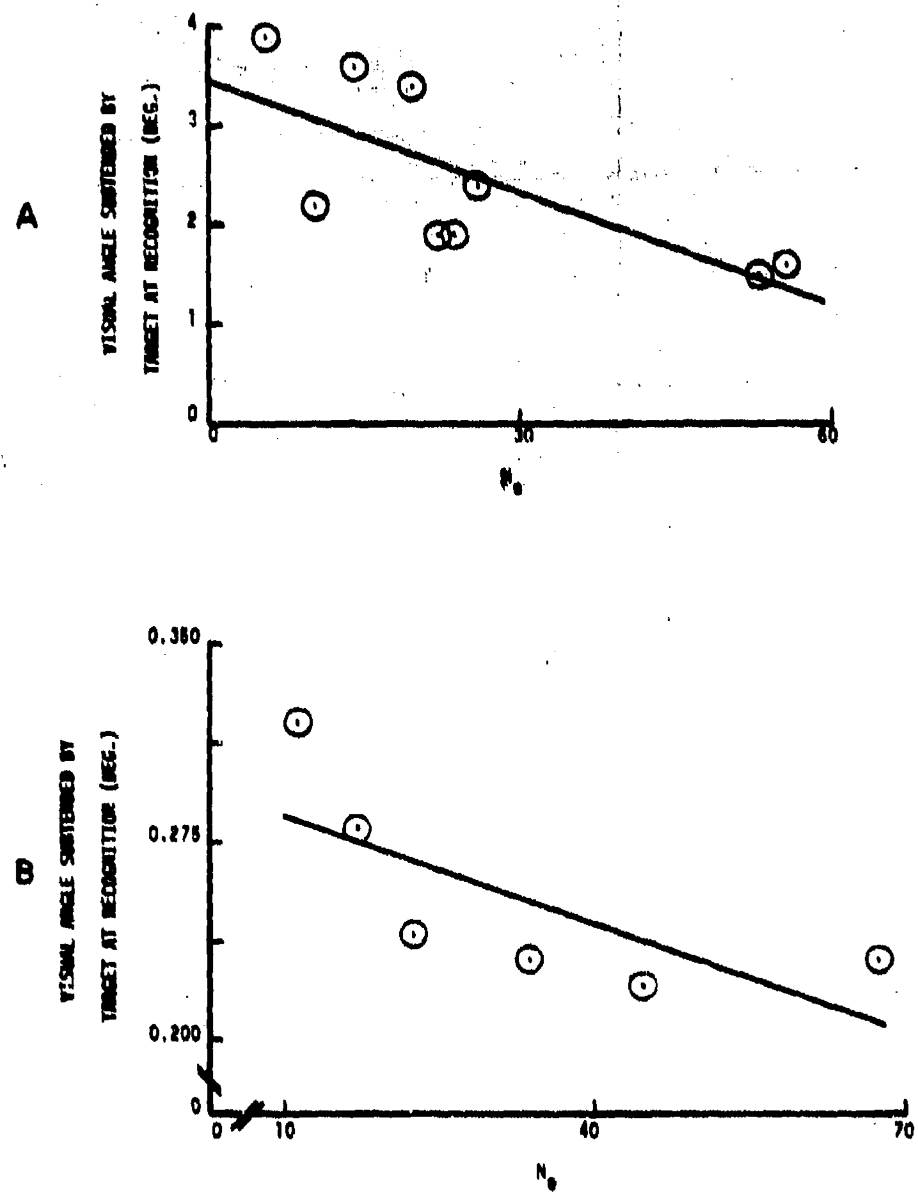

Fig. C.37. A) Graph of angle subtended by target at recognition versus N_e for the target recognition study of Chapter 4, B) graph of angle subtended by target at recognition versus N_e for the target recognition study of Chapter 5

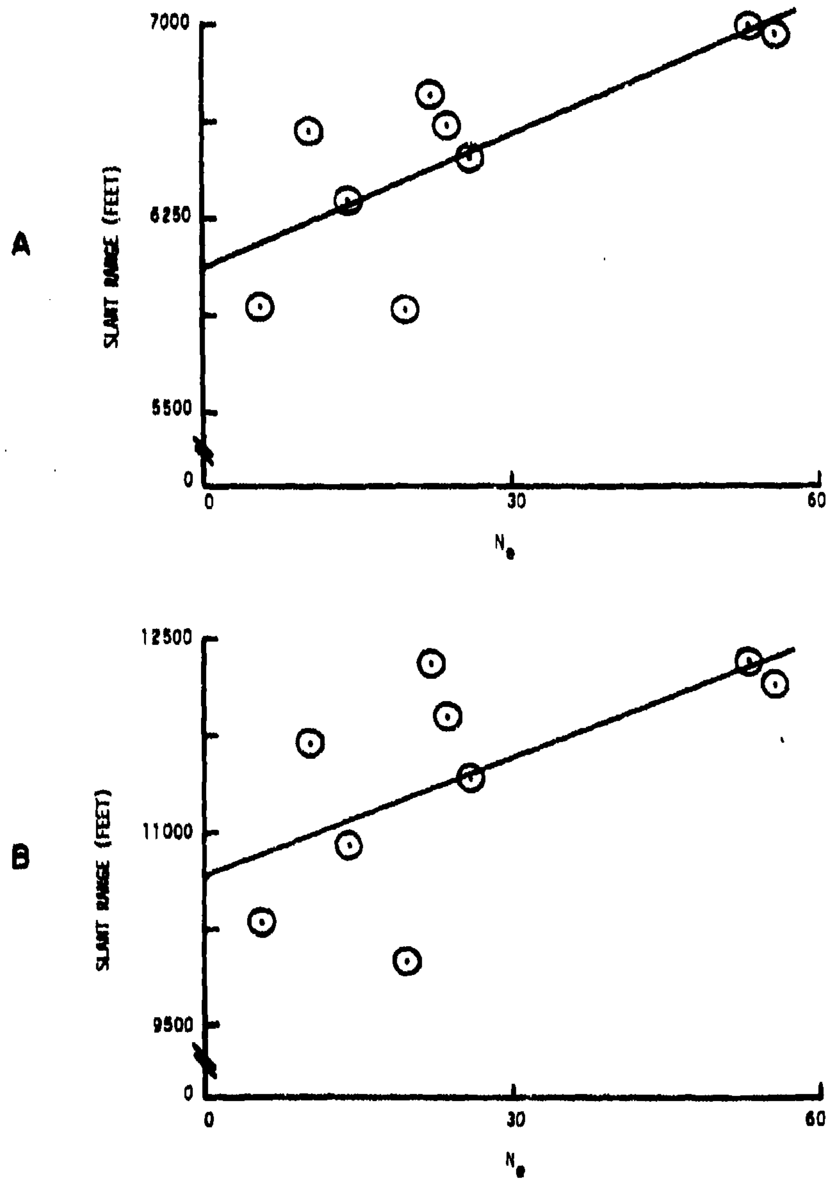

Fig. C.38. A) Graph of slant range to target at detection versus N_e for POL targets and simulated altitude of 1000 feet, B) graph of slant range to target at detection versus N_e for POL targets and simulated altitude of 2000 feet

APPENDIX D

STATISTICAL CALCULATION OF SIGNIFICANT DIFFERENCE BETWEEN CORRELATION COEFFICIENTS

A method for determining whether or not two correlation coefficients are significantly different was found in Fundamental Statistics in Psychology and Education by Guilford (1965). The method was originally developed by Hotelling (1940). Equation (28), derived by Hotelling, was used to calculate a t-value from which the level of significance was obtained from a t-table.

$$t_{d_r} = (r_{12} - r_{13}) \left\{ \frac{(N - 3)\ (1 + r_{23})}{2(1 - r_{23}^2 - r_{12}^2 - r_{13}^2 + 2r_{23}r_{12}r_{13})} \right\}^{1/2} \tag{28}$$

where

t_{d_r} = t score for a t-test

r_{12} = correlation between performance and FOM 1

r_{13} = correlation between performance and FOM 2

r_{23} = correlation between FOM 1 and FOM 2

N = number of data points

$N-3$ = degrees of freedom

If performance is represented by the variable X_1, FOM 1 by X_2, and FOM 2 by X_3, then equation (28) is applicable only if X_2 and X_3 are correlated. This was the case for all of the FOM's investigated.

The hypothesis for this one-tailed t-test is that there is no difference between $|r_{12}|$ and $|r_{13}|$ or that $|r_{13}|$ is greater than $|r_{12}|$. The level of significance indicates the probability that this hypothesis is true.

REFERENCES

Borough, H. C., Fallis, R. F., Warnock, T. H., and Britt, J. H. Quantitative determination of image quality. Boeing Report D2-114058-1, May 1967.

Brock, G. C. Reflections on thirty years of image evaluation. Photo. Sci. Eng., 1967, 11 356-362.

Brown, H. E., Collins, F. A., and Hawkins, J. A. Analysis of optical and electro-optical imaging systems using modulation transfer functions. Technical Report: DRL-TR-68-13, Defense Research Laboratory, University of Texas at Austin, March 1969 (AD832159).

Campbell, Fergus W., Nachmias, Jacob, and Jukes, John. Spatial-frequency discrimination in human vision. J. Opt. Soc. Am., 1970, 60 (4), 555-559.

Campbell, F. W. and Robson, J. G. Application of Fourier analysis to the visibility of gratings. J. Physiol., 1968, 197 551-566.

Carlson, Curtis R. and Cohen, Roger W. A model for predicting the just-noticeable difference in image structure as a function of display modulation transfer. SID 78 Digest, April 1978, 30-31.

Cornsweet, Tom N. Visual Perception. Academic Press, New York, NY (1970).

Cornsweet, Tom N. and Pinsker, H. M. Luminance discrimination of brief flashes under various conditions of adaption. J. Physiol. (London), 1965, 176, 294-310.

DePalma, J. J. and Lowry, E. M. Sine-wave response of the visual system. II. Sine-wave and square-wave contrast sensitivity. J. Opt. Soc. Amer., 1962, 52, 328-335.

Dyall, William T. "Televiewers: What do you mean by high resolution?" Electro-Optical Systems Design, March 1978, p. 26.

Fitts, Paul M. The information capacity of the human motor system in controlling the amplitude of movement. J. Exp. Psych., 1954, 47 (6), 381-387.

Freund, John E. Mathematical Statistics. Prentice-Hall, Englewood Cliffs, N.J. (1962).

Gaskill, Jack D. Linear Systems, Fourier Transforms, and Optics, John Wiley and Sons, Inc., New York, N.Y. (1978).

Graham, Clarence H. (ed.). Vision and Visual Perception, John Wiley and Sons, Inc., New York, N.Y. (1965).

Granger, E. M. Subjective assessment and specification of color image quality. Proceedings Soc. Photo-Opt. Inst. Eng. May 1974, 46, 86-91.

Granger, E. M. and Cupery, K. N. An optical merit function (SQF), which correlates with subjective image judgments. Photo Sci. Eng., 1972, 16, 221.

Guilford, J. P. Fundamental Statistics in Psychology and Education. McGraw-Hill Book Company, New York, N.Y. (1965).

Hotelling, H. The selection of variates for use in prediction, with some comments on the general problem of nuisance parameters. Ann. Math. Stat., 1940, 11, 271-283.

Johnson, John. Analytical description of night vision devices. Proceedings of the Seminar on Direct-Viewing Electro-Optical Aids to Night Vision, Biberman, L., editor, Institute for Defense Analyses Study S254, October 1966.

Martin, Wayne L., Task, H. Lee, Woodruff, Kenneth R., and Pinkus, Alan R. Element density and percent active area design requirements for liquid crystal displays. Technical Report: AMRL-TR-75-235, Aerospace Medical Research Laboratory, Wright-Patterson AFB, Ohio, February 1976.

Riggs, Lorrin A. Visual acuity. In Vision and Visual Perception, Graham, Clarence H., editor, John Wiley and Sons, Inc., New York, N.Y. (1965) pp. 321-323.

Rosell, Frederick A. and Willson, Robert H. Performance synthesis (electro-optical sensors). USAF Report AFAL-TR-71-137, May 1971.

Rosell, Frederick A. and Willson, R. H. Recent psychophysical experiments and the display signal-to-noise ratio concept. Technical Report: Westinghouse ADTM No. 110, Westinghouse Electric Corporation, Defense and Electronics System Center, Systems Development Division, Baltimore, Maryland, September 1972.

Rosell, Frederick A. and Willson, Robert H. Performance synthesis of electro-optical sensors. Technical Report: AFAL-TR-74-104, Air Force Avionics Laboratory, Wright-Patterson AFB, Ohio, April 1974.

RCA Electro-Optics Handbook, Technical Series EOH-11, Commercial Engineering, Harrison, New Jersey (1974).

Schade, O. H. Image gradation, graininess and sharpness in television and motion-picture systems. Part III: The grain structure of television images. J. SMPTE, 1953, 61, 97-164.

Schindler, Richard. Optical power spectrum analysis of display imagery. Phase I: Concept validity. Technical Report: AMRL-TR-76-96, Aerospace Medical Research Laboratory, Wright-Patterson AFB, Ohio, November 1976.

Snyder, Harry L. Visual search and image quality. Technical Report: AMRL-TR-73-114, Aerospace Medical Research Laboratory, Wright-Patterson AFB, Ohio, October 1974a (ADA008007).

Snyder, Harry L. Image quality and face recognition on a television display. Human Factors, 1974b, 16 (3), 300-307.

Snyder, Harry L. Visual search and image quality: final report. Technical Report: AMRL-TR-76-89, Aerospace Medical Research Laboratory, Wright-Patterson AFB, Ohio, December 1976.

Sperling, George. The information available in brief visual presentations. Psych. Mon.: Gen. and Appl., 1960, 74 (11), 1-27.

Task, H. Lee, Pinkus, Alan R., and Hornseth, John P. A comparison of several television display image quality measures. SID 78 Digest, April 1978, 32-33.

Task, H. Lee and Verona, Robert W. A new measure of television display quality relatable to observer performance. Technical Report: AMRL-TR-76-73, Aerospace Medical Research Laboratory, Wright-Patterson AFB, Ohio, August 1976.

van Meeteren, A. Visual aspects of image intensification. Perception Tech. Note, Soesterberg, Netherlands, 1973.

Willson, Robert H., Rosell, Frederick A., and Walmsley, Heru R. Effects of vibration and G loading on airborne E-O sensor augmented observers. Technical Report: AFAL-TR-75-172, Air Force Avionics Laboratory, Wright-Patterson AFB, Ohio, April 1976.

☆ U. S. GOVERNMENT PRINTING OFFICE: 1979-658-697